Genome-wide Meta-analysis Unravels Novel Interactions between Magnesium Homeostasis and Metabolic Phenotypes

JASN

Genome-wide Meta-analysis Unravels Novel Interactions between Magnesium Homeostasis and Metabolic Phenotypes

Journal:	*Journal of the American Society of Nephrology*
Manuscript ID	JASN-2017-03-0267.R2
Manuscript Type:	Original Article - Meta-analysis
Date Submitted by the Author:	16-Jul-2017

Complete List of Authors:	Corre, Tanguy; Lausanne University Hospital, Institute for Social and Preventive Medicine; Universite de Lausanne, Department of Computational Biology; Swiss Institute of Bioinformatics Arjona, Francisco; Radboud university medical center, Physiology Hayward, Caroline; Institute of Genetics and Molecular Medicine, Western General Hospital Youhanna, Sonia; Zurich Center for Integrative Human Physiology, University of Zurich, Institute of Physiology de Baaij, Jeroen; Radboud university medical center, Physiology Belge, Hendrica; University of Zurich, Institute of Physiology Nagele, Nadine; Institute of Physiology, University of Zurich, Debaix, Huguette; University of Zurich, Institute of Physiology Blanchard, Maxime; Radboud university medical center, Physiology Traglia, Michela; Ospedale San Raffaele, Division of Genetics and cell Biology Harris, Sarah; University of Edinburgh, Centre for Cognitive Ageing and Cognitive Epidemiology; University of Edinburgh Centre for Genomic and Experimental Medicine and MRC Institute of Genetics and Molecular Medicine, Medical Genetics Section Ulivi, Sheila; irccs burlo garofolo, medical genetics Rueedi, Rico; Universite de Lausanne, Department of Computational Biology; Swiss Institute of Bioinformatics Lamparter, David; Universite de Lausanne, Department of Computational Biology; Swiss Institute of Bioinformatics Macé, Aurélien; Lausanne University Hospital, Institute for Social and Preventive Medicine; Swiss Institute of Bioinformatics Sala, Cinzia; Ospedale San Raffaele, Division of Genetics and cell Biology Lenarduzzi, Stefania; irccs burlo garofolo, medical genetics Ponte, Belen; University Hospital of Geneva, Nephrology; Pruijm, Menno; University Hospital of Lausanne, Nephrology Ackermann, Daniel; Inselspital, University Hospital and University of Bern, Nephrology, Hypertension and Clinical Pharmacology Ehret, Georg; Geneva University Hospital, Cardiology, Department of Specialties of Internal Medicine Baptista, Daniela; Geneva University Hospital, Cardiology, Department of Specialties of Internal Medicine

Polasek, Ozren; Andrija Stampar School of Public Health, University of Zagreb Medical School, Rockefellerova 4, 10000 Zagreb, Croatia,
Rudan, Igor; University of Edinburgh, Centre for Population Health Sciences
Hurd, Toby; University of Michigan Medical School, Internal Medicine
Hastie, Nicholas; Western General Hospital, Institute of Genetics and Molecular Medicine
Vitart, Veronique; University of Edinburgh, Institute of Genetics and Molecular Medicine
Waeber, Geràrd; Lausanne University Hospital, Department of Medicine
Kutalik, Zoltan; Lausanne University Hospital, Institute for Social and Preventive Medicine; Swiss Institute of Bioinformatics
Bergmann, Sven; Universite de Lausanne, Department of Computational Biology; Swiss Institute of Bioinformatics; University of Cape Town, Department of Integrative Biomedical Sciences
Vargas-Poussou, Rosa; Hôpital Européen Georges Pompidou, Genetics
Konrad, Martin; University Children's Hospital, General Pediatrics, Pediatric Nephrology
Gasparini, Paolo; University of Trieste, Department of Medical, Surgical and Health Sciences; Sidra, Department of Experimental Genetics
Deary, Ian; University of Edinburgh, Centre for Cognitive Ageing and Cognitive Epidemiology; University of Edinburgh, Department of Psychology
Starr, John; University of Edinburgh, Centre for Cognitive Ageing and Cognitive Epidemiology; University of Edinburgh, Alzheimer Scotland Dementia Research Centre
Toniolo, Daniela; San Raffaele Scientific Institute, Division of Genetics and cell Biology
Vollenweider, Peter; Centre Hospitalier Universitaire Vaudois, Department of Medicine
Hoenderop, Joost G.J.; Radboud university medical center, Physiology
Bindels, Rene J.M.; Radboud University Medical Center, 286 Physiology;
Bochud, Murielle; Institute for Social and Preventive Medicine, Community Prevention Unit
Devuyst, Olivier; University of Zurich, Institute of Physiology

Keywords: zebrafish, Genetic determinants, Magnesium homeostasis, Metabolic syndrome, Gene-environment interaction, Tubular transport

JASN-2017-03-0267. R2

Genome-wide Meta-analysis Unravels Novel Interactions between Magnesium Homeostasis and Metabolic Phenotypes

Tanguy Corre*[,1-3], Francisco J. Arjona*[,4], Caroline Hayward*[,5], Sonia Youhanna[6], Jeroen H.F. de Baaij[4], Hendrica Belge[6], Nadine Nägele[6], Huguette Debaix[6], Maxime G. Blanchard[4], Michela Traglia[7], Sarah E. Harris[8,9], Sheila Ulivi[10], Rico Rueedi[2,3], David Lamparter[2,3], Aurélien Macé[1,3], Cinza Sala[7], Stefania Lenarduzzi[10], Belen Ponte[11], Menno Pruijm[12], Daniel Ackermann[13], Georg Ehret[14], Daniela Baptista[14], Ozren Polasek[15], Igor Rudan[16], Toby Hurd[5], Nicholas D. Hastie[5], Veronique Vitart[5], Gerard Waeber[17], Zoltán Kutalik[1,3], Sven Bergmann[2,3,18], Rosa Vargas-Poussou[19,20], Martin Konrad[21], Paolo Gasparini[22,23], Ian J. Deary[8,24], John M. Starr[8,25], Daniela Toniolo[7], Peter Vollenweider[17], Joost G.J. Hoenderop [4], René J.M. Bindels[#,4], Murielle Bochud[#,1], and Olivier Devuyst[#,6]

[1] Institute of Social and Preventive Medicine, Lausanne University Hospital, Lausanne, Switzerland
[2] Department of Computational Biology, University of Lausanne, Lausanne, Switzerland
[3] Swiss Institute of Bioinformatics, Switzerland
[4] Department of Physiology, Radboud Institute for Molecular Life Sciences, Radboud university medical center, Nijmegen, The Netherlands
[5] Medical Research Council Human Genetics Unit, Institute of Genetics and Molecular Medicine, University of Edinburgh, Edinburgh EH4 2XU, UK
[6] Institute of Physiology, University of Zürich, Zürich, Switzerland
[7] Division of Genetics and cell Biology, San Raffaele Scientific Institute, Milano, Italy
[8] Centre for Cognitive Ageing and Cognitive Epidemiology, University of Edinburgh, Edinburgh, UK
[9] Medical Genetics Section, University of Edinburgh Centre for Genomic and Experimental Medicine and MRC Institute of Genetics and Molecular Medicine, Western General Hospital, Edinburgh, UK
[10] Institute for Maternal and Child Health - IRCCS "Burlo Garofolo" – Trieste, Italy
[11] Service of Nephrology, University Hospital of Geneva (HUG), Switzerland
[12] Service of Nephrology, University Hospital of Lausanne (CHUV), Switzerland
[13] University Clinic for Nephrology and Hypertension, Inselspital, Bern University Hospital, University of Bern, Switzerland
[14] Cardiology, Department of Specialties of Internal Medicine, University Hospital of Geneva (HUG), Switzerland
[15] Faculty of Medicine, University of Split, Split, Croatia
[16] Usher Institute of Population Health Sciences and Informatics, University of Edinburgh, Edinburgh, EH8 9AG, UK
[17] Department of Medicine, Internal Medicine, Lausanne University Hospital, 1011 Lausanne, Switzerland

[18] Department of Integrative Biomedical Sciences, University of Cape Town, Cape Town, South Africa
[19] Hôpital Européen Georges Pompidou, Assistance Publique Hôpitaux de Paris, Département de Génétique, Paris, France
[20] Centre de Référence des Maladies Rénales Héréditaires de l'Enfant et de l'Adulte, Paris, France
[21] Department of General Pediatrics, University Hospital Münster, Münster, Germany
[22] Department of Medical, Surgical and Health Sciences, University of Trieste, Trieste, Italy.
[23] Department of Experimental Genetics, Sidra, Doha, Qatar.
[24] Department of Psychology, University of Edinburgh, Edinburgh, UK
[25] Alzheimer Scotland Dementia Research Centre, University of Edinburgh, Edinburgh, UK

* T.C., F.J.A. and C.H. have equally contributed to the study

[#] O.D., M.B. and R.J.M.B. have co-directed the study

Running Title: Genetic determinants of magnesium homeostasis and metabolism

Corresponding authors: Prof. Dr. Olivier Devuyst, E-mail: olivier.devuyst@uzh.ch; or Prof. Murielle Bochud, E-mail: murielle.bochud@chuv.ch.

ABSTRACT

Magnesium (Mg^{2+}) homeostasis is critical for metabolism. The genetic determinants of the renal handling of Mg^{2+}, which is crucial for Mg^{2+} homeostasis, and their potential influence on metabolic traits in the general population are unknown. Plasma and urine parameters were obtained of 9,099 individuals from 7 cohorts for the first genome-wide meta-analysis of Mg^{2+} homeostasis. Two novel loci, *TRPM6* (rs3824347, $P = 4.4\times10^{-13}$) and *ARL15* (rs35929, $P = 2.1\times10^{-11}$), for urinary Mg^{2+} (uMg) were identified, accounting together for 2.3% of the variation in 24-h uMg excretion. In human kidney cells, ARL15 was shown to regulate TRPM6-mediated currents. In zebrafish, the expression of the highly conserved *ARL15* ortholog~~ue~~, *arl15b*, was regulated by dietary Mg^{2+} and *arl15b*-knockdown resulted in renal Mg^{2+} wasting and metabolic disturbances. The association of uMg with fasting insulin and fat mass was modified by *ARL15* rs35929 in a general population. The combined observational and experimental approach uncovers a novel gene-environment interaction linking Mg^{2+} deficiency to insulin resistance and obesity.

INTRODUCTION

Magnesium (Mg^{2+}) is an essential cation for multiple enzymatic reactions, including those involving DNA and protein synthesis and energy metabolism [1]. Abnormal Mg^{2+} levels in serum are associated with common diseases such as diabetes and metabolic disorders [2]. Interventional and longitudinal observational studies in humans show that high dietary Mg^{2+} protects against the risk of developing type 2 diabetes [3-6] and improves glycemic control in diabetic patients [7] as well as in overweight non-diabetic subjects [8-10]. In young adults, high Mg^{2+} intake is significantly associated with lower incidence of metabolic syndrome [11]. Furthermore, there is evidence linking Mg^{2+} intake to body weight regulation, with low intake potentially impairing lean body mass growth [12, 13], whereas Mg^{2+} supplementation may increase lean body mass and decrease fat mass in overweight women [14].

Plasma Mg^{2+} levels are closely regulated and remain constant throughout life, despite the fact that dietary Mg^{2+} intake and intestinal absorption decrease with age [15]. The control of Mg^{2+} balance is ensured by a tightly regulated reabsorption of Mg^{2+} in the distal tubular segments of the kidney. In particular, the Mg^{2+} filtered in the glomerulus is reabsorbed in the proximal tubule and thick ascending loop of Henle (TAL) *via* paracellular routes, while downstream, in the distal convoluted tubule (DCT), Mg^{2+} is efficiently reabsorbed through transcellular mechanisms involving the transient receptor potential cation channel, subfamily M, member 6 (TRPM6) [2]. The reabsorption of Mg^{2+} in the DCT determines the final urinary Mg^{2+} (uMg) excretion since no reabsorption of Mg^{2+} occurs in posterior segments. Subjects harboring inherited or acquired dysfunctions of the renal tubular handling of Mg^{2+} show inappropriate urinary loss of Mg^{2+} causing chronic hypomagnesemia and severe, multi-systemic manifestations [2, 16, 17].

The genetic component of Mg^{2+} homeostasis is indicated by a significant heritability (15-39%) of serum Mg^{2+} [18, 19] and by rare monogenic disorders disturbing renal tubular

transport of Mg^{2+} [20-23]. Yet, most of the regulatory genes of renal Mg^{2+} channels and transporters remain unknown. A genome-wide association study (GWAS) on serum Mg^{2+} in European ancestry adults identified six loci, one of which included the gene encoding TRPM6 [24]. Two more recent studies in children [25] and in African-Americans [26] did not reveal additional loci. However, changes in uMg excretion precede changes in circulating serum Mg^{2+} levels, being thus a more sensitive indicator of any disturbance in Mg^{2+} homeostasis [27]. Furthermore, Mg^{2+} depletion can be found in individuals with apparently normal total serum Mg^{2+} levels [28], which underscores the limitations of total serum Mg^{2+} as a marker of Mg^{2+} status. Assessment of uMg in GWAS is therefore crucial to elucidate new genes involved in Mg^{2+} homeostasis. Furthermore, studying the association between the genetic determinants of uMg and metabolic phenotypes linked to disturbed Mg^{2+} balance (e.g. obesity and diabetes) may provide novel insights on links between Mg^{2+} and common diseases. Indeed, plasma triglycerides and glucose are major determinants of the Mg^{2+} balance in diabetic patients [29].

In order to shed light on the genetic factors and molecular mechanisms linking Mg^{2+} handling and metabolic disorders, we performed a meta-analysis of GWAS for the renal handling of Mg^{2+} by combining genetic isolates and population-based studies and investigating the biological relevance of the identified loci using cellular systems and model organisms. Given the known relationships of Mg^{2+} intake with metabolic disorders, we also explored whether the identified loci modified these relationships. These studies establish a novel biological control of renal Mg^{2+} handling, and a novel gene-environment interaction sustaining the link between Mg^{2+} homeostasis, insulin resistance and obesity.

RESULTS

Meta-analyses of GWAS for magnesium homeostasis

The initial discovery phase consisted of a GWAS (2.5 M markers) performed on the population-based CoLaus cohort (5,150 samples) testing for association with uMg-to-creatinine ratio. The analysis revealed a single genome wide significant signal at rs3824347 ($P = 3.6\times10^{-8}$), corresponding to the *TRPM6* locus on chromosome 9, and six suggestive loci with *P* values below 10^{-5} (Suppl. Fig. 1). These association results were combined with the genome-wide association scans from six additional European cohorts (LBC1936, CROATIA-Split, CROATIA-Vis, Carlantino, CROATIA-Korcula, and Val Borbera) into a single meta-analysis (9,099 samples). As shown on the Manhattan plot (Fig. 1a), two signals showed a *P* value below 5×10^{-8}. The QQ plot showed no problematic inflation (λ=1.014, se=$3.16\text{x}10^{-5}$) (Suppl. Fig. 2a). Both the forest plots (Fig. 1b) and the low I-square values (Table 1) indicated little heterogeneity across cohorts. No secondary signals were detected in the approximate conditional analysis using the lead single nucleotide polymorphisms (SNPs) as covariates in the regression (Suppl. Fig 2b and 2c). The lowest combined *P* value (4.4×10^{-13}) was observed for the SNP rs3824347 on chromosome 9, at a locus comprising five genes, *TRPM6*, *C9orf40*, *C9orf41*, *NMRK1* and *OSTF1* (Fig. 1c). The second strongest signal maps to chromosome 5 with a *P* value of 2.1×10^{-11} for the lead SNP rs35929 (Fig. 1d). This SNP and all other genome-wide significant SNPs at this locus lie in the first intron of the ADP ribosylation factor like GTPase 15 (*ARL15*) gene. None of the two signals showed significant association with urinary creatinine.

Results from the versatile gene-based association study (VEGAS analysis) [30] of uMg/creatinine ratio identified *C9orf40*, *C9orf41* and *TRPM6* as the only genes with a statistically significant result ($P < 2.8\times10^{-6}$), however these signals are overlapping with the single SNP association in the meta-analysis (rs3824347). None of the discovered SNPs tag

copy number variations (CNVs). A pathway analysis has been performed using the Magenta algorithm, but no enrichment appeared to be significant after multiple testing correction. Sex-stratified analyses did not reveal additional genome-wide significant loci. No significant eQTL is referenced for rs35929 nor rs3824347 in the GTEx portal.

A meta-GWAS of serum Mg^{2+} levels replicated the previously published locus on chromosome 1 [24] containing among many others the gene *MUC1* ($P = 4.45\times10^{-14}$) (Suppl. Table 1, Suppl. Fig. 3). Our meta-analysis on fractional excretion of Mg^{2+} (FEMg) yielded 12 suggestive loci with a $P < 10^{-5}$ (Suppl. Fig. 4) but no genome-wide significant association (the sample size was reduced to cohorts having serum and urine from the same time point, therefore without LBC1936, Split and Vis; n = 7,976). The association of rs35929 ($P = 2.8\text{x}10^{-4}$) and rs3824347 ($P = 1.4\text{x}10^{-5}$) with FEMg were nominally, but not genome-wide, significant.

A genetic score including rs35929 and rs3824347 associates with uMg traits

Urinary Mg-to-creatinine ratio (Fig. 2a, CoLaus cohort), FEMg in spot urine (Fig. 2b, CoLaus cohort) and uMg excretion in 24-h urine (Fig. 2c, Swiss Kidney Project on Genes in Hypertension (SKIPOGH) cohort), but not serum Mg^{2+} (Fig. 2d, CoLaus), were strongly and linearly associated with an additive unweighted genetic risk score including rs35929-A (*ARL15*) and rs3824347-G (*TRPM6*) alleles. The genetic score explained 2.3% of 24-h uMg excretion in the SKIPOGH study and 1.0% of uMg-to-creatinine ratio in CoLaus.

ARL15 regulates TRPM6 channel activity

To validate the association between uMg excretion and *ARL15* and *TRPM6* variants, we first showed that the highest mRNA expression of *Arl15* was in distal nephron segments including the TAL and DCT, the DCT being also strongly positive for *Trpm6* (Fig. 3a). At protein

level, ARL15 is localized predominantly in the TAL and the DCT segments (Fig. 3b), which are enriched in Tamm-Horsfall (TH) protein and the Na^+-Cl^--co-transporter (NCC) respectively. Importantly, TRPM6 is also distinctly localized in the DCT segment [31]. The spatial correlation between TRPM6 and ARL15 expression in the DCT prompted us to postulate a functional interaction between these two proteins. In addition, functional protein association network analyses for ARL15 (Suppl. Fig. 5) showed that ARL15 interacts with key proteins for endocytic trafficking (RAB11 and ARFGEF families), a process that may increase the abundance and channel activity of TRPM6 in the plasma membrane.

To assess the potential effect of ARL15 on TRPM6 channel activity, human embryonic kidney 293 (HEK293) cells were transfected with wild type (WT) TRPM6 in parallel with a mock transfect, WT ARL15 or a dominant negative (T46N) ARL15 mutant. The T46N ARL15 mutant was predicted to be of dominant negative nature by comparative analysis with T27N ARF6, a dominant negative mutant affecting a protein (ARF6) that belongs to the same protein family as ARL15 [32]. Patch clamp recordings showed characteristic slowly developing outwardly-rectifying currents in all conditions (Fig. 3c-f). A significant increase in TRPM6 channel activity was observed in the presence of WT ARL15, but not with the T46N ARL15 mutant (Fig. 3e). HEK293 cells express endogenous TRPM7 channels [33]. Here, these currents were small (< 50 pA/pF) and were not significantly increased by expression of WT ARL15 (Fig. 3f).

Physiological relevance of ARL15 in model organisms

To support the important role of ARL15 in Mg^{2+} homeostasis, we investigated the regulation of TRPM6 and ARL15 gene expression in mice upon exposure to variable Mg^{2+} diets, known to affect the expression of critical genes in the mouse kidney and intestine [34], where *Arl15* is expressed (Suppl. Fig. 6a). Metabolic profiling (Suppl. Tables 6-7) revealed a remarkable

adaptation after exposure to high and low Mg^{2+} diets, reflected by significant changes in the renal mRNA expression of *Trpm6* and parvalbumin (*Pvalb*), contrasting with the stable expression of *Arl15* and other segmental markers of the TAL and DCT (Suppl. Fig. 6b). A similar effect was observed in the ileum and the caecum, also involved in Mg^{2+} handling [2, 34] (Suppl. Fig. 6c-d).

We further tested the biological relevance of ARL15 by using a zebrafish model, which shows tubular segmentation patterns that are equivalent to the mammalian kidney [35]. Two distinct orthologs of mammalian ARL15 were identified in zebrafish: *arl15a* and *arl15b*, presenting 68% and 83% of AA identity respectively when aligned to the human counterpart (Suppl. Fig. 7a). Given the higher AA conservation of *arl15b* compared to *arl15a*, *arl15b* was selected to study the function of its mammalian ortholog ARL15. As mammalian *ARL15*, *arl15b* was ubiquitously expressed in all adult zebrafish tissues tested (Suppl. Fig. 7b). When adult zebrafish were fed different Mg^{2+} diets for 3 weeks, *arl15b* expression patterns reflected compensatory mechanisms to cope with Mg^{2+} deficiency (kidney and gills) or Mg^{2+} surplus (gut) (Suppl. Fig. 7c-e).

A loss-of-function approach using morpholinos (MOs) against *arl15b* in zebrafish larvae, where *arl15b* is expressed in the pronephros (Suppl. Fig. 8), was used to relate ARL15 function to renal Mg^{2+} wasting. Since intestinal Mg^{2+} absorption does not take place during the time frame where the knockdown is applied, a change in zebrafish larvae Mg content reflects a change in the renal and/or skin (renal-like tissue [36]) uptake of Mg^{2+}. Total Mg^{2+} content decreased consistently in *arl15b* morphants compared with controls, indicating renal Mg^{2+} wasting since the pronephric kidney is the only extrusion route for Mg^{2+} (Fig. 4a-b). In parallel, cardiovascular impairments and morphological phenotypes characterized by a poorly metabolized yolk in comparison with controls, indicative of metabolic disturbances, were also observed (Fig. 4c-g). Co-injection of *arl15b*-MO with human WT *ARL15* cRNA

induced a rescue of all phenotypes observed, whereas co-injection with T46N *ARL15* cRNA did not result in any rescue (Fig. 4h-k). These rescue experiments demonstrated the specificity of the renal Mg^{2+} wasting and metabolic defects associated to dysfunctional ARL15.

Genetic background influences the link between uMg and metabolism phenotypes

The functional relevance of ARL15 for Mg^{2+} homeostasis, as demonstrated in this study, in combination with the association between *ARL15* and obesity and insulin biology [37] urged us to investigate a possible link between genetic background, renal Mg^{2+} handling and metabolic traits in general population cohorts.

Urinary Mg-to-creatinine ratio was associated positively with circulating fasting adiponectin ($P < 0.001$) and glucose levels ($P = 0.001$) ~~as well as the presence of type 2 diabetes (P=0.03)~~, and negatively with body mass index (BMI) ($P = 0.001$), ~~fasting triglycerides ($P = 0.012$), fasting insulin (P = 0.03)~~, homocysteine ($P < 0.001$) and γ-glutamyl transeptidase (GGT) ($P < 0.001$), independently of serum Mg^{2+}, in CoLaus (the largest cohort available). In CoLaus, the positive associations with adiponectin and fasting glucose, as well as the negative associations with BMI, GGT and homocystein, remained significant ($P < 0.05$) upon adjustment for all the other metabolic phenotypes. In SKIPOGH, 24-h uMg excretion was negatively associated with fasting serum insulin ($P < 0.001$), even after adjustment for the all other metabolic covariates ($P = 0.003$). The negative associations of 24-h uMg excretion with fasting triglycerides or glucose disappeared upon adjustment for fasting insulin; we found no association of 24-h uMg excretion with BMI nor with fat mass ($P > 0.40$).

In CoLaus, the negative association of the *ARL15* rs35929 variant with uMg excretion was stronger in overweight people ($P = 0.005$ for interaction between BMI and rs35929 for

their effect on uMg concentration in spot urine), in people with high fat mass (*P* interaction = 0.024) (Fig. 5a), and in people with high fasting insulin levels (*P* interaction = 0.012) (Fig. 5b), highlighting a SNP-by-environment interaction. In SKIPOGH, the negative association of daytime uMg excretion with fasting insulin was stronger in carriers of the *ARL15* rs35929 A allele (*P* interaction = 0.035), which is consistent with results in CoLaus in that rs35929 appears to modify the association between uMG excretion and fasting insulin. The corresponding *P* values for interaction were 0.140 and 0.143 when replacing fasting insulin by BMI or fat mass, respectively.

DISCUSSION

In this multi-step study (Fig. 6), we conducted the first genome-wide meta-analysis for uMg levels using data from seven population-based studies of European descent. We identified two genome-wide significant loci associated with uMg-to-creatinine ratio: *i*) rs3824347 located on chromosome 9, near the *TRPM6* gene coding for a Mg^{2+} channel; *ii*) rs35929 located on chromosome 5, an intronic variant of the *ARL15* gene known for its association with adiponectin [38] and lipid levels [39, 40], type 2 diabetes [40], fasting insulin levels [41] and coronary heart disease [38], but without a prior physiological link to Mg^{2+} homeostasis. Using a multi-level approach, we provide robust evidence that ARL15 influences renal Mg^{2+} reabsorption through regulation of the Mg^{2+} channel TRPM6. An additive genetic score including the rs35929 A (*ARL15*) and rs3824347 G (*TRPM6*) alleles is strongly associated with 24-h uMg^{2+} excretion, a physiological test of Mg^{2+} status, which integrates both intestinal absorption and renal wasting [42]. In addition, the association of *ARL15* rs35929 with uMg levels is modified by the metabolic status, and the association of uMg excretion with metabolic phenotypes is modified by *ARL15* rs35929 in the general adult population. Altogether, these findings suggest a gene-diet interaction relating Mg^{2+} homeostasis to metabolic disorders in the general population. If replicated in independent populations, the observed genetic effect sizes are sufficiently large to be of clinical and public health relevance.

In contrast to *TRPM6*, little is known about the function of the *ARL15* gene, except its association with adiponectin and lipid levels, type 2 diabetes and higher fasting insulin levels in humans [38-40, 43]. We found that ARL15 is highly expressed in the TAL and DCT, where Mg^{2+} reabsorption is mostly regulated and where the main bulk of Mg^{2+} is reabsorbed. Particularly, we show that ARL15 is enriched along with the well-characterized Mg^{2+} channel TRPM6 in the DCT, and that ARL15 increases TRPM6-mediated currents in renal

epithelial cells. Since TRPM6 is the gatekeeper in transepithelial Mg^{2+} transport, its regulation by ARL15 supports a key role of the latter in the transepithelial Mg^{2+} transport in the distal part of the nephron. ARL15 is structurally similar to Ras-related GTP-binding proteins, which regulate intracellular vesicle trafficking [44]. It interacts with proteins of the RAB11 and ARFGEF families, which are also involved in endocytic traffic, suggesting that ARL15 regulates the trafficking of vesicular TRPM6 to the plasma membrane, thereby influencing Mg^{2+} reabsorption in the kidney. In this sense, our *in vivo* data substantiated ARL15 as a key protein for the maintenance of Mg^{2+} homeostasis. This conclusion is supported by the high sensitivity of *ARL15* expression to dietary Mg^{2+} , as demonstrated by the regulation of the highly conserved zebrafish ortholog of *ARL15*, *arl15b*, in the gut, kidney and gills of fish exposed to different Mg^{2+} diets – as it was already observed for the zebrafish ortholog of *TRPM6* [45]. Conversely, *Arl15* expression in intestine and kidney remained unchanged in mice fed different Mg^{2+} diets. This discrepancy between the mouse and the zebrafish model might be due to that in zebrafish, and freshwater fish in general, active transcellular Mg^{2+} reabsorption is more prominent than in terrestrial vertebrates, as freshwater fish are hyperosmotic respect to the surrounding aquatic medium [46, 47]. Thus, the dietary Mg^{2+} challenge performed with mice in the present study is not sufficiently severe to evoke regulation of *Arl15* expression.

The association of the *ARL15* rs35929 variant with uMg excretion in the present GWAS predicted a physiological relevance of ARL15 in Mg^{2+} homeostasis. In agreement with these findings, knockdown experiments in the zebrafish recognized ARL15 as a relevant key protein that determines renal Mg^{2+} excretion. In agreement with previous GWAS linking *ARL15* variants with risk of congestive heart disease [38], cardiovascular impairments, i.e. deficient tail blood circulation, was recognized in zebrafish *arl15b* morphants. Furthermore, previous links between *ARL15* and lipid metabolism [37-39, 43] were functionally supported in

zebrafish where *arl15b* morphants showed a poor mobilization of yolk metabolite reserves. In zebrafish larvae, the yolk serves mainly as a lipid store [48, 49], therefore the deficiency in yolk absorption observed in *arl15b* morphants revealed poor lipid mobilization. The zebrafish *arl15b* morphants also accumulated fluid in the pericardial cavity and in the pronephros in the form of cysts showing kidney dysfunction. However, when lowering the intensity of the *arl15b*-knockdown (by using doses of 1 and 2 ng exon 4 skipping *arl15b*-MO/embryo), renal Mg^{2+} wasting was the only phenotype observed in the fish morphants. Therefore, the disturbances in Mg^{2+} balance observed in *arl15b* morphants are a primary effect of Arl15b dysfunction and not a secondary disturbance to the kidney/metabolic/cardiovascular phenotypes observed. The phenotype rescue experiments performed with normal or mutant versions of human ARL15 confirmed that renal Mg^{2+} wasting and metabolic defects were directly due to ARL15 knockdown. Altogether, the ARL15 functions unraveled in the present study illustrate an unprecedented case of shared pathophysiological genetics of renal Mg^{2+} wasting, cardiovascular disease and metabolic disorders, and demonstrate the pleiotropic nature of ARL15, that was inferred from the present and published GWAS. The importance of *ARL15* is also supported by recent genetic evidence for its positive selection among adaptive loci identified in cattle [50]. Thus far, no mutations in *ARL15* have been associated with a monogenic disorder, including unidentified forms of renal Mg^{2+} wasting (Data not shown).

Could the metabolic traits linked to *ARL15* variants be connected? By integrating intestinal absorption and renal wasting, uMg^{2+} excretion represents a physiological test of Mg^{2+} status, more suitable than total serum Mg^{2+} levels [42]. Urinary Mg-to-creatinine ratio was associated with multiple metabolic phenotypes, independently of serum Mg^{2+}, in the population-based CoLaus study, providing novel insights into the metabolic consequences of Mg^{2+} deficiencies. Our results are in line with longitudinal studies in humans suggesting that

self-reported dietary Mg^{2+} intake may protect against type 2 diabetes, insulin resistance [51] and metabolic syndrome [52]. Growing experimental evidence in favor of a beneficial role of Mg^{2+} intake on type 2 diabetes is accumulating in humans. Mg^{2+} supplements were found to significantly improve glucose tolerance and insulin sensitivity in diabetic and non-diabetic people [53]. Whether such benefit would persist over years is currently unknown. The public health relevance of dietary Mg^{2+} intake is further underscored by an association with all-cause mortality and risk of cardiovascular disease [51]. The novelty of our results is that we benefit from an objective measure of Mg^{2+} intake, namely uMg excretion, which, unlike circulating Mg^{2+}, was found to be associated with the risk of ischemic heart disease [54].

In population-based studies, the association between uMg and metabolic phenotypes (i.e. BMI, fat mass, fasting insulin levels) tended to differ by *ARL15* rs35929 variants. These results are in line with human studies showing that Mg^{2+} intake exerts more protective effects on type 2 diabetes in overweight compared to non-overweight people [3]. Such gene-diet interaction has already been observed for type 2 diabetes, for which the increased risk conferred by the rs7903146 *TCF7L2* genotype was only observed in the absence of lifestyle intervention [55]. Therefore, the *ARL15* gene may modulate the beneficial effect of Mg^{2+} intake on insulin resistance in humans, offering a novel paradigm in nutrigenetics. Furthermore, the beneficial effect of high Mg^{2+} intake on metabolic disorders, such as type 2 diabetes and obesity, may not be uniform across individuals.

In conclusion, the translational data described in this study (Fig. 6) offer novel insights for the understanding of Mg^{2+} homeostasis and its relation with metabolic phenotypes, and identify ARL15 as a key and central player for these processes.

CONCISE METHODS

Genome-wide meta-analyses

Seven European population-based cohorts with Caucasian ethnicity (CoLaus, CROATIA-Vis, CROATIA-Korcula, CROATIA-Split, Lothian Birth Cohort 1936, INGI-Val Borbera, INGI-Carlantino, described in the Supplementary Information) participated in the study, with a total of 9,099 individuals. A variety of electrolytes including Mg^{2+} as well as creatinine, were measured in both urine and serum (methods and mean values described in the Supplementary Information).

All cohorts were whole genome genotyped before imputation using HapMap CEU panel as reference (Supplementary Information). Serum Mg^{2+} measurements and FEMg were subjected to quantile-quantile normalization in order to reach normality prior to performing linear regression. Urinary Mg^{2+} measurements expressed in mg/dl were first standardized to urinary creatinine, then corrected for age, sex and study specific covariates (such as ancestry principal components, study center…) before undergoing a quantile-quantile normalization. The approximately 2.5M SNPs passing quality control checks were subjected to a linear regression of the residuals for each phenotype, and association summary statistics were collected.

Even though quantile-quantile plots of the individual GWAS showed minimal inflation, ruling out the presence of population substructure, a genomic-control (GC) correction based on the lambda factor was applied to the association *P* values. Subsequently, a meta-analysis was conducted using the inverse variant weighting method implemented in METAL [56]. A new GC correction was applied to combined statistics.

SKIPOGH cohort

SKIPOGH is a population-based family-based multicentric study focusing on blood pressure regulation and renal function [57]. Each participant collected 24-h urine. The study was approved by the institutional ethical committees of each participating university hospital and participants signed written informed consent.

VEGAS analysis

The SNP association *P* values from the meta-analysis of uMg were analysed using VEGAS [30], a program for performing gene-based tests for association using the summary statistics from genetic association studies. VEGAS assigns SNPs to genes and combines their association *P* values into a gene-based test statistic. Permutations are used to calculate the null distribution of the test statistic for each gene in order to derive an empirical gene-wise *P* value. The gene-based approach also reduces the multiple-testing problem of GWAS by only considering statistical tests for 17,787 genes giving a Bonferroni-corrected threshold of $P < 2.8E{-}6$.

Pathway analysis

We used Magenta [58] to check enrichment for pathways in either the BIOCARTA KEGG REACTOME databases which were contained in the msigdb version 4.0 (http://www.broadinstitute.org/gsea/msigdb/collections.jsp#C2).

Metabolome analysis

Nuclear magnetic resonance spectroscopy data obtained from urine samples was binned and normalized to produce metabolome features [59]. These features were then associated with the

SNPs of interest, including relevant covariates among standard covariates (age, sex, genotype principal components) and lifestyle factors (smoking, caffeine use, dietary intake, etc.).

CNV analysis

In house datasets have been used to call CNVs and to check their correlation with the SNPs of interest. The CNVs call has been done using pennCNV software [60]. A SNP by sample matrix with the copy number status has been created. Then the square correlation (Pearson's correlation) between value of each SNP of interest and the SNPs copy number status in a +/- 100 kb region has been calculated. For the SNPs of interest for which no correspondence has been found in the datasets, they have been replaced by the closest SNPs in high linkage disequilibrium (LD) and present in the datasets. LD between the SNPs of interest and a list of SNPs tagging CNVs from the Genetic Investigation of ANthropometric Traits (GIANT) consortium has also been calculated. The SNPs from the GIANT list are in LD higher than 0.8 with their corresponding CNV [60].

Laboratory measurements

Electrolytes, haematology parameters and glycaemia were dosed in the biochemical platform of the University of Zürich using standard clinical laboratory methods. Creatinine was measured using Jaffe kinetic compensated method (Roche Diagnostics, Switzerland, intra-assay variability 0.7-2.9%). The Chronic Kidney Disease Epidemiology Collaboration (CKD-EPI) formula was used to calculate the estimated glomerular filtration rate (eGFR). In CoLaus, urinary uromodulin, creatinine, electrolytes and osmolality concentrations were measured in morning spot urine samples.

All urinary biochemical parameters were measured from samples stored at -80°C, using the same biochemical platform UniCel® DxC 800 Synchron® Clinical System

(Beckman Coulter, Nyon, Switzerland) at the University of Zürich. Appropriate controls and sets of calibration standards were used before running each sample batch. All cohorts were subjected to the same measurement protocol, in the same laboratory.

Tissue distribution and localization of ARL15

The tissue distribution of *ARL15* and of its highly conserved zebrafish ortholog *arl15b* was studied in adult mouse, adult zebrafish and zebrafish larvae, as described in the Supplementary Information. Segmental expression of ARL15 in the mouse (C57BL/6J) kidney was studied at both protein and mRNA level. Five-µm sections of fixed frozen kidney samples were co-stained for ARL15 and specific segment markers: breast cancer resistance protein (BCRP) for the proximal tubule (PT), TH for the TAL, NCC for the DCT, and aquaporin-2 (AQP2) for the collecting duct (CD). For mRNA expression, kidneys were dissected and minced, before isolation of well-characterized nephron segments. For more details of the immunohistochemistry, micro-dissection studies and mRNA analyses in the nephron segments, see the Supplementary Information.

Functional studies in cells and animal models

To study the regulation of TRPM6 channel activity by ARL15, human embryonic kidney 293 (HEK293) cells were transfected with 1 µg of human TRPM6 cDNA [33] and 250 ng of empty vector (mock), human WT ARL15 or a human dominant negative (T46N) ARL15 mutant as negative control. Whole-cell patch clamp recordings were performed to determine the electrophysiological properties of the cells transfected with the constructs mentioned above (see details in the Supplementary Information).

The regulation of *ARL15* gene expression by dietary Mg^{2+} was studied in C57BL/6J mice and Tupfel long-fin zebrafish (details in the Supplementary Information). These studies

were followed by a loss-of-function approach in zebrafish larvae using two non-overlapping splice-site blocking morpholinos (MOs): 5'-AAACACTGAAAGACGGGACAAAGAC-3' and 5'-GTTAAGCGAGTATTAGGTTACCTCT-3' (Gene Tools, Philomath, OR, USA), designated as exon skipping 3 and 4 *arl15b*-MO respectively. These antisense oligonucleotides were used to knockdown the highly conserved *ARL15* ortholog in the zebrafish, *arl15b*. Phenotype rescue experiments were performed by co-injecting *arl15b*-MOs with human *ARL15* cRNA as previously described [61] and detailed in the Supplementary Information. The use of two non-overlapping *arl15b*-MOs and the combination with rescue experiments with human *ARL15* cRNA served to rule out potential off-target effects in our knockdown approach.

Statistical analyses in experiments performed in cellular and animal models

All results are depicted as mean ± standard error of the mean (SEM). Statistical analyses were conducted by one-way ANOVA followed by the Tukey's multiple comparison post-test. When only two experimental groups were affected by the factor of variance, an unpaired Student's *t*-test was used. Statistical significance was set at $P < 0.05$.

Metabolic factors associated with uMg excretion

We used multiple linear regression to explore the association between square-root-transformed uMg-to-creatinine ratio in spot urine and several metabolic markers (i.e. fasting triglycerides, total cholesterol, HDL-cholesterol, glucose, insulin, homocysteine, adiponectin, GGT and BMI), taken one–at–a–time as the dependent variable, while adjusting for serum Mg^{2+} and other potential confounders in SKIPOGH and CoLaus cohorts. In SKIPOGH, we used multivariate linear mixed effect regression to explore the association of fasting insulin with 24-h uMg excretion, while adjusting for potential confounders. We used a conservative

P value (0.05/9=0.0056) threshold to consider the associations of urinary Mg with metabolic phenotypes as statistically significant.

SNP-by-environment interaction on uMg levels

We explored the role of metabolic phenotypes on the association of *ARL15* rs35929 with uMg levels in spot urine among CoLaus participants. We conducted multiple linear regression to explore the modifying effect of BMI, fat mass and fasting insulin levels on the association of the *ARL15* rs35929 with square-root transformed uMg concentration, while including age, sex, height, lean mass, CKD-EPI, urinary creatinine (square-root), serum Mg^{2+}, serum and urine Ca^{2+} (square-root) and menopausal status. The *P* values for interaction were not corrected for multiple testing, as we tested a single global hypothesis ("does the association between rs35929 and urinary Mg differ by metabolic status?") guided by prior knowledge.

Note: The datasets and summary statistics are available in the IUMSP Research Data Repository, under the link https://data.iumsp.ch/index.php/catalog/6.

ID Number: CHE-GWAS-V01. Created on July 12, 2017.

ACKNOWLEDGEMENTS

We thank Dr. Sjoerd Verkaart, Anke Hoefnagels and Sami G. Mohammed for their excellent technical support during the performance of the functional analyses and acknowledge Drs. Erwin van Wijk and Gert Flik for providing the facilities for zebrafish experimentation.

FUNDING

This work was supported by the Long-Term Fellowship from the European Renal Association - European Dialysis and Transplant Association (ERA LTF 175-2014) and the Impulsion Grant from the ERA-EDTA Working Group on Inherited Kidney Disorders (WGIKD) to FJA; and by the grant from the Netherlands Organization for Scientific Research (NWO VICI 016.130.668) to JGJH. JHFdB is supported by the grant from NWO (Rubicon 825.14.021) and RJMB by the EURenOmics project from the European Union Seventh Framework Programme (FP7/2007–2013, agreement no 305608). ZK received financial support from the Leenaards Foundation, the Swiss National Science Foundation (31003A-143914) and SystemsX.ch (51RTP0_151019). MBO and TC are supported by the Swiss National Centre of Competence in Research Kidney Control of Homeostasis (NCCR Kidney.CH) program. OD is supported by grants from the European Community's Seventh Framework Programme (305608 EURenOmics), the Swiss National Centre of Competence in Research Kidney Control of Homeostasis (NCCR Kidney.CH) program, the Swiss National Science Foundation (31003A_169850) and the Rare Disease Initiative Zurich (radiz), a clinical research priority program of the University of Zurich, Switzerland.

The SKIPOGH study is supported by a grant from the Swiss national science foundation (FN 33CM30-124087). The CoLaus study is supported by research grants from GlaxoSmithKline, the Faculty of Biology and Medicine of Lausanne, and the Swiss National Science Foundation (grants 33CSCO-122661, 33CS30-139468 and 33CS30-148401). The

CROATIA-Korcula and CROATIA-Split studies were funded by grants from the Medical Research Council (UK), European Commission Framework 6 project EUROSPAN (Contract No. LSHG-CT-2006-018947) and Republic of Croatia Ministry of Science, Education and Sports research grants to I.R. (108-1080315-0302). We would like to acknowledge the invaluable contributions of the recruitment team in Korcula and Split, the administrative teams in Croatia and Edinburgh and the people of Korcula and Split. The SNP genotyping for the CROATIA-Korcula cohort was performed in Helmholtz Zentrum München, Neuherberg, Germany. The SNP genotyping for the CROATIA-Split cohort was performed by AROS Applied Biotechnology, Aarhus, Denmark. INGI-Carlantino : We thank Anna Morgan and Angela D'Eustacchio for technical support; the municipal administrators for their collaboration on the project and for logistic support; and all participants to this study. For the INGI-VALBORBERA study, the research was supported by funds from Compagnia di San Paolo, Torino, Italy; Fondazione Cariplo, Italy and Ministry of Health, Ricerca Finalizzata 2008 to DT. Phenotype collection in LBC1936 was supported by Age UK (The Disconnected Mind project). Genotyping was funded by the BBSRC (BB/F019394/1). The work was undertaken by the University of Edinburgh Centre for Cognitive Ageing and Cognitive Epidemiology, part of the cross council Lifelong Health and Wellbeing Initiative (MR/K026992/1). Funding from the BBSRC and Medical Research Council (MRC) is gratefully acknowledged. We thank the LBC1936 participants, the LBC1936 team for data collection and collation, and the staff at the Wellcome Trust Clinical Research Facility for bio-sample collection and genotyping.

COMPETING FINANCIAL INTERESTS: None.

REFERENCES

1. Feeney, KA, Hansen LL, Putker M, Olivares-Yañez C, Day J, Eades LJ, Larrondo LF, Hoyle NP, O'Neill JS, van Ooijen G: Daily magnesium fluxes regulate cellular timekeeping and energy balance. *Nature* 532**:** 375-379, 2016.

2. de Baaij JHF, Hoenderop JGJ, Bindels RJM: Magnesium in man: implications for health and disease. *Physiol Rev* 95**:** 1-46, 2015.

3. Dong JY, Xun P, He K, Qin LQ: Magnesium intake and risk of type 2 diabetes: meta-analysis of prospective cohort studies. *Diabetes Care,* 34**:** 2116-2122, 2011.

4. Hruby A, Meigs JB, O'Donnell CJ, Jacques PF, McKeown NM: Higher magnesium intake reduces risk of impaired glucose and insulin metabolism and progression from prediabetes to diabetes in middle-aged americans. *Diabetes Care,* 37**:** 419-427, 2014.

5. Lopez-Ridaura R, Willett WC, Rimm EB, Liu S, Stampfer MJ, Manson JE, Hu FB: Magnesium intake and risk of type 2 diabetes in men and women. *Diabetes Care,* 27**:** 134-140, 2004.

6. Schulze MB, Schulz M, Heidemann C, Schienkiewitz A, Hoffmann K, Boeing H: Fiber and magnesium intake and incidence of type 2 diabetes: a prospective study and meta-analysis. *Arch Intern Med* 167**:** 956-965, 2007.

7. Song Y, He K, Levitan EB, Manson JE, Liu S: Effects of oral magnesium supplementation on glycaemic control in Type 2 diabetes: a meta-analysis of randomized double-blind controlled trials. *Diabet Med* 23**:** 1050-1056, 2006.

8. Chacko SA, Sul J, Song Y, Li X, LeBlanc J, You Y, Butch A, Liu S: Magnesium supplementation, metabolic and inflammatory markers, and global genomic and proteomic profiling: a randomized, double-blind, controlled, crossover trial in overweight individuals. *Am J Clin Nutr* 93**:** 463-473, 2011.

9. Mooren FC, Krüger K, Völker K, Golf SW, Wadepuhl M, Kraus A: Oral magnesium supplementation reduces insulin resistance in non-diabetic subjects - a double-blind, placebo-controlled, randomized trial. *Diabetes, Obes Metab* 13**:** 281-284, 2011.

10. Guerrero-Romero F, Tamez-Perez HE, González-González G, Salinas-Martínez AM, Montes-Villarreal J, Treviño-Ortiz JH, Rodríguez-Morán M: Oral magnesium supplementation improves insulin sensitivity in non-diabetic subjects with insulin resistance. A double-blind placebo-controlled randomized trial. *Diabetes Metab* 30**:** 253-258, 2004.

11. He K, Liu K, Daviglus ML, Morris SJ, Loria CM, Van Horn L, Jacobs DR, Savage PJ: Magnesium intake and incidence of metabolic syndrome among young adults. *Circulation,* 113**:** 1675-1682, 2006.

12. Bertinato J, Lavergne C, Rahimi S, Rachid H, Vu NA, Plouffe LJ, Swist E: Moderately low magnesium intake impairs growth of lean body mass in obese-prone and obese-resistant rats fed a high-energy diet. *Nutrients,* 8**:** E253, 2016.

13. Ried JS, Jeff M J, Chu AY, Bragg-Gresham JL, van Dongen J, Huffman JE, Ahluwalia TS, Cadby G, Eklund N, Eriksson J, Esko T, Feitosa MF, Goel A, Gorski M, Hayward C, Heard-Costa NL, Jackson AU, Jokinen E, Kanoni S, Kristiansson K, Kutalik Z, Lahti J, Luan J, Mägi R, Mahajan A, Mangino M, Medina-Gomez C, Monda KL, Nolte IM, Pérusse L, Prokopenko I, Qi L, Rose LM, Salvi E, Smith MT, Snieder H, Stančáková A, Ju Sung Y, Tachmazidou I, Teumer A, Thorleifsson G, van der Harst P, Walker RW, Wang SR, Wild SH, Willems SM, Wong A, Zhang W, Albrecht E, Couto Alves A, Bakker SJ, Barlassina C, Bartz TM, Beilby J, Bellis C, Bergman RN, Bergmann S, Blangero J, Blüher M, Boerwinkle E, Bonnycastle LL, Bornstein SR, Bruinenberg M, Campbell H, Chen YI, Chiang CW, Chines PS, Collins FS, Cucca F, Cupples LA, D'Avila F, de Geus EJ, Dedoussis G, Dimitriou M, Döring

A, Eriksson JG, Farmaki AE, Farrall M, Ferreira T, Fischer K, Forouhi NG, Friedrich N, Gjesing AP, Glorioso N, Graff M, Grallert H, Grarup N, Gräßler J, Grewal J, Hamsten A, Harder MN, Hartman CA, Hassinen M, Hastie N, Hattersley AT, Havulinna AS, Heliövaara M, Hillege H, Hofman A, Holmen O, Homuth G, Hottenga JJ, Hui J, Husemoen LL, Hysi PG, Isaacs A, Ittermann T, Jalilzadeh S, James AL, Jørgensen T, Jousilahti P, Jula A, Marie Justesen J, Justice AE, Kähönen M, Karaleftheri M, Tee Khaw K, Keinanen-Kiukaanniemi SM, Kinnunen L, Knekt PB, Koistinen HA, Kolcic I, Kooner IK, Koskinen S, Kovacs P, Kyriakou T, Laitinen T, Langenberg C, Lewin AM, Lichtner P, Lindgren CM, Lindström J, Linneberg A, Lorbeer R, Lorentzon M, Luben R, Lyssenko V, Männistö S, Manunta P, Leach IM, McArdle WL, Mcknight B, Mohlke KL, Mihailov E, Milani L, Mills R, Montasser ME, Morris AP, Müller G, Musk AW, Narisu N, Ong KK, Oostra BA, Osmond C, Palotie A, Pankow JS, Paternoster L, Penninx BW, Pichler I, Pilia MG, Polašek O, Pramstaller PP, Raitakari OT, Rankinen T, Rao DC, Rayner NW, Ribel-Madsen R, Rice TK, Richards M, Ridker PM, Rivadeneira F, Ryan KA, Sanna S, Sarzynski MA, Scholtens S, Scott RA, Sebert S, Southam L, Sparsø TH, Steinthorsdottir V, Stirrups K, Stolk RP, Strauch K, Stringham HM, Swertz MA, Swift AJ, Tönjes A, Tsafantakis E, van der Most PJ, Van Vliet-Ostaptchouk JV, Vandenput L, Vartiainen E, Venturini C, Verweij N, Viikari JS, Vitart V, Vohl MC, Vonk JM, Waeber G, Widén E, Willemsen G, Wilsgaard T, Winkler TW, Wright AF, Yerges-Armstrong LM, Hua Zhao J, Carola Zillikens M, Boomsma DI, Bouchard C, Chambers JC, Chasman DI, Cusi D, Gansevoort RT, Gieger C, Hansen T, Hicks AA, Hu F, Hveem K, Jarvelin MR, Kajantie E, Kooner JS, Kuh D, Kuusisto J, Laakso M, Lakka TA, Lehtimäki T, Metspalu A, Njølstad I, Ohlsson C, Oldehinkel AJ, Palmer LJ, Pedersen O, Perola M, Peters A, Psaty BM, Puolijoki H, Rauramaa R, Rudan I, Salomaa V, Schwarz PE,

Shudiner AR, Smit JH, Sørensen TI, Spector TD, Stefansson K, Stumvoll M, Tremblay A, Tuomilehto J, Uitterlinden AG, Uusitupa M, Völker U, Vollenweider P, Wareham NJ, Watkins H, Wilson JF, Zeggini E, Abecasis GR, Boehnke M, Borecki IB, Deloukas P, van Duijn CM, Fox C, Groop LC, Heid IM, Hunter DJ, Kaplan RC, McCarthy MI, North KE, O'Connell JR, Schlessinger D, Thorsteinsdottir U, Strachan DP, Frayling T, Hirschhorn JN, Müller-Nurasyid M, Loos RJ: A principal component meta-analysis on multiple anthropometric traits identifies novel loci for body shape. *Nat Commun* 7**:** 13357, 2016.

14. Moslehi N, Vafa M, Sarrafzadeh J, Rahimi-Foroushani A: Does magnesium supplementation improve body composition and muscle strength in middle-aged overweight women? A double-blind, placebo-controlled, randomized clinical trial. *Biol Trace Elem Res* 153**:** 111-118, 2013.

15. Barbagallo M, Belvedere M, Dominguez LJ: Magnesium homeostasis and aging. *Magnes Res* 22**:** 235-246, 2009.

16. Glaudemans B, Knoers NVAM, Hoenderop JGJ, Bindels RJM: New molecular players facilitating Mg^{2+} reabsorption in the distal convoluted tubule. *Kidney Int* 77**:** 17-22, 2010.

17. Devuyst O, Knoers NV, Remuzzi G, Schaefer F: Rare inherited kidney diseases: challenges, opportunities, and perspectives. *Lancet* 383**:** 1844-1859, 2014.

18. Hunter DJ, de Lange M, Snieder H, MacGregor AJ, Swaminathan R, Thakker RV, Spector TD: Genetic contribution to renal function and electrolyte balance: a twin study. *Clin Sci* 103**:** 259-265, 2002.

19. Moulin F, Ponte B, Pruijm M, Ackermann D, Bouatou Y, Guessous I, Ehret G, Bonny O, Pechère-Bertschi A, Staessen JA, Paccaud F, Martin PY, Burnier M, Vogt B, Devuyst

O, Bochud M: Heritability and distribution of renal handling of electrolytes: a population-based approach. *Kidney Int*: in press, 2017.

20. Simon DB, Lu Y, Choate KA, Velázquez H, Al-Sabban E, Praga M, Casari G, Bettinelli A, Colussi G, Rodríguez-Soriano J, McCredie D, Milford D, Sanjad S, Lifton RP: Paracellin-1, a renal tight junction protein required for paracellular Mg^{2+} resorption. *Science* 285**:** 103-106, 1999.

21. Konrad M, Schaller A, Seelow D, Pandey AV, Waldegger S, Lesslauer A, Vitzhum H, Suzuki Y, Luk JM, Becker C, Schlingmann KP, Schmid M, Rodríguez-Soriano J, Ariceta G, Cano F, Enríquez R, Juppner H, Bakkaloglu SA, Hediger MA, Gallati S, Neuhauss SC, Nurnberg P, Weber S: Mutations in the tight-junction gene claudin 19 (CLDN19) are associated with renal magnesium wasting, renal failure, and severe ocular involvement. *Am J Hum Genet* 79**:** 949-957, 2006.

22. Schlingmann KP, Weber S, Peters M, Nejsum LN, Vitzthum H, Klingel K, Kratz M, Haddad E, Ristoff E, Dinour D, Syrrou M, Nielsen S, Sassen M, Waldegger S, Seyberth HW, Konrad M: Hypomagnesemia with secondary hypocalcemia is caused by mutations in TRPM6, a new member of the TRPM gene family. *Nat Genet* 31**:** 166-170, 2002.

23. Walder RY, Landau D, Meyer P, Shalev H, Tsolia M, Borochowitz Z, Boettger MB, Beck GE, Englehardt RK, Carmi R, Sheffield VC: Mutation of TRPM6 causes familial hypomagnesemia with secondary hypocalcemia. *Nat Genet* 31**:** 171-174, 2002.

24. Meyer TE, Verwoert GC, Hwang SJ, Glazer NL, Smith AV, van Rooij FJ, Ehret GB, Boerwinkle E, Felix JF, Leak TS, Harris TB, Yang Q, Dehghan A, Aspelund T, Katz R, Homuth G, Kocher T, Rettig R, Ried JS, Gieger C, Prucha H, Pfeufer A, Meitinger T, Coresh J, Hofman A, Sarnak MJ, Chen YD, Uitterlinden AG, Chakravarti A, Psaty

BM, van Duijn CM, Kao WH, Witteman JC, Gudnason V, Siscovick DS, Fox CS, Köttgen A, Genetic Factors for Osteoporosis Consortium, Meta Analysis of Glucose and Insulin Related Traits Consortium: Genome-wide association studies of serum magnesium, potassium, and sodium concentrations identify six loci influencing serum magnesium levels. *PLoS Genet* 6**:** e1001045, 2010.

25. Chang X, Li J, Guo Y, Wei Z, Mentch FD, Hou C, Zhao Y, Qiu H, Kim C, Sleiman PM, Hakonarson H: Genome-wide association study of serum minerals levels in children of different ethnic background. *PLoS One* 10**:** e0123499, 2015.
26. Tin A, Köttgen A, Folsom AR, Maruthur NM, Tajuddin SM, Nalls MA, Evans MK, Zonderman AB, Friedrich CA, Boerwinkle E, Coresh J, Kao WH: Genetic loci for serum magnesium among African-Americans and gene-environment interaction at MUC1 and TRPM6 in European-Americans: the Atherosclerosis Risk in Communities (ARIC) study. *BMC Genet* 16**:** 56, 2015.
27. Fleming CR, George L, Stoner GL, Tarrosa VB, Moyer TP: The importance of urinary magnesium values in patients with gut failure. *Mayo Clin Proc,* 71**:** 21-24, 1996.
28. Barbagallo M, Dominguez LJ: Magnesium and type 2 diabetes. *World J Diabetes* 6**:** 1152-1157, 2015.
29. Kurstjens S, de Baaij JHF, Bouras H, Bindels RJM, Tack CJ, Hoenderop JGJ: Determinants of hypomagnesemia in patients with type 2 diabetes mellitus. *Eur J Endocrinol* 176**:** 11-19, 2017.
30. Liu JZ, McRae AF, Nyholt DR, Medland SE, Wray NR, Brown KM, AMFS Investigators, Hayward NK, Montgomery GW, Visscher PM, Martin NG, Macgregor S: A versatile gene-based test for genome-wide association studies. *Am J Hum Genet* 87**:** 139-145, 2010.

31. Nijenhuis T, Vallon V, van der Kemp AWCM, Loffing J, Hoenderop JGJ, Bindels RJM: Enhanced passive Ca^{2+} reabsorption and reduced Mg^{2+} channel abundance explains thiazide-induced hypocalciuria and hypomagnesemia. *J Clin Invest* 115**:** 1651-1658, 2005.

32. Lawrence JTR, Birnbaum MJ: ADP-ribosylation factor 6 delineates separate pathways used by endothelin 1 and insulin for stimulating glucose uptake in 3T3-L1 adipocytes. *Mol Cell Biol* 21**:** 5276-5285, 2001.

33. Voets T, Nilius B, Hoefs S, van der Kemp AW, Droogmans G, Bindels RJM, Hoenderop JGJ: TRPM6 forms the Mg^{2+} influx channel involved in intestinal and renal Mg^{2+} absorption. *J Biol Chem* 279**:** 19-25, 2004.

34. Groenestege WM, Hoenderop JGJ, van den Heuvel L, Knoers N, Bindels, RJM: The epithelial Mg^{2+} channel transient receptor potential melastatin 6 is regulated by dietary Mg^{2+} content and estrogens. *J Am Soc Nephrol* 17**:** 1035-1043, 2006.

35. Wingert RA, Davidson AJ: The zebrafish pronephros: A model to study nephron segmentation. *Kidney Int* 73**:** 1120-1127, 2008.

36. Hwang P-P, Chou M-Y: Zebrafish as an animal model to study ion homeostasis. *Pflügers Arch* 465**:** 1233-1247, 2013.

37. Shungin D, Winkler TW, Croteau-Chonka DC, Ferreira T, Locke AE, Mägi R, Strawbridge RJ, Pers TH, Fischer K, Justice AE, Workalemahu T, Wu JM, Buchkovich ML, Heard-Costa NL, Roman TS, Drong AW, Song C, Gustafsson S, Day FR, Esko T, Fall T, Kutalik Z, Luan J, Randall JC, Scherag A, Vedantam S, Wood AR, Chen J, Fehrmann R, Karjalainen J, Kahali B, Liu CT, Schmidt EM, Absher D, Amin N, Anderson D, Beekman M, Bragg-Gresham JL, Buyske S, Demirkan A, Ehret GB, Feitosa MF, Goel A, Jackson AU, Johnson T, Kleber ME, Kristiansson K, Mangino M, Mateo Leach I, Medina-Gomez C, Palmer CD, Pasko D,

Pechlivanis S, Peters MJ, Prokopenko I, Stančáková A, Ju Sung Y, Tanaka T, Teumer A, Van Vliet-Ostaptchouk JV, Yengo L, Zhang W, Albrecht E, Ärnlöv J, Arscott GM, Bandinelli S, Barrett A, Bellis C, Bennett AJ, Berne C, Blüher M, Böhringer S, Bonnet F, Böttcher Y, Bruinenberg M, Carba DB, Caspersen IH, Clarke R, Daw EW, Deelen J, Deelman E, Delgado G, Doney AS, Eklund N, Erdos MR, Estrada K, Eury E, Friedrich N, Garcia ME, Giedraitis V, Gigante B, Go AS, Golay A, Grallert H, Grammer TB, Gräßler J, Grewal J, Groves CJ, Haller T, Hallmans G, Hartman CA, Hassinen M, Hayward C, Heikkilä K, Herzig KH, Helmer Q, Hillege HL, Holmen O, Hunt SC, Isaacs A, Ittermann T, James AL, Johansson I, Juliusdottir T, Kalafati IP, Kinnunen L, Koenig W, Kooner IK, Kratzer W, Lamina C, Leander K, Lee NR, Lichtner P, Lind L, Lindström J, Lobbens S, Lorentzon M, Mach F, Magnusson PK, Mahajan A, McArdle WL, Menni C, Merger S, Mihailov E, Milani L, Mills R, Moayyeri A, Monda KL, Mooijaart SP, Mühleisen TW, Mulas A, Müller G, Müller-Nurasyid M, Nagaraja R, Nalls MA, Narisu N, Glorioso N, Nolte IM, Olden M, Rayner NW, Renstrom F, Ried JS, Robertson NR, Rose LM, Sanna S, Scharnagl H, Scholtens S, Sennblad B, Seufferlein T, Sitlani CM, Vernon Smith A, Stirrups K, Stringham HM, Sundström J, Swertz MA, Swift AJ, Syvänen AC, Tayo BO, Thorand B, Thorleifsson G, Tomaschitz A, Troffa C, van Oort FV, Verweij N, Vonk JM, Waite LL, Wennauer R, Wilsgaard T, Wojczynski MK, Wong A, Zhang Q, Hua Zhao J, Brennan EP, Choi M, Eriksson P, Folkersen L, Franco-Cereceda A, Gharavi AG, Hedman ÅK, Hivert MF, Huang J, Kanoni S, Karpe F, Keildson S, Kiryluk K, Liang L, Lifton RP, Ma B, McKnight AJ, McPherson R, Metspalu A, Min JL, Moffatt MF, Montgomery GW, Murabito JM, Nicholson G, Nyholt DR, Olsson C, Perry JR, Reinmaa E, Salem RM, Sandholm N, Schadt EE, Scott RA, Stolk L, Vallejo EE, Westra HJ, Zondervan KT, ADIPOGen Consortium, CARDIOGRAMplusC4D

Consortium, CKDGen Consortium, GEFOS Consortium, GENIE Consortium, GLGC, ICBP, International Endogene Consortium, LifeLines Cohort Study, MAGIC Investigators, MuTHER Consortium, PAGE Consortium, ReproGen Consortium, Amouyel P, Arveiler D, Bakker SJ, Beilby J, Bergman RN, Blangero J, Brown MJ, Burnier M, Campbell H, Chakravarti A, Chines PS, Claudi-Boehm S, Collins FS, Crawford DC, Danesh J, de Faire U, de Geus EJ, Dörr M, Erbel R, Eriksson JG, Farrall M, Ferrannini E, Ferrières J, Forouhi NG, Forrester T, Franco OH, Gansevoort RT, Gieger C, Gudnason V, Haiman CA, Harris TB, Hattersley AT, Heliövaara M, Hicks AA, Hingorani AD, Hoffmann W, Hofman A, Homuth G, Humphries SE, Hyppönen E, Illig T, Jarvelin MR, Johansen B, Jousilahti P, Jula AM, Kaprio J, Kee F, Keinanen-Kiukaanniemi SM, Kooner JS, Kooperberg C, Kovacs P, Kraja AT, Kumari M, Kuulasmaa K, Kuusisto J, Lakka TA, Langenberg C, Le Marchand L, Lehtimäki T, Lyssenko V, Männistö S, Marette A, Matise TC, McKenzie CA, McKnight B, Musk AW, Möhlenkamp S, Morris AD, Nelis M, Ohlsson C, Oldehinkel AJ, Ong KK, Palmer LJ, Penninx BW, Peters A, Pramstaller PP, Raitakari OT, Rankinen T, Rao DC, Rice TK, Ridker PM, Ritchie MD, Rudan I, Salomaa V, Samani NJ, Saramies J, Sarzynski MA, Schwarz PE, Shuldiner AR, Staessen JA, Steinthorsdottir V, Stolk RP, Strauch K, Tönjes A, Tremblay A, Tremoli E, Vohl MC, Völker U, Vollenweider P, Wilson JF, Witteman JC, Adair LS, Bochud M, Boehm BO, Bornstein SR, Bouchard C, Cauchi S, Caulfield MJ, Chambers JC, Chasman DI, Cooper RS, Dedoussis G, Ferrucci L, Froguel P, Grabe HJ, Hamsten A, Hui J, Hveem K, Jöckel KH, Kivimaki M, Kuh D, Laakso M, Liu Y, März W, Munroe PB, Njølstad I, Oostra BA, Palmer CN, Pedersen NL, Perola M, Pérusse L, Peters U, Power C, Quertermous T, Rauramaa R, Rivadeneira F, Saaristo TE, Saleheen D, Sinisalo J, Slagboom PE, Snieder H, Spector TD, Thorsteinsdottir U, Stumvoll M, Tuomilehto J,

Uitterlinden AG, Uusitupa M, van der Harst P, Veronesi G, Walker M, Wareham NJ, Watkins H, Wichmann HE, Abecasis GR, Assimes TL, Berndt SI, Boehnke M, Borecki IB, Deloukas P, Franke L, Frayling TM, Groop LC, Hunter DJ, Kaplan RC, O'Connell JR, Qi L, Schlessinger D, Strachan DP, Stefansson K, van Duijn CM, Willer CJ, Visscher PM, Yang J, Hirschhorn JN, Zillikens MC, McCarthy MI, Speliotes EK, North KE, Fox CS, Barroso I, Franks PW, Ingelsson E, Heid IM, Loos RJ, Cupples LA, Morris AP, Lindgren CM, Mohlke KL: New genetic loci link adipose and insulin biology to body fat distribution. *Nature,* 518**:** 187-196, 2015.

38. Richards JB, Waterworth D, O'Rahilly S, Hivert M-F, Loos RJF, Perry JRB, Tanaka T, Timpson NJ, Semple RK, Soranzo N, Song K, Rocha N, Grundberg E, Dupuis J, Florez JC, Langenberg C, Prokopenko I, Saxena R, Sladek R, Aulchenko Y, Evans D, Waeber G, Erdmann J, Burnett M-S, Sattar N, Devaney J, Willenborg C, Hingorani A, Witteman JCM, Vollenweider P, Glaser B, Hengstenberg C, Ferrucci L, Melzer D, Stark K, Deanfield J, Winogradow J, Grassl M, Hall AS, Egan JM, Thompson JR, Ricketts SL, König IR, Reinhard W, Grundy S, Wichmann H-E, Barter P, Mahley R, Kesaniemi YA, Rader DJ, Reilly MP, Epstein SE, Stewart AFR, Van Duijn CM, Schunkert H, Burling K, Deloukas P, Pastinen T, Samani NJ, McPherson R, Smith GD, Frayling TM, Wareham NJ, Meigs JB, Mooser V, Spector TD, GIANT Consortium: A genome-wide association study reveals variants in ARL15 that influence adiponectin levels. *Plos Genet* 5**:** e1000768, 2009.

39. Global Lipid Genetics Consortium, Willer CJ, Schmidt EM, Sengupta S, Peloso GM, Gustafsson S, Kanoni S, Ganna A, Chen J, Buchkovich ML, Mora S, Beckmann JS, Bragg-Gresham JL, Chang HY, Demirkan A, Den Hertog HM, Do R, Donnelly LA, Ehret GB, Esko T, Feitosa MF, Ferreira T, Fischer K, Fontanillas P, Fraser RM, Freitag DF, Gurdasani D, Heikkilä K, Hyppönen E, Isaacs A, Jackson AU, Johansson

A, Johnson T, Kaakinen M, Kettunen J, Kleber ME, Li X, Luan J, Lyytikäinen LP, Magnusson PK, Mangino M, Mihailov E, Montasser ME, Müller-Nurasyid M, Nolte IM, O'Connell JR, Palmer CD, Perola M, Petersen AK, Sanna S, Saxena R, Service SK, Shah S, Shungin D, Sidore C, Song C, Strawbridge RJ, Surakka I, Tanaka T, Teslovich TM, Thorleifsson G, Van den Herik EG, Voight BF, Volcik KA, Waite LL, Wong A, Wu Y, Zhang W, Absher D, Asiki G, Barroso I, Been LF, Bolton JL, Bonnycastle LL, Brambilla P, Burnett MS, Cesana G, Dimitriou M, Doney AS, Döring A, Elliott P, Epstein SE, Eyjolfsson GI, Gigante B, Goodarzi MO, Grallert H, Gravito ML, Groves CJ, Hallmans G, Hartikainen AL, Hayward C, Hernandez D, Hicks AA, Holm H, Hung YJ, Illig T, Jones MR, Kaleebu P, Kastelein JJ, Khaw KT, Kim E, Klopp N, Komulainen P, Kumari M, Langenberg C, Lehtimäki T, Lin SY, Lindström J, Loos RJ, Mach F, McArdle WL, Meisinger C, Mitchell BD, Müller G, Nagaraja R, Narisu N, Nieminen TV, Nsubuga RN, Olafsson I, Ong KK, Palotie A, Papamarkou T, Pomilla C, Pouta A, Rader DJ, Reilly MP, Ridker PM, Rivadeneira F, Rudan I, Ruokonen A, Samani N, Scharnagl H, Seeley J, Silander K, Stancáková A, Stirrups K, Swift AJ, Tiret L, Uitterlinden AG, van Pelt LJ, Vedantam S, Wainwright N, Wijmenga C, Wild SH, Willemsen G, Wilsgaard T, Wilson JF, Young EH, Zhao JH, Adair LS, Arveiler D, Assimes TL, Bandinelli S, Bennett F, Bochud M, Boehm BO, Boomsma DI, Borecki IB, Bornstein SR, Bovet P, Burnier M, Campbell H, Chakravarti A, Chambers JC, Chen YD, Collins FS, Cooper RS, Danesh J, Dedoussis G, de Faire U, Feranil AB, Ferrières J, Ferrucci L, Freimer NB, Gieger C, Groop LC, Gudnason V, Gyllensten U, Hamsten A, Harris TB, Hingorani A, Hirschhorn JN, Hofman A, Hovingh GK, Hsiung CA, Humphries SE, Hunt SC, Hveem K, Iribarren C, Järvelin MR, Jula A, Kähönen M, Kaprio J, Kesäniemi A, Kivimaki M, Kooner JS, Koudstaal PJ, Krauss RM, Kuh D, Kuusisto J, Kyvik KO, Laakso M, Lakka TA, Lind

L, Lindgren CM, Martin NG, März W, McCarthy MI, McKenzie CA, Meneton P, Metspalu A, Moilanen L, Morris AD, Munroe PB, Njølstad I, Pedersen NL, Power C, Pramstaller PP, Price JF, Psaty BM, Quertermous T, Rauramaa R, Saleheen D, Salomaa V, Sanghera DK, Saramies J, Schwarz PE, Sheu WH, Shuldiner AR, Siegbahn A, Spector TD, Stefansson K, Strachan DP, Tayo BO, Tremoli E, Tuomilehto J, Uusitupa M, van Duijn CM, Vollenweider P, Wallentin L, Wareham NJ, Whitfield JB, Wolffenbuttel BH, Ordovas JM, Boerwinkle E, Palmer CN, Thorsteinsdottir U, Chasman DI, Rotter JI, Franks PW, Ripatti S, Cupples LA, Sandhu MS, Rich SS, Boehnke M, Deloukas P, Kathiresan S, Mohlke KL, Ingelsson E, Abecasis GR: Discovery and refinement of loci associated with lipid levels. *Nat Genet* 45**:** 1274-1283, 2013.

40. DIAbetes Genetics Replication And Meta-analysis (DIAGRAM) Consortium, Asian Genetic Epidemiology Network Type 2 Diabetes (AGEN-T2D) Consortium, South Asian Type 2 Diabetes (SAT2D) Consortium, Mexican American Type 2 Diabetes (MAT2D) Consortium, Type 2 Diabetes Genetic Exploration by Nex-generation sequencing in muylti-Ethnic Samples (T2D-GENES) Consortium, Mahajan A, Go MJ, Zhang W, Below JE, Gaulton KJ, Ferreira T, Horikoshi M, Johnson AD, Ng MC, Prokopenko I, Saleheen D, Wang X, Zeggini E, Abecasis GR, Adair LS, Almgren P, Atalay M, Aung T, Baldassarre D, Balkau B, Bao Y, Barnett AH, Barroso I, Basit A, Been LF, Beilby J, Bell GI, Benediktsson R, Bergman RN, Boehm BO, Boerwinkle E, Bonnycastle LL, Burtt N, Cai Q, Campbell H, Carey J, Cauchi S, Caulfield M, Chan JC, Chang LC, Chang TJ, Chang YC, Charpentier G, Chen CH, Chen H, Chen YT, Chia KS, Chidambaram M, Chines PS, Cho NH, Cho YM, Chuang LM, Collins FS, Cornelis MC, Couper DJ, Crenshaw AT, van Dam RM, Danesh J, Das D, de Faire U, Dedoussis G, Deloukas P, Dimas AS, Dina C, Doney

AS, Donnelly PJ, Dorkhan M, van Duijn C, Dupuis J, Edkins S, Elliott P, Emilsson V, Erbel R, Eriksson JG, Escobedo J, Esko T, Eury E, Florez JC, Fontanillas P, Forouhi NG, Forsen T, Fox C, Fraser RM, Frayling TM, Froguel P, Frossard P, Gao Y, Gertow K, Gieger C, Gigante B, Grallert H, Grant GB, Grrop LC, Groves CJ, Grundberg E, Guiducci C, Hamsten A, Han BG, Hara K, Hassanali N, Hattersley AT, Hayward C, Hedman AK, Herder C, Hofman A, Holmen OL, Hovingh K, Hreidarsson AB, Hu C, Hu FB, Hui J, Humphries SE, Hunt SE, Hunter DJ, Hveem K, Hydrie ZI, Ikegami H, Illig T, Ingelsson E, Islam M, Isomaa B, Jackson AU, Jafar T, James A, Jia W, Jöckel KH, Jonsson A, Jowett JB, Kadowaki T, Kang HM, Kanoni S, Kao WH, Kathiresan S, Kato N, Katulanda P, Keinanen-Kiukaanniemi KM, Kelly AM, Khan H, Khaw KT, Khor CC, Kim HL, Kim S, Kim YJ, Kinnunen L, Klopp N, Kong A, Korpi-Hyövälti E, Kowlessur S, Kraft P, Kravic J, Kristensen MM, Krithika S, Kumar A, Kumate J, Kuusisto J, Kwak SH, Laakso M, Lagou V, Lakka TA, Langenberg C, Langford C, Lawrence R, Leander K, Lee JM, Lee NR, Li M, Li X, Li Y, Liang J, Liju S, Lim WY, Lind L, Lindgren CM, Lindholm E, Liu CT, Liu JJ, Lobbens S, Long J, Loos RJ, Lu W, Luan J, Lyssenko V, Ma RC, Maeda S, Mägi R, Männisto S, Matthews DR, Meigs JB, Melander O, Metspalu A, Meyer J, Mirza G, Mihailov E, Moebus S, Mohan V, Mohlke KL, Morris AD, Mühleisen TW, Müller-Nurasyid M, Musk B, Nakamura J, Nakashima E, Navarro P, Ng PK, Nica AC, Nilsson PM, Njølstad I, Nöthen MM, Ohnaka K, Ong TH, Owen KR, Palmer CN, Pankow JS, Park KS, Parkin M, Pechlivanis S, Pedersen NL, Peltonen L, Perry JR, Peters A, Pinidiyapathirage JM, Platou CG, Potter S, Price JF, Qi L, Radha V, Rallidis L, Rasheed A, Rathman W, Rauramaa R, Raychaudhuri S, Rayner NW, Rees SD, Rehnberg E, Ripatti S, Robertson N, Roden M, Rossin EJ, Rudan I, Rybin D, Saaristo TE, Salomaa V, Saltevo J, Samuel M, Sanghera DK, Saramies J, Scott J,

Scott LJ, Scott RA, Segrè AV, Sehmi J, Sennblad B, Shah N, Shah S, Shera AS, Shu XO, Shuldiner AR, Sigurđsson G, Sijbrands E, Silveira A, Sim X, Sivapalaratnam S, Small KS, So WY, Stančáková A, Stefansson K, Steinbach G, Steinthorsdottir V, Stirrups K, Strawbridge RJ, Stringham HM, Sun Q, Suo C, Syvänen AC, Takayanagi R, Takeuchi F, Tay WT, Teslovich TM, Thorand B, Thorleifsson G, Thorsteinsdottir U, Tikkanen E, Trakalo J, Tremoli E, Trip MD, Tsai FJ, Tuomi T, Tuomilehto J, Uitterlinden AG, Valladares-Salgado A, Vedantam S, Veglia F, Voight BF, Wang C, Wareham NJ, Wennauer R, Wickremasinghe AR, Wilsgaard T, Wilson JF, Wiltshire S, Winckler W, Wong TY, Wood AR, Wu JY, Wu Y, Yamamoto K, Yamauchi T, Yang M, Yengo L, Yokota M, Young R, Zabaneh D, Zhang F, Zhang R, Zheng W, Zimmet PZ, Altshuler D, Bowden DW, Cho YS, Cox NJ, Cruz M, Hanis CL, Kooner J, Lee JY, Seielstad M, Teo YY, Boehnke M, Parra EJ, Chambers JC, Tai ES, McCarthy MI, Morris AP: Genome-wide trans-ancestry meta-analysis provides insight into the genetic architecture of type 2 diabetes susceptibility. *Nat Genet* 46**:** 234-244, 2014.

41. Scott RA, Lagou V, Welch RP, Wheeler E, Montasser ME, Luan J, Mägi R, Strawbridge RJ, Rehnberg E, Gustafsson S, Kanoni S, Rasmussen-Torvik LJ, Yengo L, Lecoeur C, Shungin D, Sanna S, Sidore C, Johnson PC, Jukema JW, Johnson T, Mahajan A, Verweij N, Thorleifsson G, Hottenga JJ, Shah S, Smith AV, Sennblad B, Gieger C, Salo P, Perola M, Timpson NJ, Evans DM, Pourcain BS, Wu Y, Andrews JS, Hui J, Bielak LF, Zhao W, Horikoshi M, Navarro P, Isaacs A, O'Connell JR, Stirrups K, Vitart V, Hayward C, Esko T, Mihailov E, Fraser RM, Fall T, Voight BF, Raychaudhuri S, Chen H, Lindgren CM, Morris AP, Rayner NW, Robertson N, Rybin D, Liu CT, Beckmann JS, Willems SM, Chines PS, Jackson AU, Kang HM, Stringham HM, Song K, Tanaka T, Peden JF, Goel A, Hicks AA, An P, Müller-

Nurasyid M, Franco-Cereceda A, Folkersen L, Marullo L, Jansen H, Oldehinkel AJ, Bruinenberg M, Pankow JS, North KE, Forouhi NG, Loos RJ, Edkins S, Varga TV, Hallmans G, Oksa H, Antonella M, Nagaraja R, Trompet S, Ford I, Bakker SJ, Kong A, Kumari M, Gigante B, Herder C, Munroe PB, Caulfield M, Antti J, Mangino M, Small K, Miljkovic I, Liu Y, Atalay M, Kiess W, James AL, Rivadeneira F, Uitterlinden AG, Palmer CN, Doney AS, Willemsen G, Smit JH, Campbell S, Polasek O, Bonnycastle LL, Hercberg S, Dimitriou M, Bolton JL, Fowkes GR, Kovacs P, Lindström J, Zemunik T, Bandinelli S, Wild SH, Basart HV, Rathmann W, Grallert H, DIAbetes Genetics Replication and Meta-analysis (DIAGRAM) Consortium, Maerz W, Kleber ME, Boehm BO, Peters A, Pramstaller PP, Province MA, Borecki IB, Hastie ND, Rudan I, Campbell H, Watkins H, Farrall M, Stumvoll M, Ferrucci L, Waterworth DM, Bergman RN, Collins FS, Tuomilehto J, Watanabe RM, de Geus EJ, Penninx BW, Hofman A, Oostra BA, Psaty BM, Vollenweider P, Wilson JF, Wright AF, Hovingh GK, Metspalu A, Uusitupa M, Magnusson PK, Kyvik KO, Kaprio J, Price JF, Dedoussis GV, Deloukas P, Meneton P, Lind L, Boehnke M, Shuldiner AR, van Duijn CM, Morris AD, Toenjes A, Peyser PA, Beilby JP, Körner A, Kuusisto J, Laakso M, Bornstein SR, Schwarz PE, Lakka TA, Rauramaa R, Adair LS, Smith GD, Spector TD, Illig T, de Faire U, Hamsten A, Gudnason V, Kivimaki M, Hingorani A, Keinanen-Kiukaanniemi SM, Saaristo TE, Boomsma DI, Stefansson K, van der Harst P, Dupuis J, Pedersen NL, Sattar N, Harris TB, Cucca F, Ripatti S, Salomaa V, Mohlke KL, Balkau B, Froguel P, Pouta A, Jarvelin MR, Wareham NJ, Bouatia-Naji N, McCarthy MI, Franks PW, Meigs JB, Teslovich TM, Florez JC, Langenberg C, Ingelsson E, Prokopenko I, Barroso I: Large-scale association analyses identify new loci influencing glycemic traits and provide insight into the underlying biological pathways. *Nat Genet* 44**:** 991-1005, 2012.

42. Swaminathan R: Magnesium metabolism and its disorders. *Clin Biochem Rev* 24**:** 47-66, 2003.

43. Teslovich TM, Musunuru K, Smith AV, Edmondson AC, Stylianou IM, Koseki M, Pirruccello JP, Ripatti S, Chasman DI, Willer CJ, Johansen CT, Fouchier SW, Isaacs A, Peloso GM, Barbalic M, Ricketts SL, Bis JC, Aulchenko YS, Thorleifsson G, Feitosa MF, Chambers J, Orho-Melander M, Melander O, Johnson T, Li X, Guo X, Li M, Shin Cho Y, Jin Go M, Jin Kim Y, Lee JY, Park T, Kim K, Sim X, Twee-Hee Ong R, Croteau-Chonka DC, Lange LA, Smith JD, Song K, Hua Zhao J, Yuan X, Luan J, Lamina C, Ziegler A, Zhang W, Zee RY, Wright AF, Witteman JC, Wilson JF, Willemsen G, Wichmann HE, Whitfield JB, Waterworth DM, Wareham NJ, Waeber G, Vollenweider P, Voight BF, Vitart V, Uitterlinden AG, Uda M, Tuomilehto J, Thompson JR, Tanaka T, Surakka I, Stringham HM, Spector TD, Soranzo N, Smit JH, Sinisalo J, Silander K, Sijbrands EJ, Scuteri A, Scott J, Schlessinger D, Sanna S, Salomaa V, Saharinen J, Sabatti C, Ruokonen A, Rudan I, Rose LM, Roberts R, Rieder M, Psaty BM, Pramstaller PP, Pichler I, Perola M, Penninx BW, Pedersen NL, Pattaro C, Parker AN, Pare G, Oostra BA, O'Donnell CJ, Nieminen MS, Nickerson DA, Montgomery GW, Meitinger T, McPherson R, McCarthy MI, McArdle W, Masson D, Martin NG, Marroni F, Mangino M, Magnusson PK, Lucas G, Luben R, Loos RJ, Lokki ML, Lettre G, Langenberg C, Launer LJ, Lakatta EG, Laaksonen R, Kyvik KO, Kronenberg F, König IR, Khaw KT, Kaprio J, Kaplan LM, Johansson A, Jarvelin MR, Janssens AC, Ingelsson E, Igl W, Kees Hovingh G, Hottenga JJ, Hofman A, Hicks AA, Hengstenberg C, Heid IM, Hayward C, Havulinna AS, Hastie ND, Harris TB, Haritunians T, Hall AS, Gyllensten U, Guiducci C, Groop LC, Gonzalez E, Gieger C, Freimer NB, Ferrucci L, Erdmann J, Elliott P, Ejebe KG, Döring A, Dominiczak AF, Demissie S, Deloukas P, de Geus EJ, de Faire U,

Crawford G, Collins FS, Chen YD, Caulfield MJ, Campbell H, Burtt NP, Bonnycastle LL, Boomsma DI, Boekholdt SM, Bergman RN, Barroso I, Bandinelli S, Ballantyne CM, Assimes TL, Quertermous T, Altshuler D, Seielstad M, Wong TY, Tai ES, Feranil AB, Kuzawa CW, Adair LS, Taylor HA Jr, Borecki IB, Gabriel SB, Wilson JG, Holm H, Thorsteinsdottir U, Gudnason V, Krauss RM, Mohlke KL, Ordovas JM, Munroe PB, Kooner JS, Tall AR, Hegele RA, Kastelein JJ, Schadt EE, Rotter JI, Boerwinkle E, Strachan DP, Mooser V, Stefansson K, Reilly MP, Samani NJ, Schunkert H, Cupples LA, Sandhu MS, Ridker PM, Rader DJ, van Duijn CM, Peltonen L, Abecasis GR, Boehnke M, Kathiresan S: Biological, clinical and population relevance of 95 loci for blood lipids. *Nature* 466**:** 707-713, 2010.

44. Gillingham AK, Munro S: The small G proteins of the Arf family and their regulators. *Annu Rev Cell Dev Biol* 23**:** 579-611, 2007.

45. Arjona FJ, Chen Y-X, Flik G, Bindels RJM, Hoenderop JGJ: Tissue-specific expression and in vivo regulation of zebrafish orthologues of mammalian genes related to symptomatic hypomagnesemia. *Pflügers Arch* 465**:** 1409-1421, 2013.

46. Bijvelds MJC, Van der Velden JA, Kolar ZI, Flik G: Magnesium transport in freshwater teleosts. *J Exp Biol* 201**:** 1981-1990, 1998.

47. Kersten S, Arjona FJ: Ion transport in the zebrafish kidney from a human disease angle: possibilities, considerations, and future perspectives. *Am J Physiol Renal Physiol* 312**:** F172-F189, 2017.

48. Miyares RL, de Rezende VB, Farber SA: Zebrafish yolk lipid processing: a tractable tool for the study of vertebrate lipid transport and metabolism. *Dis Model Mech* 7**:** 915-927, 2014.

49. Liu Q, Dalman M, Chen Y, Akhter M, Brahmandam S, Patel Y, Lowe J, Thakkar M, Gregory A-V, Phelps D, Riley C, Londraville RL: Knockdown of leptin A expression

dramatically alters zebrafish development. *Gen Comp Endocrinol* 178**:** 562-572, 2012.

50. Boitard S, Boussaha M, Capitan A, Rocha D, Servin B: Uncovering adaptation from sequence data: lessons from genome resequencing of four cattle breeds. *Genetics* 203**:** 433-450, 2016.

51. Fang X, Wang K, Han D, He X, Wei J, Zhao L, Imam MU, Ping Z, Li Y, Xu Y, Min J, Wang F: Dietary magnesium intake and the risk of cardiovascular disease, type 2 diabetes, and all-cause mortality: a dose-response meta-analysis of prospective cohort studies. *BMC Med* 14**:** 210, 2016.

52. Sarrafzadegan N, Khosravi-Boroujeni H, Lotfizadeh M, Pourmogaddas A, Salehi-Abargouei A: Magnesium status and the metabolic syndrome: A systematic review and meta-analysis. *Nutrition,* 32**:** 409-417, 2016.

53. Simental-Mendía LE, Sahebkar A, Rodríguez-Morán M, Guerrero-Romero F: A systematic review and meta-analysis of randomized controlled trials on the effects of magnesium supplementation on insulin sensitivity and glucose control. *Pharmacol Res* 111**:** 272-282, 2016.

54. Joosten MM, Gansevoort RT, Mukamal KJ, van der Harst P, Geleijnse JM, Feskens EJ, Navis G, Bakker SJ, PREVEND Study Group: Urinary and plasma magnesium and risk of ischemic heart disease. *Am J Clin Nutr* 97**:** 1299-1306, 2013.

55. Florez JC, Jablonski KA, Bayley N, Pollin TI, de Bakker PI, Shuldiner AR, Knowler WC, Nathan DM, Altshuler D, Diabetes Prevention Program Research Group: TCF7L2 polymorphisms and progression to diabetes in the Diabetes Prevention Program. *N Engl J Med* 355**:** 241-250, 2006.

56. Willer CJ, Li Y, Abecasis GR: METAL: fast and efficient meta-analysis of genomewide association scans. *Bioinformatics* 26**:** 2190-2191, 2010.

57. Ponte B, Pruijm M, Ackermann D, Vuistiner P, Guessous I, Ehret G, Alwan H, Youhanna S, Paccaud F, Mohaupt M, Péchère-Bertschi A, Vogt B, Burnier M, Martin PY, Devuyst O, Bochud M: Copeptin is associated with kidney length, renal function, and prevalence of simple cysts in a population-based study. *J Am Soc Nephrol* 26**:** 1415-1425, 2015.

58. Segrè AV, DIAGRAM Consortium, MAGIC Investigators, Groop L, Mootha VK, Daly MJ, Altshuler D: Common inherited variation in mitochondrial genes is not enriched for associations with type 2 diabetes or related glycemic traits. *PloS Genet* 6**:** e1001058, 2010.

59. Rueedi R, Ledda M, Nicholls AW, Salek RM, Marques-Vidal P, Morya E, Sameshima K, Montoliu I, Da Silva L, Collino S, Martin FP, Rezzi S, Steinbeck C, Waterworth DM, Waeber G, Vollenweider P, Beckmann JS, Le Coutre J, Mooser V, Bergmann S, Genick UK, Kutalik Z: Genome-wide association study of metabolic traits reveals novel gene-metabolite-disease links. *PLoS Genet* 10**:** e1004132, 2014.

60. Wang K, Li M, Hadley D, Liu R, Glessner J, Grant SF, Hakonarson H, Bucan M: PennCNV: an integrated hidden Markov model designed for high-resolution copy number variation detection in whole-genome SNP genotyping data. *Genome Res* 11**:** 1665-1674, 2007.

61. Arjona, FJ, de Baaij, JHF, Schlingmann, KP, Lameris, ALL, van Wijk, E, Flik, G, Regele, S, Korenke, GC, Neophytou, B, Rust, S, Reintjes, N, Konrad, M, Bindels, RJM, Hoenderop, JGJ: CNNM2 mutations cause impaired brain development and seizures in patients with hypomagnesemia. *PLoS Genet* 10**:** e1004267, 2014.

Table 1: Summary statistics for the meta-analysis of uMg-to-creatinine ratio.

SNP	*Effect allele*	*Other allele*	*Mean effect allele frequency*	*Effect size discovery (SE)*	*p-value discovery*	*Effect size replication (SE)*	*p-value replication*	*Effect size Combined analysis (SE)*	*p-value combined analysis*	*Direction of effects of individual cohorts*	*I^2*
rs35929	*a*	*g*	*0.21*	*-0.112 (-0.025)*	5.57×10^{-6}	*-0.135 (-0.027)*	5.95×10^{-7}	*-0.1227 (-0.183)*	2.11×10^{-11}	-----+-	*35.7*
rs3824347	*g*	*a*	*0.41*	*-0.109 (-0.02)*	3.61×10^{-8}	*-0.1125 (-0.024)*	2.02×10^{-6}	*-0.1103 (-0.152)*	4.38×10^{-13}	+++++++	*7*

The effect size sign for each individual cohort on the last but one column is represented by the sign – or +. The cohort displaying a "-" for rs32929 is LBC1936, having anyhow an effect close to 0. The last column shows the I^2 value, representing the heterogeneity across cohorts.

LEGENDS TO FIGURES

Figure 1. Genome-wide meta-analysis results for uMg-to–creatinin Urinary Mg-to-creatinine ratio.

(**a**) Manhattan plot showing -log10(*P* values) for all SNPs in the genome-wide meta-analysis for normalized uMg-to-creatinine ratio in Europeans (n = 9,099), ordered by chromosomal position. The values correspond to the association of normalized uMg-to-creatinine ratio, including age and sex as covariates in the model as well as study-specific covariates if needed. The gene closest to the SNP with the lowest *P* value is listed at each locus. Two loci reached genome-wide significance ($P < 5\times10^{-8}$) at combined analysis (*TRPM6*, rs3824347 and *ARL15,* rs35929). (**b**) Forest plot for rs35929 (*ARL15*) and rs3824347 (*TRPM6*) showing effect sizes and 95% confidence intervals across studies as well as the summary meta-analysis results. (**c**) Regional association plot at the rs3824347 (*TRPM6)* locus. Regional association plot showing -log10 *P* values for the association of SNPs at the locus of interest ordered by their chromosomal position with normalized uMg-to-creatinine ratio. The -log10 *P* value for each SNP is colored according to the correlation of the corresponding SNP with the SNP showing the lowest *P* value (index SNP) within the locus using different colors for selected levels of linkage disequilibrium (r2). Correlation structures correspond to HapMap 2 CEU. The blue line represents the recombination according to the scale shown on the right-side Y axis. (**d**) Regional association plot at the rs35929 (*ARL15*) locus. See Panel **b** legend.

Figure 2. External population-based validation using 24-h urine data.

(**a-d**) Associations of uMg excretion and fractional excretion with an unweighted genetic risk score including rs35929 (*ARL15* locus) and rs3824347 (*TRPM6* locus). Data are geometric

means and whiskers are 95% confidence intervals for Mg-related phenotypes in the CoLaus (panels **a**,**b**,**d**) and SKIPOGH (panel **c**) studies. The X axes represent the unweighted genetic score generated from rs35929 (*ARL15* locus) and rs3824347 (*TRPM6* locus), using as effect allele the one associated with lower uMg-to-creatinine ratio, i.e. the A allele for rs35929 and the G allele for rs3824347. *P* values are from non-parametric trend tests across genetic score. The numbers in each genetic score category are listed in all panels. The Y axis represents uMg-to-creatinine ratio (mg/g) (**a**), FEMg (%) (**b**), uMg excretion (mg/24h) (**c**) and serum Mg^{2+} (mg/dl) (**d**).

Figure 3. ARL15 localizes in renal DCT regulating TRPM6 channel activity.

(**a**) Gene expression analyses of *Trpm6, Arl15, Podocin, Sglt2, Snat3, Nkcc2, Ncc* and *Aqp2* in micro-dissected mouse nephron segments showed co-expression of *Arl15* and *Trpm6* in DCT. (**b**) Double immunofluorescence staining of mouse kidney cortex sections for ARL15 (in *green*) and BCRP (*red*); TH (*red*); NCC (*red*); or AQP2 (*red*) as markers of the PT, TAL, DCT or CD respectively. (**c**) Typical current-voltage curves obtained from transfected HEK293 cells 200 s after break-in. Outwardly-rectifying currents are observed in response to a 500 ms voltage ramp (from -100 to +100 mV) applied 200 s after break-in. (**d**) The average time development of the current density measured at +80 mV is shown ($n \geq 10$). The mock + ARL15 condition is not shown for clarity reasons. (**e**) WT ARL15 (red, WT, n = 47) but not the T46N ARL15 mutant (black, T46N, n = 18) increased the whole-cell current density of TRPM6. Asterisks indicate significant differences respect to the cells transfected with *TRPM6* only (blue, '-', n = 44). One-way ANOVA followed by Tukey's multiple comparisons post-test, $P < 0.05$. (**f**) Transfection of

HEK293 cells with WT *ARL15* did not evoke a significant increase in whole-cell current density when compared with mock-transfected of cells ($n \geq 10$, unpaired Student's *t*-test).

Figure 4. Physiological relevance of ARL15 in kidney.

(**a-b**) Knockdown of *arl15b* by 0.5-2 (**a**) and 2-8 (**b**) ng/embryo of the two *arl15b*-MOs used (exon skipping 3 and 4 *arl15b*-MOs) resulted in a dose-dependent decrease of the total Mg content of zebrafish *arl15b* morphants, reflecting renal Mg^{2+} wasting. The zero dose represents injection with control-MO (2 (**a**) and 8 (**b**) ng MO/embryo). (**c**) Morphological phenotypes distinguished in zebrafish larvae (5 days post-fertilization (dpf)) following treatment with *arl15b*-MO or control-MO. A complete description of each phenotype is detailed in the Supplementary Information. Metabolic defects (poor metabolization of the yolk) are indicated by arrows. (**d-g**) Distribution of morphological phenotypes in zebrafish larvae injected with 0.5-2 (**d, f**) and 2-8 (**e, g**) ng/embryo of exon skipping 3 (**d, e**), exon skipping 4 (**f, g**) *arl15b*-MO or control-MO (2 (**d, f**) and 8 (**e, g**) ng MO/embryo). (**h-k**) Rescue of renal Mg^{2+} wasting (**h, j**) and of metabolism defects (**i, k**) in morphant zebrafish by co-injection of exon skipping 3 *arl15b*-MO (0.5 ng MO/embryo, **h-i**) or exon skipping 4 *arl15b*-MO (8 ng MO/embryo, **j-k**) with cRNA encoding human WT ARL15 (50 pg cRNA/embryo). Co-injection with cRNA encoding human T46N ARL15 mutant (50 pg cRNA/embryo) did not rescue renal Mg^{2+} wasting or the defects in metabolism. (**d-g, i, k**) Numbers on top of the bars indicate the number of animals in each experiment. (**a-b, h, j**) Data are presented as mean ± SEM (n = 10, except for **b**, where n = 6-10). (**a-b, h, j**) Asterisks indicate significant differences respect to the control condition (One-way ANOVA followed by Tukey's multiple comparisons post-test, $P < 0.05$).

Figure 5. Effect modification of metabolic phenotypes on the association of uMg with the *ARL15* locus.

(**a**) Effect modification of fat mass on the association of uMg concentration with rs35929 (*ARL15*) genotypes. Data represent adjusted square-root transformed uMg levels by rs35929 genotypes and fat mass strata in CoLaus. The model was adjusted for age, sex, height, lean mass, CKD-EPI, urinary creatinine (square-root), serum Mg^{2+}, serum and urinary Ca^{2+} (square-root) and menopausal status. *P* interaction = 0.024. Fat mass strata are cut by sex-specific medians. n = 4,729. (**b**) Effect modification of fasting insulin on the association of uMg levels with rs35929 (*ARL15*) genotypes. Data represent adjusted square-root transformed uMg levels by rs35929 genotypes and fasting insulin strata in CoLaus. The model was adjusted for age, sex, height, lean mass, CKD-EPI, urinary creatinine (square-root), serum Mg^{2+}, serum and urinary Ca^{2+} (square-root) and menopausal status. *P* interaction = 0.012. Fat mass strata are cut by sex-specific medians (n = 4,729).

Figure 6. Multi-step approach used to investigate the genetic determinants of the renal handling of Mg^{2+} and their influence on metabolic traits in the general population.

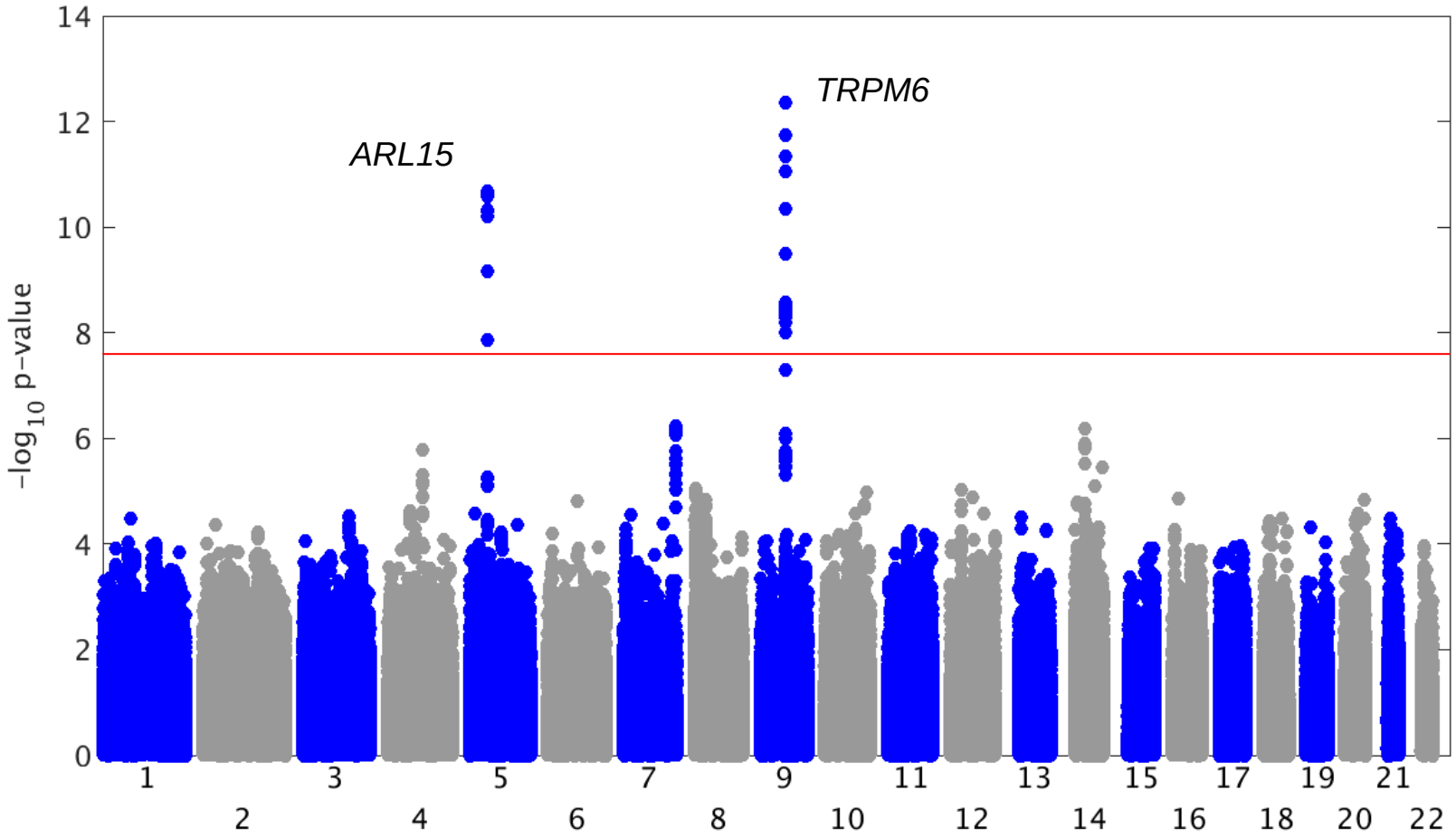
ARL15
TRPM6
−log10 p−value
0
2
4
6
8
10
12
14
1
2
3
4
5
6
7
8
9
10
11
12
13
14
15
16
17
18
19
20
21
22

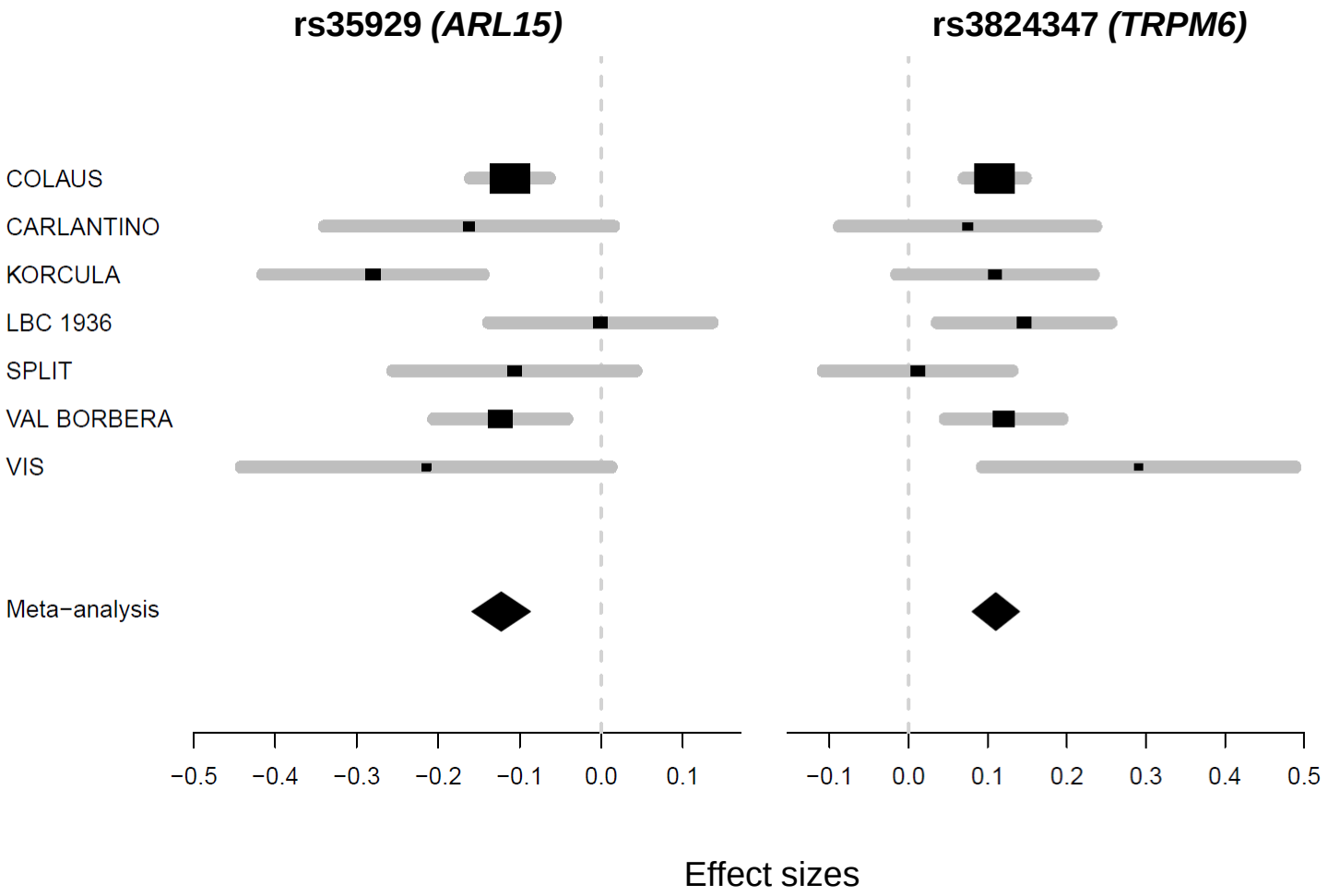
rs35929 (ARL15)
rs3824347 (TRPM6)
COLAUS
CARLANTINO
KORCULA
LBC 1936
SPLIT
VAL BORBERA
VIS
Meta−analysis
−0.5
−0.4
−0.3
−0.2
−0.1
0.0
0.1
−0.1
0.0
0.1
0.2
0.3
0.4
0.5
Effect sizes

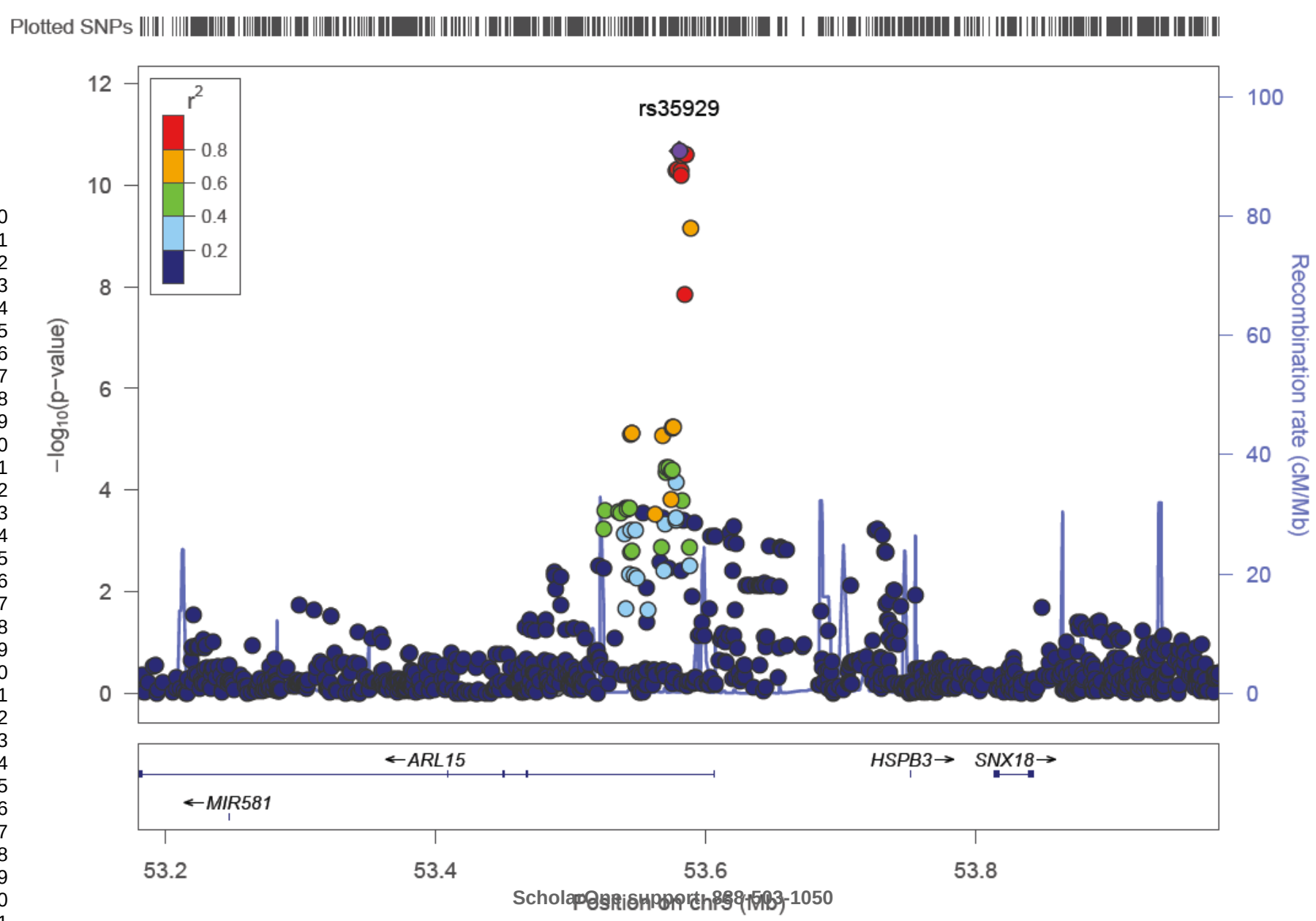

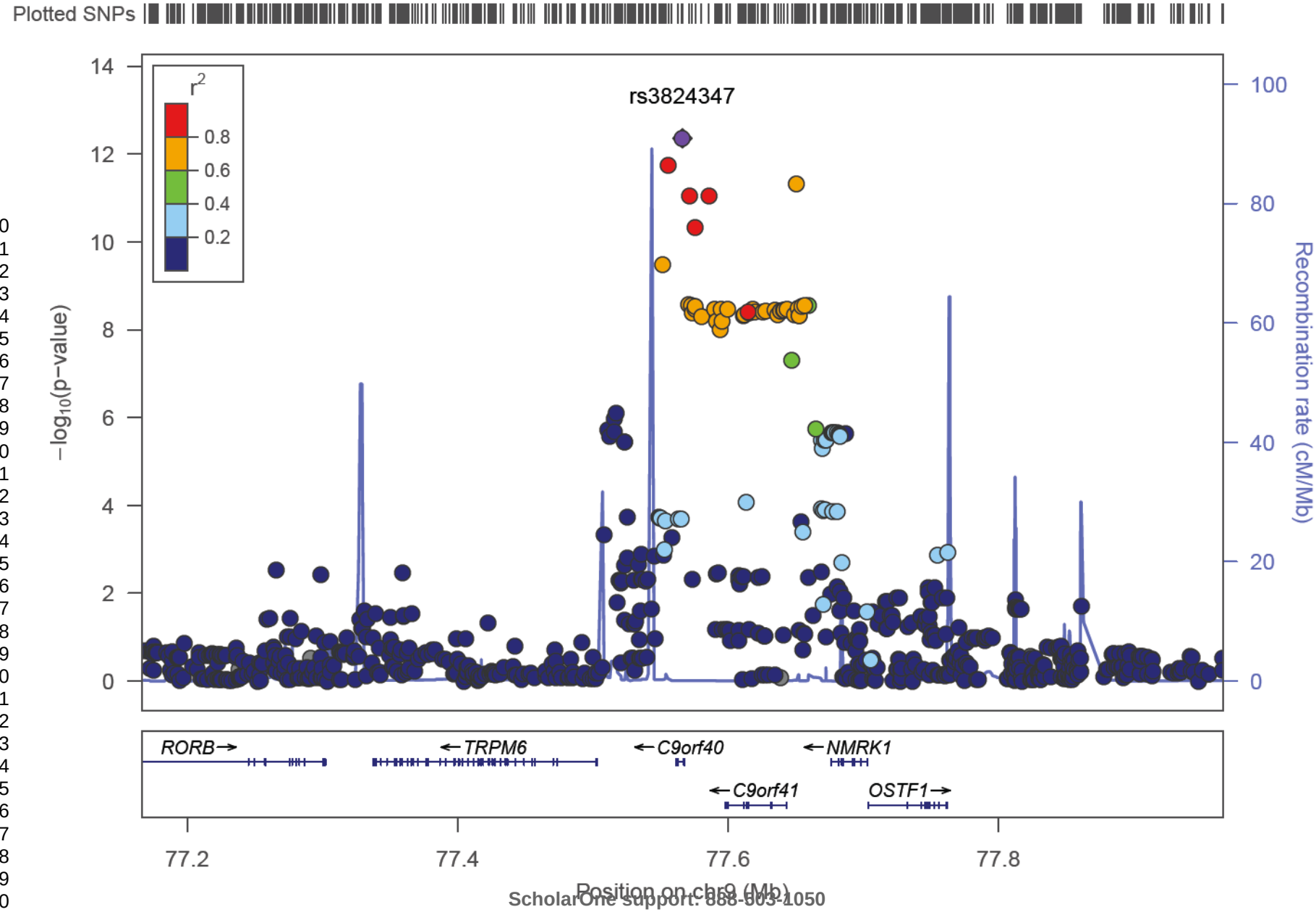

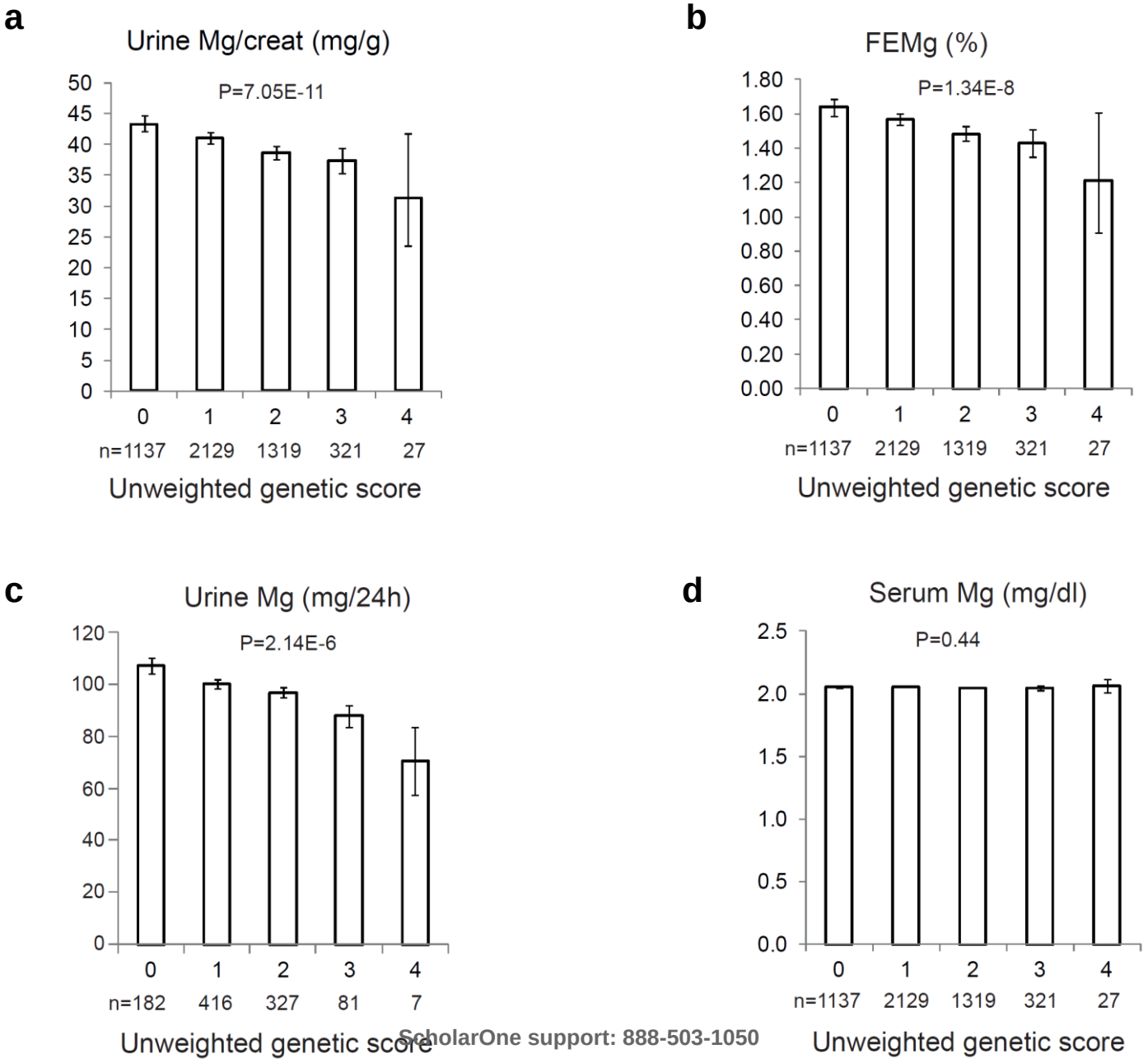

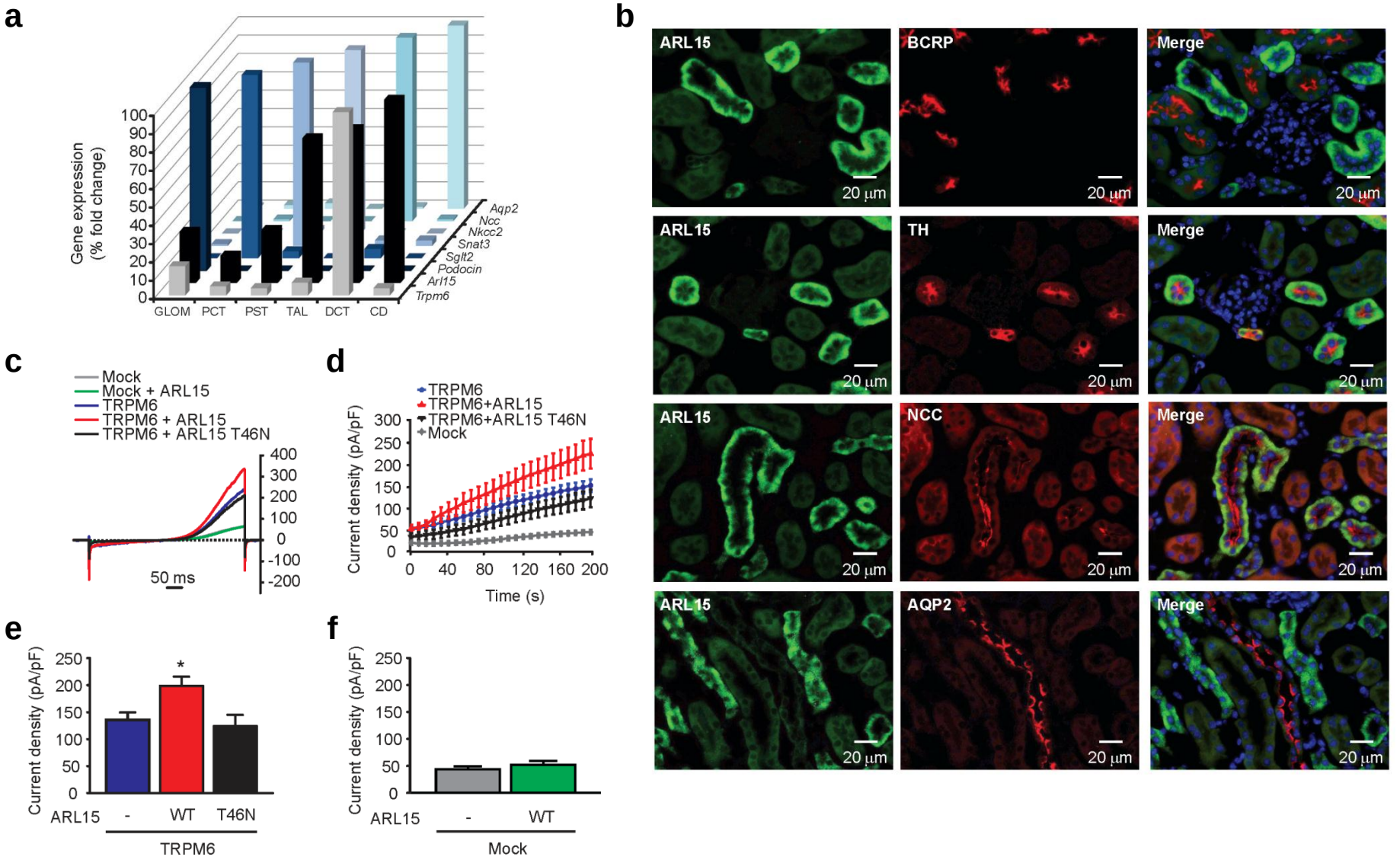
a
Gene expression (% fold change)
100
90
80
70
60
50
40
30
20
10
0
GLOM
PCT
PST
TAL
DCT
CD
Aqp2
Ncc
Nkcc2
Slnat3
Sglt2
Podocin
Arl15
Trpm6
b
ARL15
BCRP
Merge
TH
NCC
AQP2
20 μm
c
Mock
Mock + ARL15
TRPM6
TRPM6 + ARL15
TRPM6 + ARL15 T46N
400
300
200
100
0
-100
-200
50 ms
d
TRPM6
TRPM6+ARL15
TRPM6+ARL15 T46N
Mock
Current density (pA/pF)
300
250
200
150
100
50
0
0
40
80
120
160
200
Time (s)
e
Current density (pA/pF)
250
200
150
100
50
0
*
ARL15
-
WT
T46N
TRPM6
f
Current density (pA/pF)
250
200
150
100
50
0
ARL15
-
WT
Mock

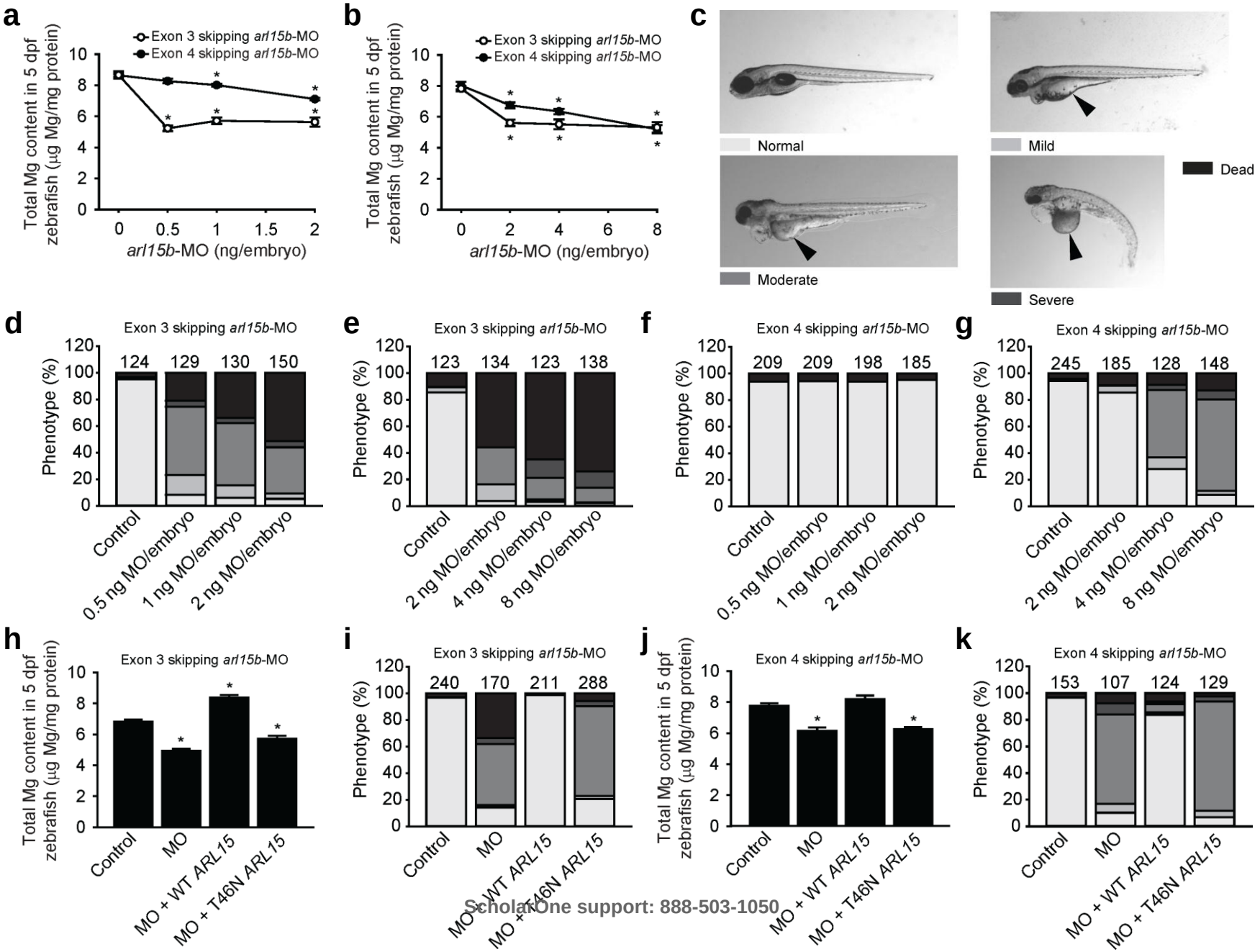

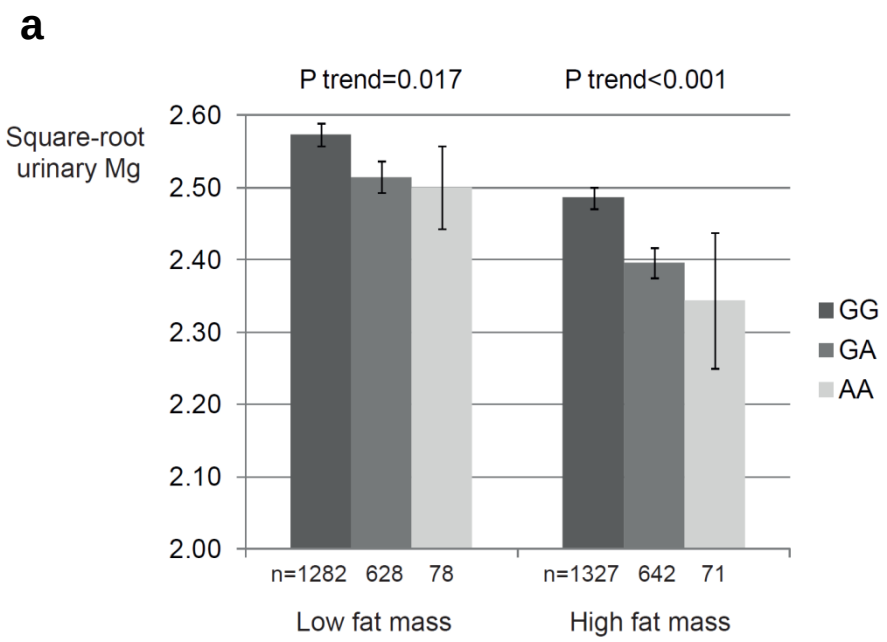
a
P trend=0.017
P trend<0.001
Square-root urinary Mg
2.60
2.50
2.40
2.30
2.20
2.10
2.00
n=1282 628 78
n=1327 642 71
Low fat mass
High fat mass
GG
GA
AA

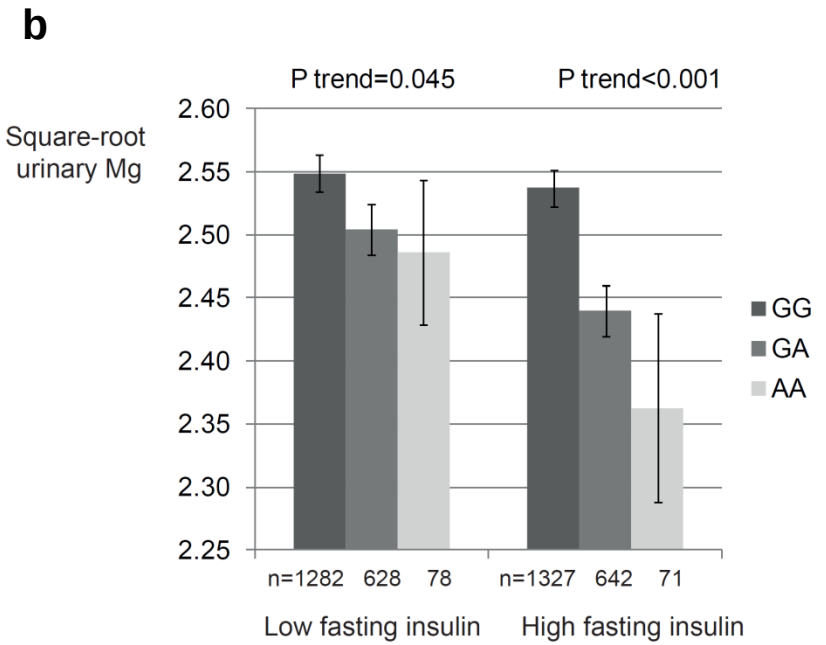
b
P trend=0.045
P trend<0.001
Square-root urinary Mg
2.60
2.55
2.50
2.45
2.40
2.35
2.30
2.25
n=1282 628 78
n=1327 642 71
Low fasting insulin
High fasting insulin
GG
GA
AA

Discovery GWAS: uMg-to-creat (CoLaus; N=5,150)
→ rs3824347 (chr 9, *TRPM6*)

Meta-GWAS: uMg-to-creat (CoLaus + LBC1936, LBC1936, CROATIA-Split, CROATIA-Vis, Carlantino, CROATIA-Korcula, Val Borbera; N=9,099)
→ rs3824347 (chr 9, *TRPM6*) + rs35929 (chr 5, *ARL15*)

Additive genetic risk score: rs3824347 + rs35929
→ uMg-to-creat and FEMg (CoLaus); uMg 24h (SKIPOGH)

Expression studies of ARL15 and TRPM6 in mouse kidney
→ mRNA (RT-qPCR) and protein (immunofluorescence)

Functional studies: Influence of ARL15 on channel activity of TRPM6
→ Patch-clamp recordings on HEK293 cells transfected with ARL15 and TRPM6

***In vivo* studies: Mouse** - Effects of magnesium diets (kidney, ileum, caecum)
→ Differential mRNA expression patterns (*Arl15*, *Trpm6*, other genes)

***In vivo* studies: Zebrafish**
→ Identification of ARL15 orthologs
→ Expression of *arl15b* in adult fish
→ Effect of magnesium diets on *arl15b* expression patterns (kidneys, gills, gut – adult fish)
→ Loss-of-function and rescue (larvae): Magnesium balance and metabolic phenotypes

Link genetic background (*ARL15* rs35929) with renal magnesium handling and metabolic traits
→ CoLaus: Association of uMg with metabolic traits
→ SKIPOGH: Association of 24h uMg with metabolic traits
→ CoLaus: Effect of body weight, BMI and fat mass on the association of rs35929 with uMg excretion
→ SKIPOGH: Effect of rs35929 on the association of uMg excretion with fasting insulin

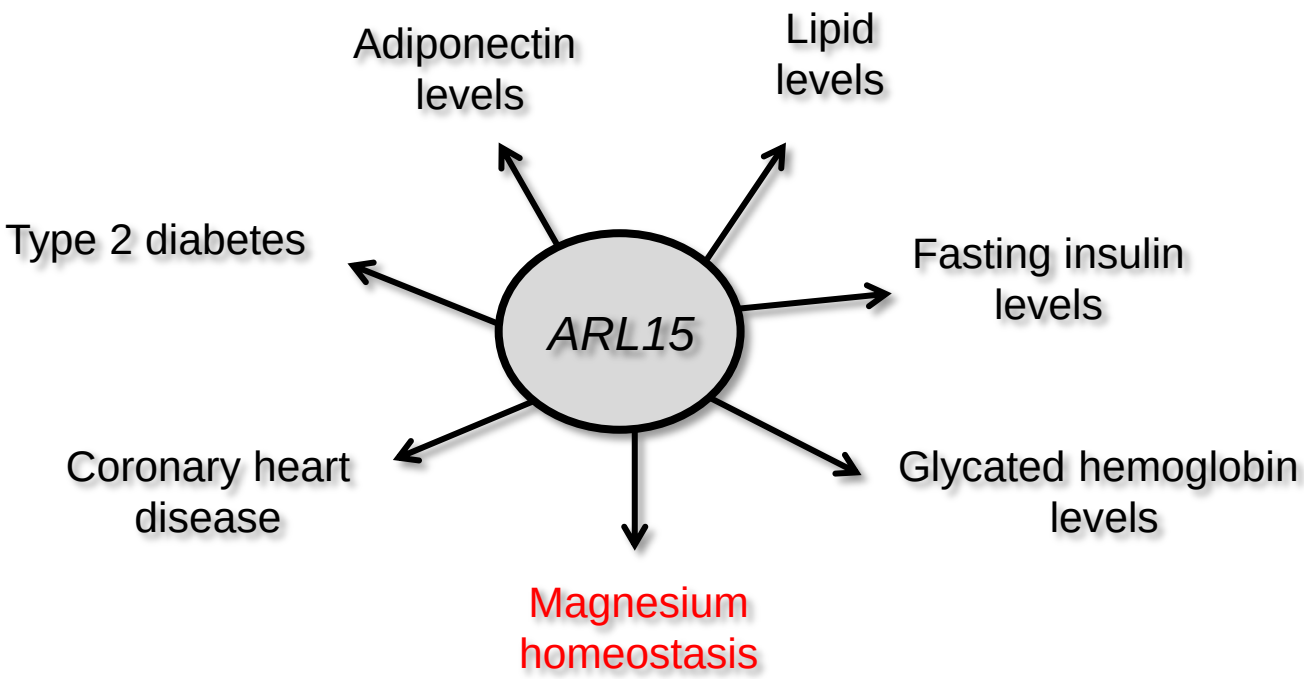
Adiponectin levels
Lipid levels
Type 2 diabetes
ARL15
Fasting insulin levels
Coronary heart disease
Glycated hemoglobin levels
Magnesium homeostasis

Supplementary Information

Genome-wide Meta-analysis Unravels Novel Interactions between Magnesium Homeostasis and Metabolic Phenotypes

Table of contents:

SUPPLEMENTARY METHODS

GWAS Cohorts

CoLaus is a population-based cohort with baseline examination conducted between 2003 and 2006. It includes 6,184 individuals of European descent aged 35-75 years randomly selected from the registry of the city of Lausanne [1]. The *CROATIA-Vis* study, Croatia, is a family-based, cross-sectional study in the isolated island of Vis that included 1,056 examinees aged 18-93. Blood samples were collected in 2003 and 2004 [2]. The *CROATIA-Korcula* study, Croatia, is a family-based, cross-sectional study in the isolated island of Korcula that included 965 examinees aged 18-95. Blood samples were collected in 2007 [3]. The *CROATIA-Split* study, Croatia, is population-based, cross-sectional study in the Dalmatian city of Split that so far includes 1,012 examinees aged 18-95. Blood samples were collected in 2009 -2011 [4]. The *Lothian Birth Cohort 1936* (LBC1936) consists of 1,091 relatively healthy older participants, most of whom took part in the Scottish Mental Survey of 1947 at the age of about 11 years. At a mean age of 69.5 years (SD 0.8) they were recruited to a study investigating influences on cognitive ageing [5]. A second wave of cognitive and physical testing occurred at approximately 73 years of age at which time a urine sample was collected [5, 6]. The *INGI-Val Borbera* population is a collection of 1,785 genotyped samples (18-102 years) collected in the Val Borbera Valley, a geographically isolated valley located within the Appennine Mountains in Northwest Italy [7]. The *INGI-Carlantino* study is a population-based, cross-sectional study in a village situated in the Southeastern part of the Apennines in a hilly area of the Puglia region. Main study characteristics are summarized in Suppl. Table 4, genotyping details on Suppl. Table 5.

Micro-dissection studies in mouse kidney

Well-characterized tubular segments were microdissected from mouse kidneys as described previously [8]. Kidneys from male C57BL/6J mice were dissected and minced before incubation with 0.1% (*w*/*v*) type 2 collagenase solution that contained 100 µg/ml soybean trypsin inhibitor for 30 min at 37°C. After digestion, the supernatant was sieved through 250- and 80-µm nylon filters. Nephron fragments remained in the 80-µm sieve and were resuspended by flushing. Distinct segments [glomeruli (GLOM), proximal convoluted and straight tubules (PCT and PST respectively), thick ascending loop of Henle (TAL), distal convoluted tubule (DCT) and collecting duct (CD)] were isolated upon their morphologic features. Three collections were snap-frozen in liquid nitrogen and conserved at -80°C.

Immunohistochemistry

Nephron immunohistochemistry was performed as described previously [9, 10]. In short, co-staining for ARL15, breast cancer resistance protein (BCRP), Tamm-Horsfall protein (TH), thiazide sensitive Na^+-Cl^- cotransporter (NCC) and aquaporin-2 (AQP2) was performed on 5-µm sections of fixed frozen mouse (C57BL/6J) kidney samples. The sections were incubated for 16 h at 4°C with the following primary antibodies: rabbit anti-ARL15 (1:100, Sigma Chemical Co., St Louis, USA), rat anti-BCRP (1:250 [10]), sheep anti-TH (1:750 [10]), rabbit anti-NCC (1:50 [11]) or rabbit anti-AQP2 (1:1000, kindly provided by Dr. Deen, Nijmegen, The Netherlands). For detection, kidney sections were incubated with Alexa Fluor-conjugated secondary antibodies. Images were taken with a Zeiss Axio Imager 1 microscope (Oberkochen, Germany) equipped with a HXP120 Kubler Codix fluorescence lamp and a Zeiss Axiocam MRm digital camera.

Cell culture and transfection

Human embryonic kidney 293 (HEK293) cells were grown at 37°C in DMEM (Biowhittaker Europe, Vervier, Belgium) supplemented with 10% (*v/v*) FCS (PAA Laboratories, Linz, Austria), non-essential amino acids (AAs), and 2 mM L-glutamine in a humidified 5% (*v/v*) CO_2 atmosphere.

Cells were seeded in 12-well plates and subsequently transfected with a total of 1.25 µg of cDNA (per well in a 12 wells plate) using Lipofectamine 2000 (Invitrogen, Breda, The Netherlands). HA-tagged human TRPM6 was in the pCINeo-IRES-GFP mammalian expression vector [12]. A human ARL15 clone was obtained from Source BioScience (Berlin, Germany) and subcloned into the pCINeo-IRES-mCherry vector, used for transfections. The T46N mutation was inserted in the ARL15 construct using the QuikChange site-directed mutagenesis kit (Stratagene, La Jolla, CA, USA) according to the manufacturer's protocol. All constructs were verified by sequence analysis. Mock conditions were obtained by transfecting the empty pCINeo-IRES-mCherry vector. Approximately 36 h after transfection, cells were seeded on glass coverslips coated with 50 µg/ml fibronectin (Roche Diagnostics, Mannheim, Germany). Experiments were started 2 h after seeding the cells. Cells displaying both GFP and mCherry fluorescence were chosen for recording.

Electrophysiology

All experiments were performed at room temperature. Whole-cell recordings were undertaken and analyzed using an EPC-9 amplifier and the Patchmaster software (HEKA electronics,

Lambrecht, Germany). The sampling interval was set to 100 µs (10 kHz) with a low-pass filter set at 2.9 kHz. Pipettes were pulled from thin wall borosilicate glass (Harvard Apparatus, March-Hugstetten, Germany) and had resistance between 1 and 3 MΩ when filled with the pipette solution. Series resistance compensation was set to 75-95% in all experiments. Currents were elicited by a series of 500 ms voltage ramps (from -100 to +100 mV) applied every two seconds from a holding voltage of 0 mV. Current densities were obtained by normalizing the current amplitude to the cell capacitance.

The extracellular solution contained (in mM): 150 NaCl, 1 $CaCl_2$, 10 HEPES and pH adjusted to 7.4 using NaOH. The pipette solution was made of (in mM): 150 NaCl, 10 Na_2EDTA, 10 HEPES and pH adjusted to 7.2 using NaOH.

Conservation of ARL15 proteins

TBLASTN searches were performed on the mouse, cow and zebrafish genome database at NCBI (http://blast.ncbi.nlm.nih.gov/Blast.cgi) using the human ARL15 as query AA sequence. Sequences with a significant homology with human ARL15 were selected. Multiple sequence alignments were carried out using ClustalW (http://www.ebi.ac.uk/Tools/clustalw/) and the degree of AA conservation across species was discerned.

Distribution of *Arl15* gene expression and dietary Mg^{2+} challenge in mice

To study the tissue distribution of *Arl15* gene expression, three C57BL/6J mice were sacrificed; lung, bone, kidney, peritoneum, stomach, brain, heart, liver and muscle tissues were collected. The dietary Mg^{2+} challenge was performed on age- and gender-matched C57BL/6J wild type (WT) littermates. Mice were housed in a temperature- and light-controlled room with *ad libitum* access to standard pellet chow (SSNIFF Spezialdiäten, Soest, Germany) and deionized drinking water for 4 weeks until the start of the experiment. Three groups of mice were next fed a control diet (0.19% (*w/w*) Mg; n = 10), a Mg^{2+}-deficient diet (0.0005% (*w/w*) Mg; n = 10), or a Mg^{2+}-enriched diet (0.48% (*w/w*) Mg; n = 10) (SSNIFF Spezialdiäten, Soest, Germany) for 10 days. Mice were housed individually in metabolic cages overnight at baseline, day 5 and day 10 for urine collection (16 h sampling). Venous blood samples were obtained from the inferior vena cava during sacrifice at day 10, and kidneys and intestine (ileum and caecum) were harvested as previously described [13]. All protocols were conducted in accordance with the National Research Council Guide for the Care and Use of Laboratory animals and were approved by the local Ethics Committee.

Distribution of *arl15b* gene expression and dietary Mg^{2+} challenge in zebrafish

Zebrafish from the Tupfel long-fin (TLF) strain were used for experimentation. For the study of the tissue distribution of the highly conserved ARL15 zebrafish ortholog (*arl15b*) in adult zebrafish tissues, 3 females and 3 males were dissected following anaesthesia (0.1% (*v/v*) 2-phenoxyethanol (Sigma Chemical Co., St Louis, USA)) and brain, ovary, gills, testis, heart, spleen, kidney, gut, operculum, scales and liver tissues were collected and stored at -80°C until analysis. In 5 days post-fertilization (dpf) larvae, animals were anaesthetised with tricaine/Tris pH 7.0 solution and pronephric tissue was isolated with fine-point needles under the microscope (Leica Microsystems Ltd). After removal of the yolk and swim bladder, the pronephros could be distinguished by the pigments that surround the pronephric tubules (Suppl. Fig. 8). Then, pronephric-enriched tissue was scratched and subsequently aspirated with a Pasteur pipette. Samples were constituted by 10 pronephros each, which were stored at -80°C until further analysis. Control genes were used to verify the purity of the pronephric tissue isolated: *ncc*, uniquely expressed in the pronephros [14], served as positive control; and *ncc-like*, whose gene expression is restricted to the skin [15], served as negative control.

To study the regulation of *arl15b* gene expression by the Mg^{2+} status in zebrafish ionoregulatory tissues (gills, kidney and gut), fish Mg^{2+} balance was challenged by different Mg^{2+} diets as previously reported [16]. Briefly, 27 adult zebrafish were weighed and randomly divided into 3 groups of 9 animals each and kept in 3 separate 2-liter tanks. During 2 weeks (acclimation to control conditions), all fish were fed a Mg^{2+}-control diet (Hope Farms, Woerden, The Netherlands; 0.07% (*w/w*) Mg) at a daily ration of 2% (*w/w*) of the total body weight. After this period, for 2 groups, the control diet was replaced by a Mg^{2+}-deficient diet (Hope Farms; 0.01% (*w/w*) Mg) or a Mg^{2+}-enriched diet (Hope Farms; 0.7% (*w/w*) Mg). These 2 groups were kept under these feeding regimes for 3 weeks, while the remaining group (fed a Mg^{2+}-control diet) served as a control. At the end of this period, all groups were sampled. Sampling took place 24 h after the last feeding. Fish were anaesthetised in 0.1% (*v/v*) 2-phenoxyethanol (Sigma). After anaesthesia, death of animals was induced by spinal transaction and organs were collected, immediately frozen in liquid nitrogen and stored at -80°C until analysis. All animal procedures detailed here were performed in accordance with national and international legislation and were approved by the ethical review committee of the Radboud University Nijmegen.

Knockdown of the zebrafish ortholog of human ARL15 and rescue experiments

WT TLF zebrafish were bred and raised under standard conditions (28.5°C and 14 h of light: 10 h of dark cycle) in accordance with international and institutional guidelines. Zebrafish eggs were obtained from natural spawning. The following splice-site blocking morpholinos (MOs) were designed to knockdown *arl15b* expression: 5'-AAACACTGAAAGACGGGACAAAGAC-3' and GTTAAGCGAGTATTAGGTTACCTCT-3' (Gene Tools, Philomath, OR, USA), designated as exon 3 and 4 skipping *arl15b*-MO respectively. A standard mismatch MO, directed against a human β-globin intron mutation, 5'-CCTCTTACCTCAGTTACAATTTATA-3', was also used in the experiments to control for toxic effects of the MO molecule. MOs were diluted in deionized, sterile water supplemented with 0.5% (*w*/*v*) phenol red and injected in a volume of 1 nl into the yolk of one- to two-cell stage embryos using a Pneumatic PicoPump pv280 (World Precision Instruments, Sarasota, FL, USA). WT embryos (uninjected) were also included in the experiments to control for the effects of the injection procedure *per se*. To determine the most effective dose of the *arl15b*-MO, 0.5, 1 and 2 ng *arl15b*-MO; and 2, 4 and 8 ng *arl15b*-MO were injected in two sets of experiments. In these experiments, control embryos were injected with 2 or 8 ng of the standard mismatch control-MO (the highest dose for each set of experiments respectively). After injection, embryos from the same experimental condition were placed in 3 Petri dishes and cultured at 28.5°C in E3 embryo medium (5 mM NaCl, 0.17 mM KCl, 0.33 mM $CaCl_2$, 0.33 mM $MgSO_4$), which was refreshed daily.

Morphological phenotypes characterizing kidney function and yolk metabolization were analyzed in larvae at 5 dpf. Larvae were classified into different classes of phenotypes on the basis of comparisons with stage-matched control embryos (injected with the control-MO) of the same clutch. In *arl15b* morphant larvae (5 dpf), 4 different phenotypes were distinguished: normal; mild, larvae with mild-moderate pericardial edema (indicative of kidney dysfunction) and metabolic defects (poor metabolization of the yolk); moderate, moderate pericardial edema accompanied by kidney cysts in approximately 75% of the cases, metabolic defects (poor metabolization of the yolk) and cardiovascular defects (poor blood circulation in the tail); severe, severe pericardial edema accompanied by kidney cysts in approximately 80% of the cases, metabolic defects (poor metabolization of the yolk) and cardiovascular defects (poor blood circulation or absence in the tail and severe bradychardia (heart beat rate below 100 beats per minute)). Representative images were obtained with a DFC450C camera (Leica Microsystems Ltd) after anaesthetising larvae with tricaine/Tris pH 7.0 solution.

For electrolyte measurements or RNA isolation, 7-10 zebrafish larvae were pooled as one sample. Samples were then snap frozen in liquid nitrogen and stored at -80°C in order to ensure euthanasia of animals.

In vivo cRNA rescue experiments were performed with human WT ARL15 and dominant negative mutant (T46N) ARL15 cRNAs. Constructs were sub-cloned into the pT7Ts expression vector, suitable for rescue experiments in zebrafish [17], and cRNAs were prepared using the mMESSAGE mMACHINE Kit (Ambion, Austin, TX, USA) according to the manufacturer's instructions. The cRNAs, in an amount of 50 pg, as based on previous studies [18, 19], were (co)injected together with MOs as described above. Zebrafish larvae were phenotyped at 5 dpf.

Electrolyte measurements in animal studies

In mice, urinary creatinine and electrolytes as well as plasma urea and creatinine (enzymatic determination) were measured on a Synchron Unicel DxC 800 analyzer (Beckman Coulter, Brea, USA). In zebrafish, sample processing started by washing twice the samples with nanopure water in order to avoid contamination of remaining waterborne Mg^{2+}. Fish were then dried and digested as described previously [19]. The total Mg content in each sample was determined with a colorimetric assay (Roche). Within-run precision and accuracy was controlled by means of an internal control Precinorm (CV = 0.8%). Furthermore, samples were normalized by protein content, which was determined with the Pierce BCA protein assay kit (Pierce Biotechnology, Rockford, IL, USA).

RNA isolation and cDNA synthesis

In mouse, total RNA was extracted from different tissues using the Aurum™ Total RNA Fatty and Fibrous Tissue Kit (Bio-Rad, Hercules, CA), following the manufacturer's protocol. In zebrafish, RNA was isolated from zebrafish tissues and larvae using TRIzol reagent (Invitrogen, Carlsbad, CA, USA) according to the manufacturer's instructions in which glycogen (Fermentas GmbH, St. Leon-Rot, Germany) was used in order to maximize the RNA recovery. This method allowed the isolation of more than 3 µg RNA per tissue or whole-larvae sample (n = 7-10 larvae/sample), and of more than 200 ng RNA per pronephric samples (10 pronephros/sample). In both, mouse and zebrafish RNA samples, one µg of RNA, or 200 ng in the case of pronephric samples, was subjected to DNase treatment to prevent genomic DNA contamination and subsequently used to perform the reverse transcriptase reaction.

Reverse transcription quantitative polymerase chain reaction (RT-qPCR)

Changes in target genes mRNA levels were determined by relative RT-qPCR following the MIQUE guidelines [20] with a CFX96™ Real-Time PCR Detection System (Bio-Rad Laboratories, Hercules, CA) using iQ™ SYBR Green Supermix (Bio-Rad) detection of single PCR product accumulation. To study the effect of dietary Mg^{2+} on gene expression in mouse kidney, ileum and caecum, the geNorm algorithm was used with 5 reference genes to calculate the normalization factor (software geNorm version 3.4). The reference genes used encoded for β-actin (*Actb*), glyceraldehyde 3-phosphate dehydrogenase (*Gapdh*), peptidylprolyl isomerase A (*Ppia*), attachment region binding protein (*Arbp*) and hypoxanthine phosphoribosyltransferase 1 (*Hprt1*). In the rest of procedures with mice (tissue distribution and gene expression profile in different mouse nephron segments) and in the zebrafish studies, gene expression levels were normalized to the expression levels of the standard species-specific reference genes *Gapdh* (for mice [21, 22]) and elongation factor-1α (*elf1α*, for zebrafish [16, 23]). Here, relative mRNA expression was analysed using the Livak method ($2^{-\Delta\Delta Ct}$). Primer sequences are shown in Suppl. Table 8.

Efficacy of the splice-site blocking *arl15b*-morpholinos. To determine the efficacy of the splice blocking induced by the exon 3 skipping *arl15b*-MO, cDNA from 5 dpf control (injected with 0.5 ng control-MO) and morphant (injected with 0.5 ng *arl15b*-MO) larvae was used for PCR analysis. The primers used were 5'- CGAGGTCACAGGGGTGTTTC-3' as forward primer and 5'- GACGAAGCGCTGTCCAAAAC-3' as reverse primer. Fragments thus obtained were extracted from a 1.5% agarose gel and Sanger-sequenced (Suppl. Fig. 9) to confirm the splice blocking induced.

In the case of the exon 4 skipping *arl15b*-MO, cDNA was generated from fish injected with 2 ng control or *arl15b*-MO. Primers used were 5'- CTGACGGGTTCTGGGAAGAC-3' as forward primer and 5'- ACCGTGCTTCCCTCTAGGAT-3' as reverse primer. Given the absence of a spliced-*arl15b* transcript in 2-5 dpf fish (as a result of nonsense-mediated decay of *arl15b* mRNA by the exon 4 skipping *arl15b*-MO, Suppl. Fig. 10), the efficacy of the approach was further studied by RT-qPCR using specific primers that discriminate for the functional (non-spliced) *arl15b* transcript: the forward primer targets the exon 3-4 junction and the reverse primer targets exon 4 (Suppl. Table 8).

SUPPLEMENTARY FIGURES

Supplementary Figure 1. Manhattan plot from the GWAS on uMg-to-creatinine ratio for the CoLaus cohort.

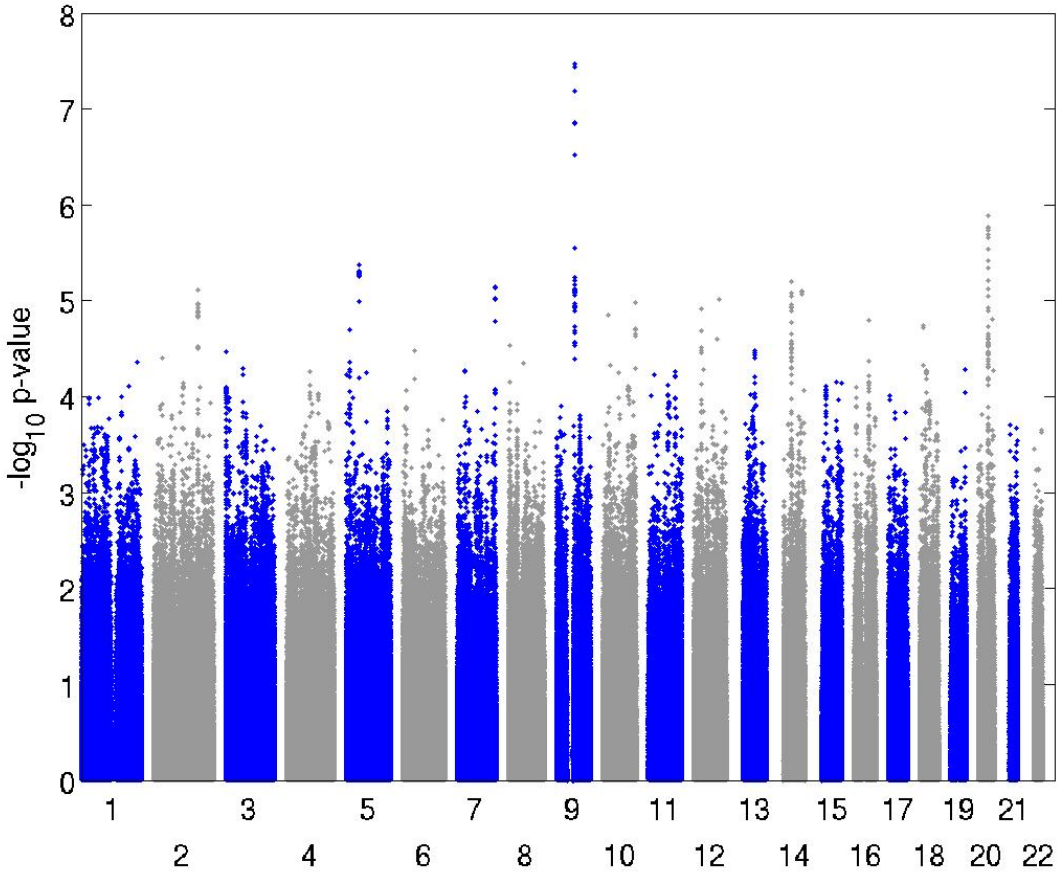

Manhattan plot showing -log10(*P* values) for all SNPs in the genome-wide association for normalized uMg-to-creatinine ratio in CoLaus (n=5,150), ordered by chromosomal position. The values correspond to the association of normalized uMg-to-creatinine ratio, including as covariates age, sex and the first principal components generated from all genotypes to take population structure into account. One locus (*TRPM6*) reached genome-wide significance ($P < 5\times10^{-8}$).

Supplementary Figure 2. QQ plot and conditional analyses for the uMg-to-creatinine ratio.

(**a**) QQ plot from the meta-analysis of uMg-to-creatinine ratio.

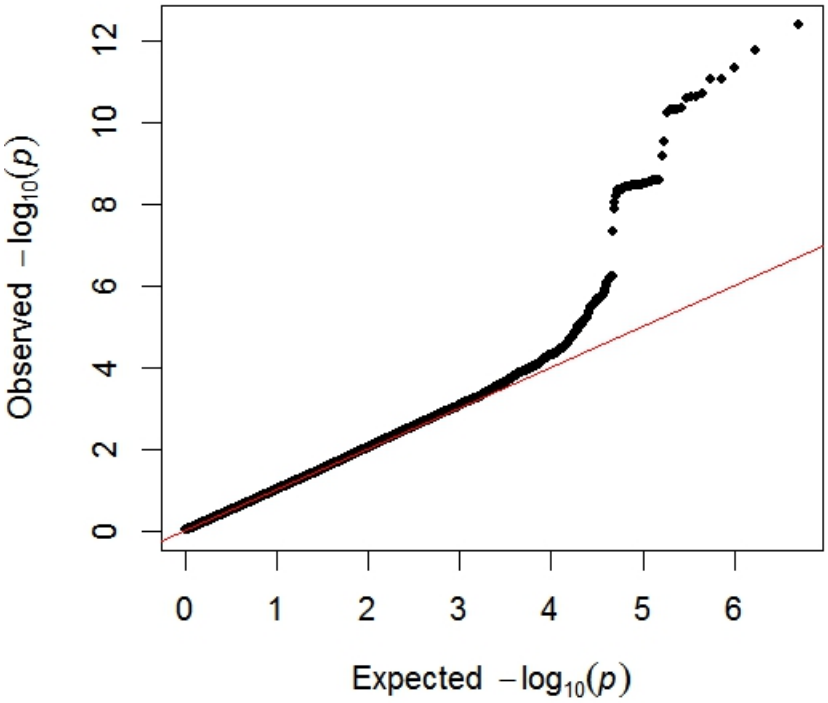

(**b**) Zoom plot showing the *TRPM6* region's associations to uMg-to-creatinine ratio after conditioning the analysis for rs3824347.

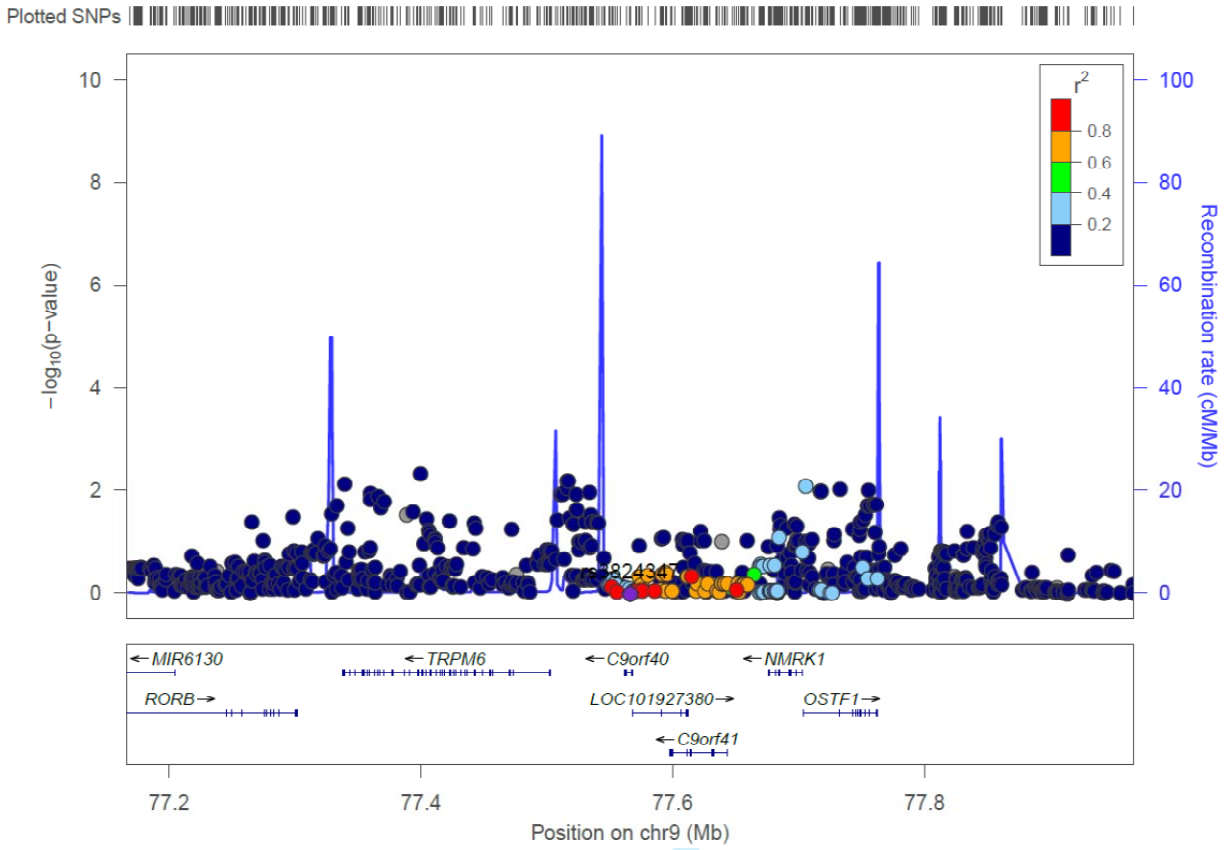

(**c**) Zoom plot showing the *ARL15* region's associations to uMg-to-creatinine ratio after conditioning the analysis for rs35929.

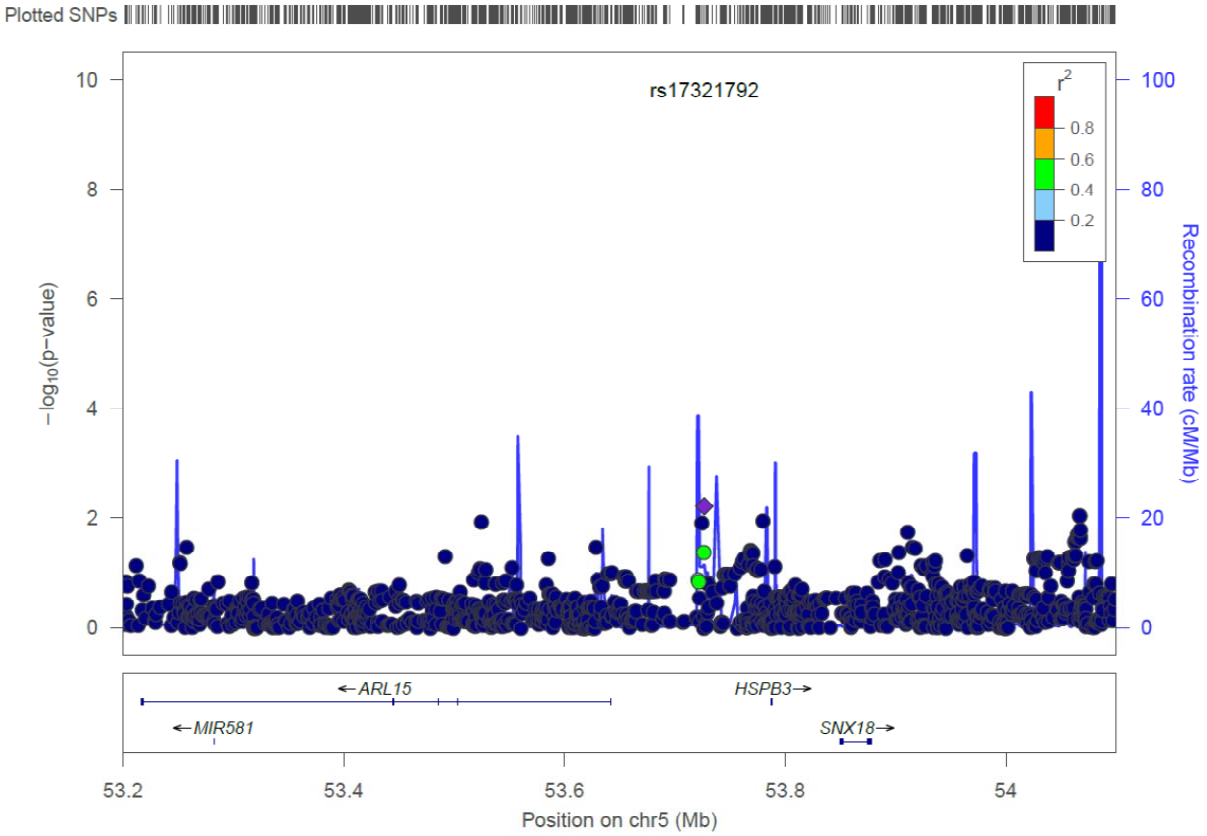

Supplementary Figure 3. Manhattan plot from the GWAS on serum Mg^{2+} levels for the meta-analysis.

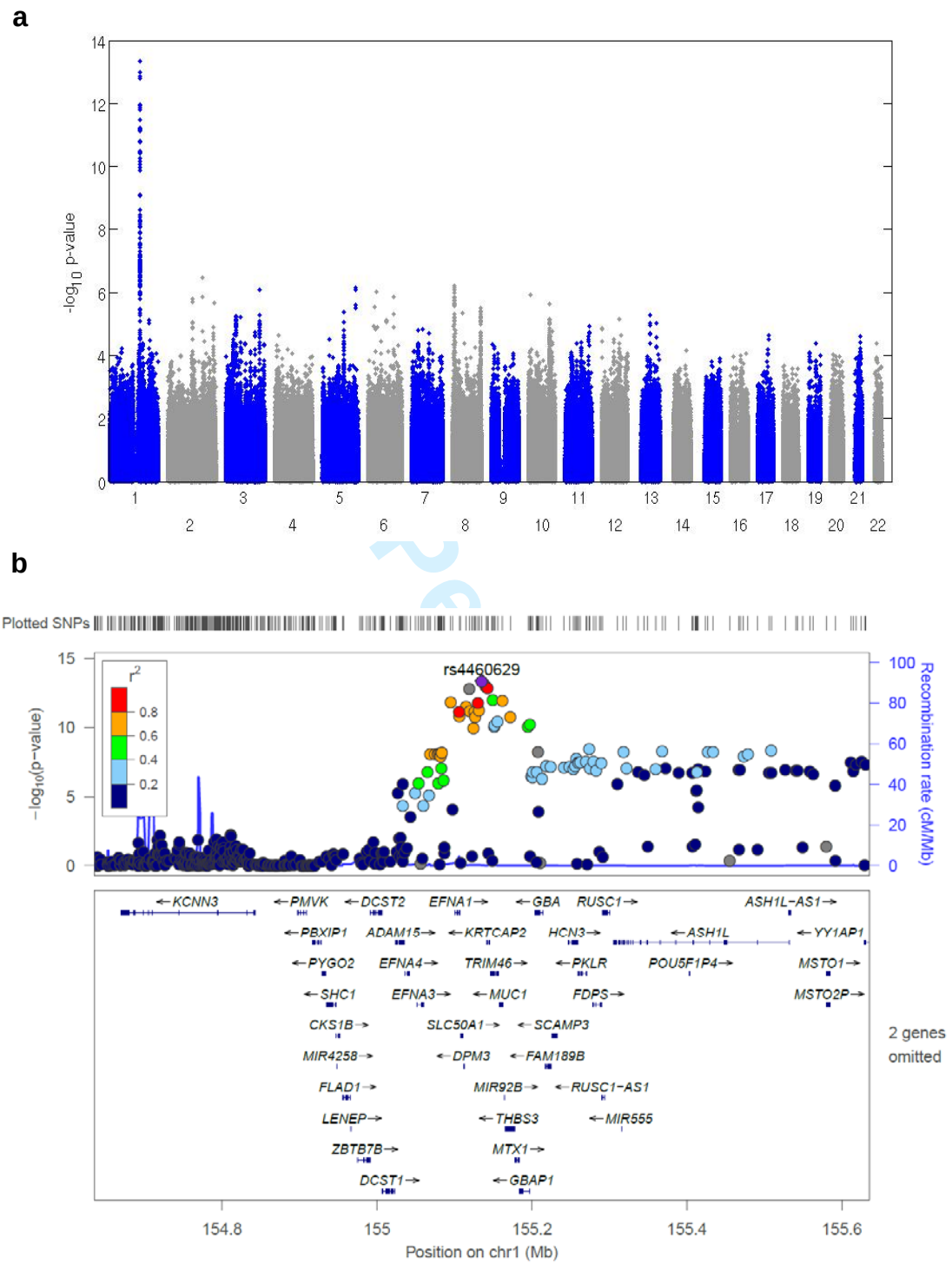

(**a**) Manhattan plot showing all –log10(*P* values) for the combined analysis of the GWAS on serum Mg^{2+}, ordered by chromosome position. A locus on chromosome one reaches genome-wide significance. (**b**) Regional association plot of the region on chromosome one identified on the Manhattan plot on panel A. It shows a gene-rich locus, with no obvious candidate for being the gene involved.

Supplementary Figure 4. Manhattan plot from the meta-analysis of fractional excretion of Mg^{2+} (FEMg) GWASs.

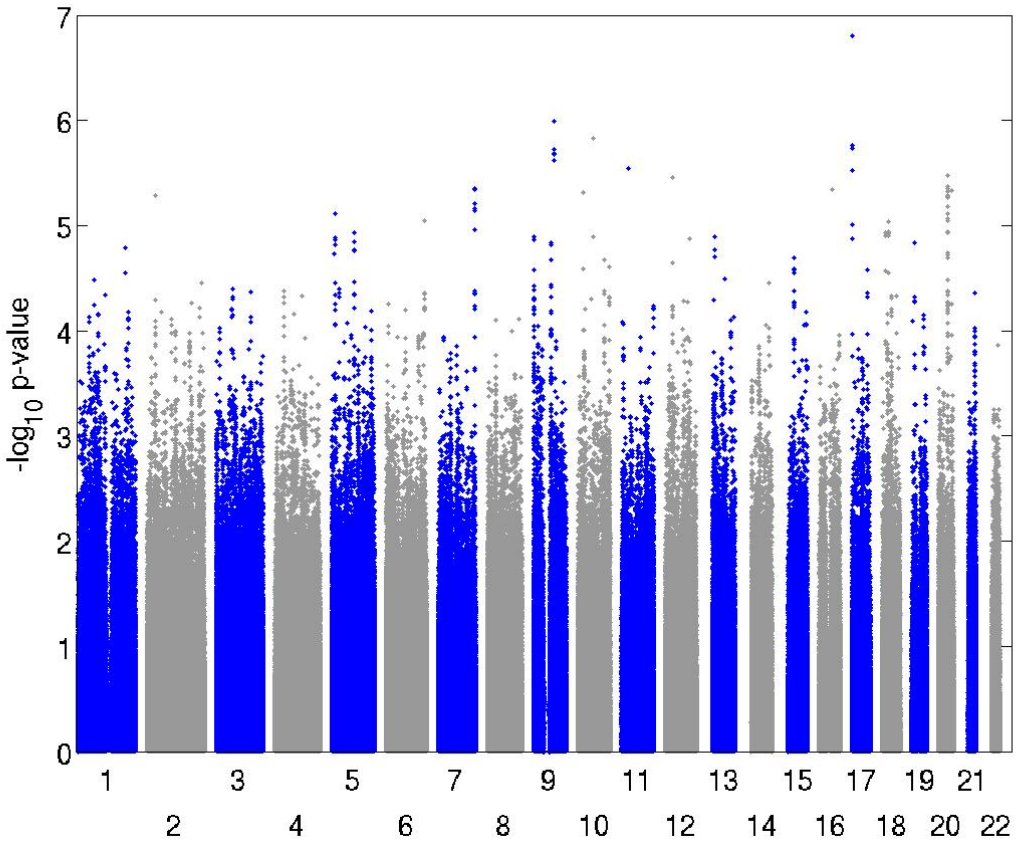

Manhattan plot showing all –log10(*P* values) for the combined analysis of the GWAS on FEMg, ordered by chromosome position. No signal reaches genome-wide significance.

Supplementary Figure 5. Functional protein association network analyses for ARL15.

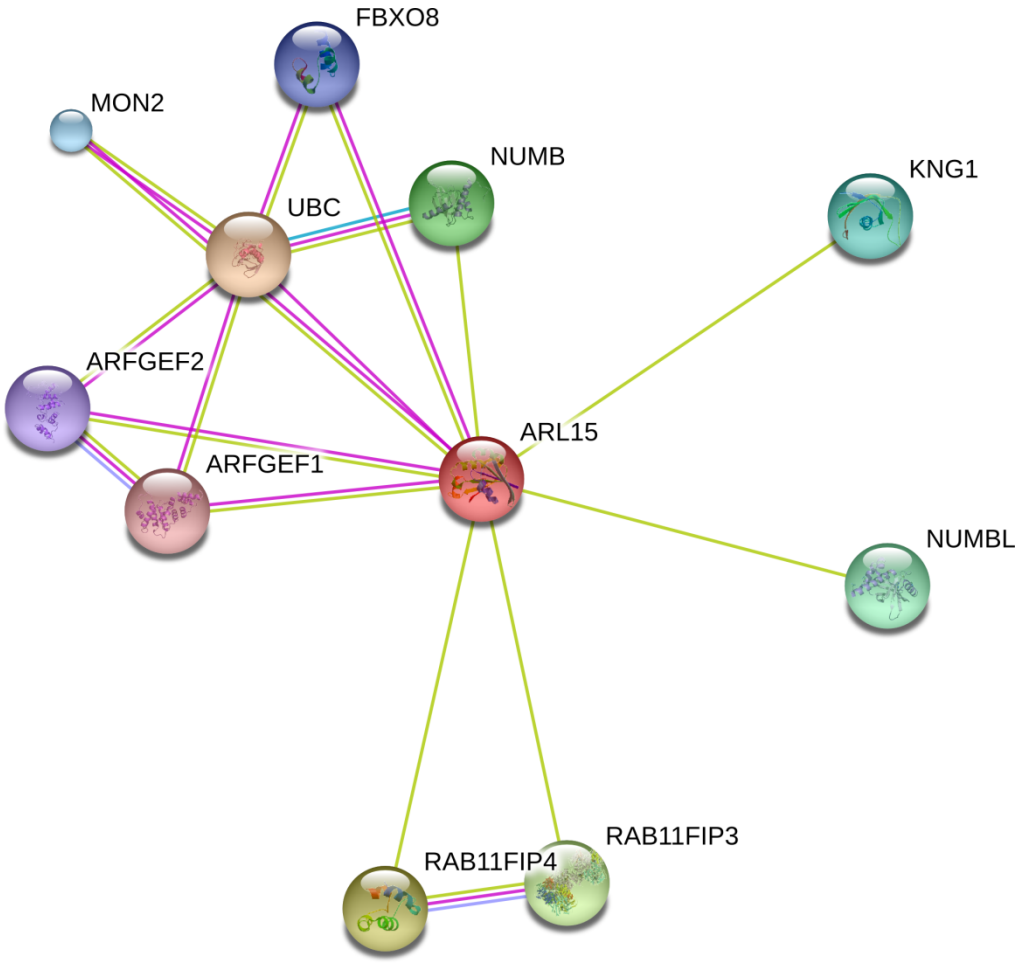

ARL15 interacts with regulators of endocytic (RAB11FIP4, UBC) and vesicular (ARFGEF1) trafficking, factors involved in maintenance of cell polarity (ARFGEF1), factors influencing sodium handling (KNG1) and regulators of ubiquitination (UBC). (http://string-db.org/cgi/network.pl?taskId=NPTdrqbgkFZS). Network nodes represent proteins, whereas different colored nodes refer to different proteins. Small nodes (MON2) refer to proteins of unknown 3D structure while large nodes represent proteins whose 3D structure is known or predicted (ARL15, KNG1, NUMBL, RAB11FIP3, RAB11FIP4, ARFGEF1, ARFGEF2, UBC, NUMB, FBXO8). Edges represent protein-protein associations: blue, interactions from curated databases (e.g. UBC-NUMB); magenta, experimentally determined interactions (e.g. ARL15-ARFGEF1, ARL15-ARFGEF2, ARL15-UBC, ARL15-MON2, ARL15-FBXO8); green, interactions derived from text mining (e.g. ARL15-RAB11FIP3, ARL15-RAB11FIP4, ARL15-NUMBL, ARL15-KNG1, ARL15-NUMB); purple, interactions deduced by protein homology (e.g. ARFGEF1-ARFGEF2).

Supplementary Figure 6. Tissue distribution of *Arl15* gene expression in mouse tissues and regulation of gene expression by dietary Mg^{2+} in mouse tissues relevant for Mg^{2+} handling.

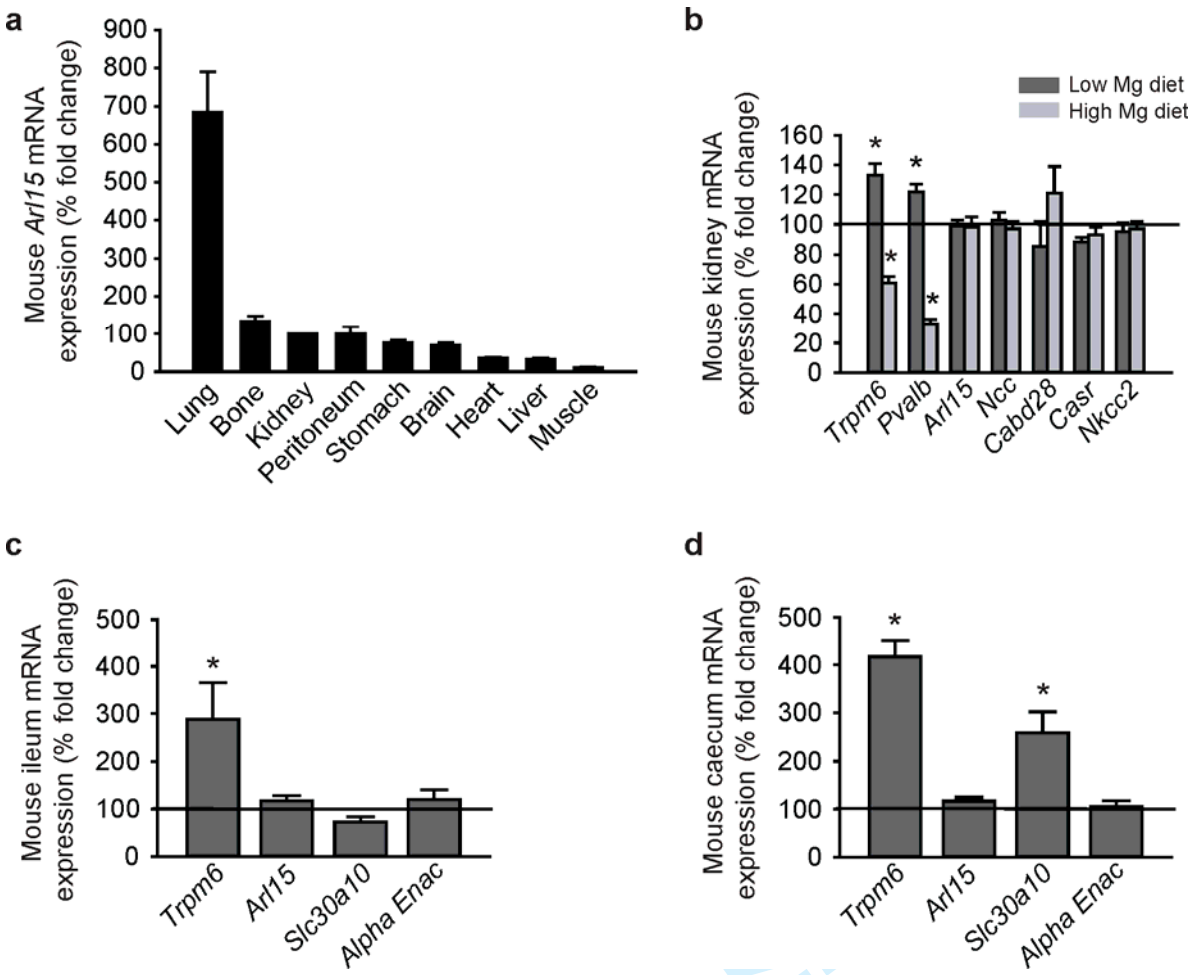

(**a**) Tissue distribution of *Arl15* gene expression in mouse tissues. Relative gene expression in mouse tissues and organs was analysed using the Livak method ($2^{-\Delta\Delta Ct}$), where results are normalized against the reference genes *Gapdh* and expressed relative (%) to the gene expression in the kidney, chosen as calibrator. Data are presented as mean ± SEM (n = 3). (**b-d**) Gene expression levels of *Trpm6*, parvalbumin (*Pvalb*), *Arl15*, the Na^+-Cl^- cotransporter (*Ncc*), calbindin D-28k (*Cabd28*), the calcium-sensing receptor (*Casr*) and the Na^+-K^+-Cl^- cotransporter isoform 2 (*Nkcc2*) in mouse kidney (**b**); of *Trpm6*, *Arl15*, the zinc transporter 10 (*Slc30a10*) and the alpha subunit of the epithelial sodium channel (*Alpha Enac*) in mouse ileum (**c**); and *Trpm6*, *Arl15*, *Slc30a10* and *Alpha Enac* in mouse caecum (**d**). Mice were fed a control diet (0.19% (*w/w*) Mg), a Mg^{2+}-deficient diet (0.0005% (*w/w*) Mg), or a Mg^{2+}-enriched diet (0.48% (*w/w*) Mg) for 10 days. Gene expression data were calculated using the geNorm algorithm and represent the mean fold difference (mean ± SEM, n = 10 for kidney and n = 5 for ileum and caecum) from the control group (mice on the control diet). $^*P < 0.05$ compared with the control group.

Supplementary Figure 7. The zebrafish Arl15b protein is a highly conserved ortholog of human ARL15 being its gene expression is magnesiotropic in kidney, gills and gut.

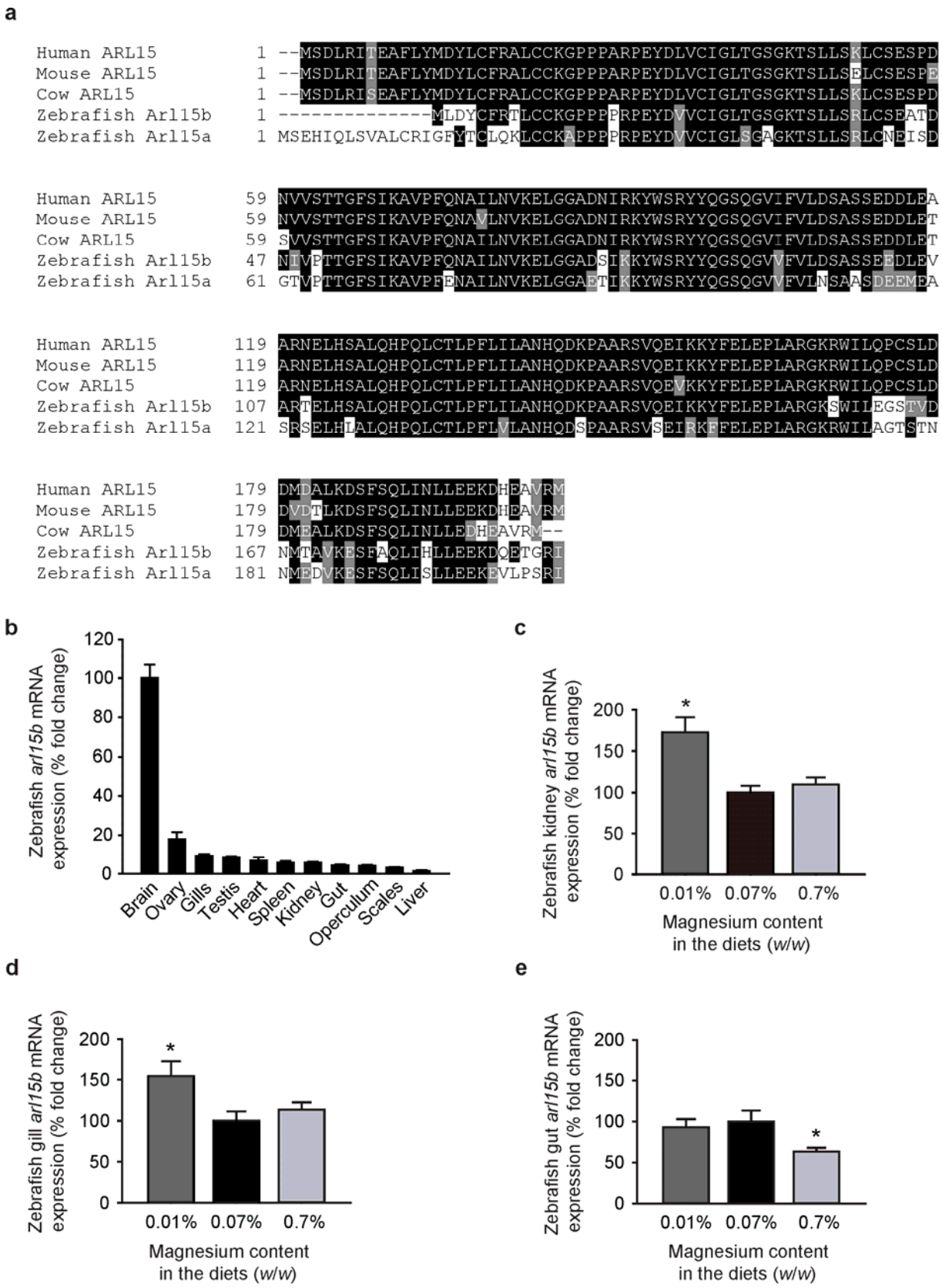

(**a**) Alignment of the human, mouse and cow ARL15 proteins (GenBank accession no. NP_061960, NP_766183 and NP_001014943 respectively) and zebrafish Arl15 paralogs: Arl15a and Arl15b (GenBank accession no. NP_001093503 and XP_001923547 respectively). Identical AA are boxed in black, conservative substitutions in gray. Sequence identity of zebrafish Arl15a with human, mouse and cow ARL15 is 68, 66 and 67% respectively. Zebrafish Arl15b displayed a strikingly high degree of AA conservation with its mammalian counterparts: 83, 81 and 79% with human, mouse and cow ARL15 respectively. (**b**) Tissue distribution of *arl15b* gene expression in zebrafish tissues. Relative gene expression in mouse and zebrafish tissues and organs was analysed using the Livak method ($2^{-\Delta\Delta Ct}$), where results are normalized against the translational *elf1α* and expressed relative (%) to the gene expression in the brain, chosen as calibrator. Data are presented as mean ± SEM (n = 6, except for the ovary and testis where n = 3). (**c-e**) Gene expression levels of *arl15b* in kidney (**c**), gills (**d**) and gut (**e**) of zebrafish on a Mg^{2+}-deficient diet (0.01% (*w*/*w*) Mg), Mg^{2+}-control diet (0.07% (*w*/*w*) Mg) and Mg^{2+}-enriched diet (0.7% (*w*/*w*) Mg) for 21 days. Data were calculated using the Livak method ($2^{-\Delta\Delta Ct}$) and they represent the mean fold difference (mean ± SEM, n = 8-9) from the control group (fish on the control diet). $^{*}P < 0.05$ was considered statistically significant when compared with the control group.

Supplementary Figure 8. The *arl15b* gene is expressed in the pronephric kidney of zebrafish larvae.

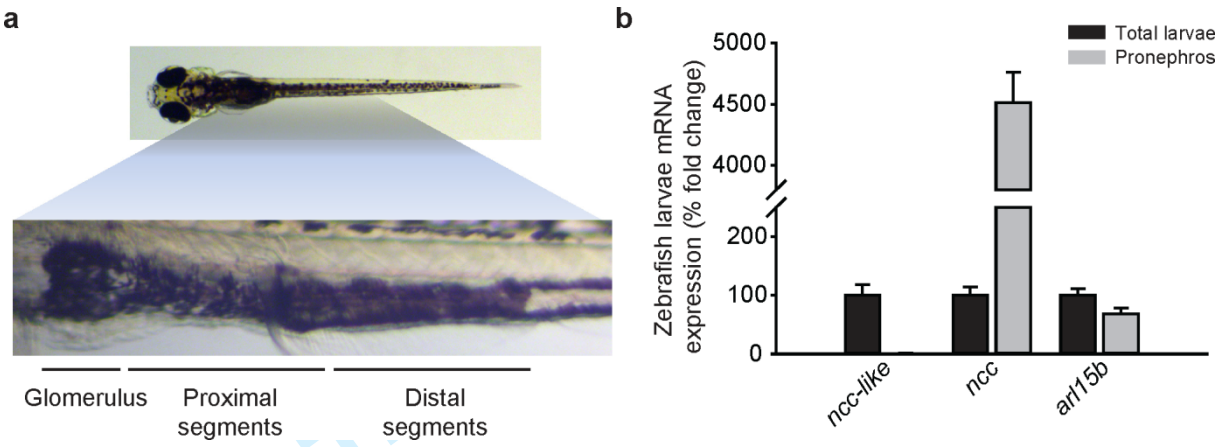

(**a**) The pronephros of 5 dpf zebrafish larva after dissection for collection of pronephric-enriched tissue. Pronephric tubules can be distinguished by the black pigments that develop around the tubuli. (**b**) Gene expression of *arl15b* and the control genes *ncc* (uniquely expressed in the pronephros, as positive control) and *ncc-like* (distinctly expressed in the skin, as negative control) in the pronephros and total larvae. Relative gene expression was analysed using the Livak method ($2^{-\Delta\Delta Ct}$), where results are normalized against the reference gene *elf1α* and expressed relative (%) to the gene expression in total larvae. Data are presented as mean ± SEM (n = 3).

Supplementary Figure 9. Efficacy of the exon 3 skipping *arl15b*-MO used.

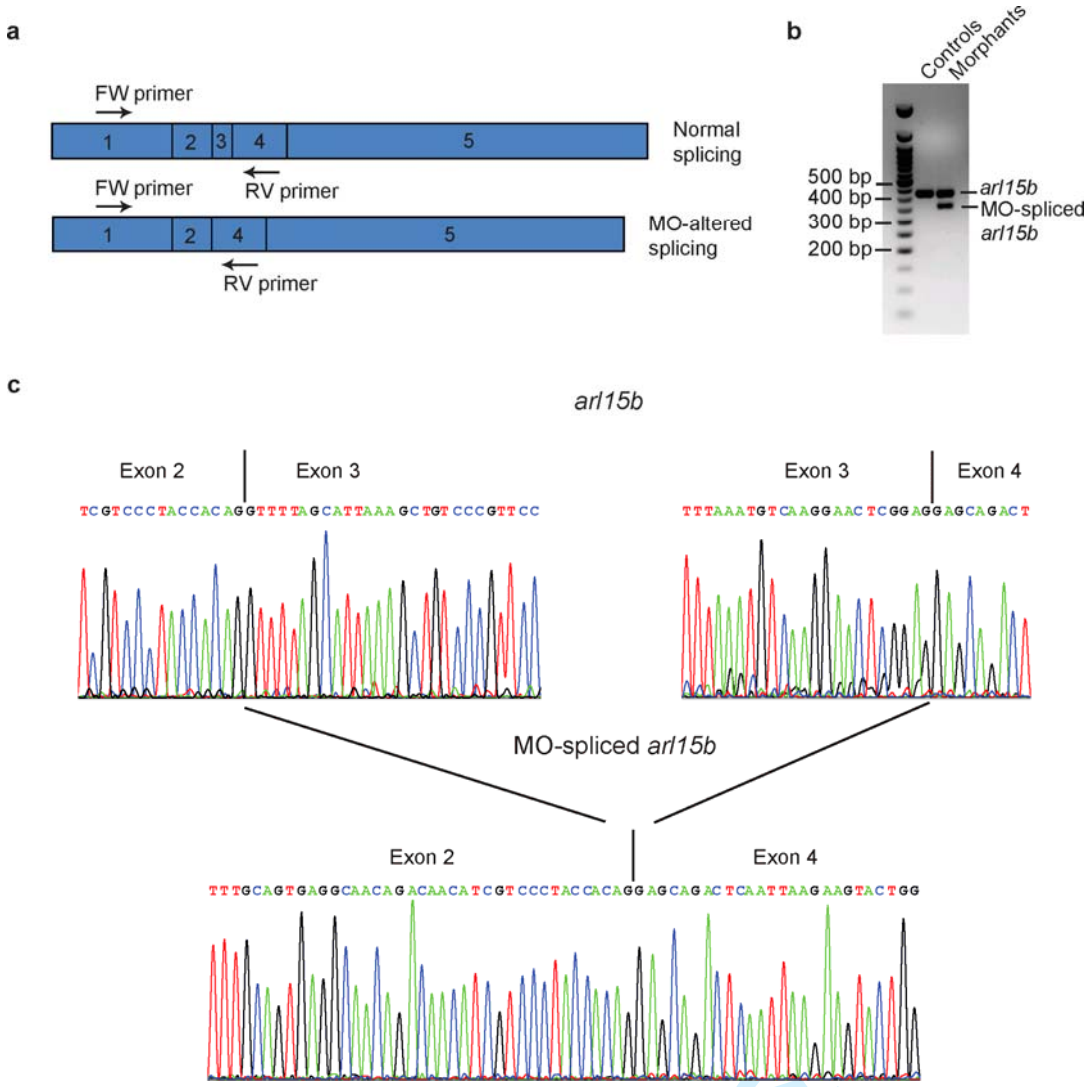

(**a**) Expected PCR products using forward (FW) and reverse (RV) primers located in exon 1 and 4 respectively on *arl15b* mRNA with normal splicing or altered splicing evoked by the *arl15b*-MO. (**b**) Gel electrophoresis image showing defects in the splicing process following injection of *arl15b*-MO (morphants, dose of 0.5 ng *arl15b*-MO/embryo) or control-MO (controls, dose of 0.5 ng control-MO/embryo). Bands showing correctly spliced *arl15b* mRNA and MO-spliced *arl15b* mRNA are shown. PCR was performed on cDNA prepared from larvae 5 days after injection. Shown on the left are the sizes (in bp) of the major bands of the DNA ladder. The expected amplicon size of the correctly spliced *arl15b* mRNA and the MO-spliced *arl15b* mRNA using FW and RV primers is of 411 bp and 351 bp respectively. (**c**) Chromatograms obtained from Sanger sequencing of the amplicons in the correctly spliced *arl15b* mRNA and the MO-spliced *arl15b* mRNA. The *arl15b*-MO evoked exon 3 skipping yielding a knockdown of Arl15b function. By skipping exon 3 with the *arl15b*-MO, the resulting protein lacks active domains such as the complete switch I region and part of the switch II region (switch regions are surface loops that undergo conformational changes upon GTP binding) and G3 box.

Supplementary Figure 10. Efficacy of the exon 4 skipping *arl15b*-MO used.

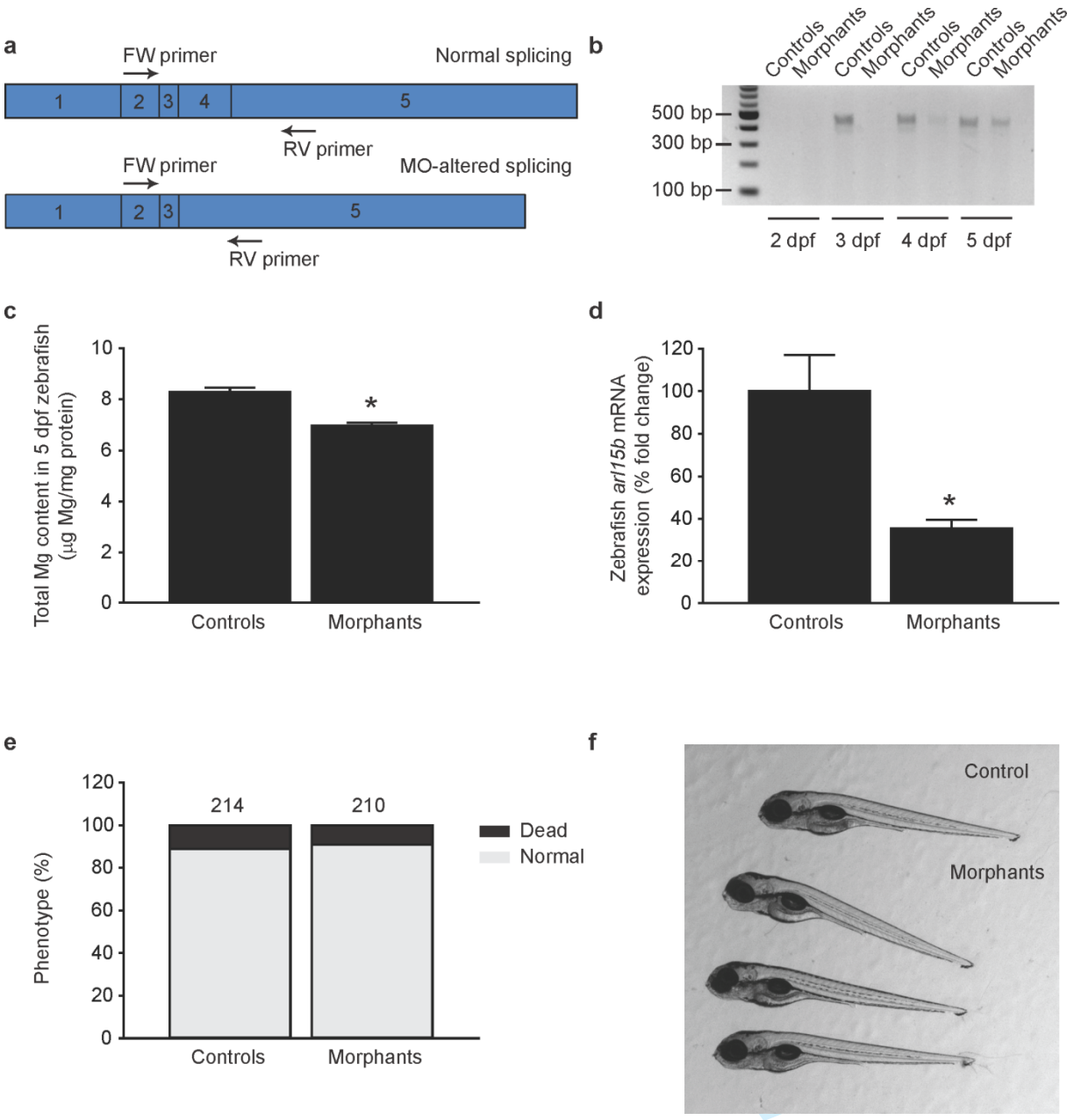

(**a**) Expected PCR products using forward (FW) and reverse (RV) primers located in exon 2 and 5 respectively on *arl15b* mRNA with normal splicing or altered splicing evoked by the *arl15b*-MO. (**b**) Gel electrophoresis image showing knockdown of *arl15b* gene expression following injection of *arl15b*-MO (morphants, dose of 2 ng *arl15b*-MO/embryo) or control-MO (controls, dose of 2 ng control-MO/embryo) in 2-5 dpf zebrafish larvae. Bands showing correctly spliced *arl15b* mRNA are shown, while bands showing MO-spliced *arl15b* mRNA could not be detected so that the exon 4 skipping *arl15b*-MO evoked nonsense-mediated decay of *arl15b* transcripts. Shown on the left are the sizes (in bp) of the major bands of the DNA ladder. The expected amplicon size of the correctly spliced *arl15b* mRNA and the MO-spliced *arl15b* mRNA (not detected) using FW and RV primers is of 413 bp and 204 bp respectively. (**c-f**) Characterization of the knockdown evoked by injection of 2 ng of exon 4 skipping *arl15b*-MO. Controls were injected with 2 ng of control-MO. **C,** total Mg content in

5 dpf morphant and control zebrafish larvae. Data are presented as mean ± SEM (n = 10). $^{*}P < 0.05$ was considered statistically significant when compared with the control group. (**d**) Quantification of the knockdown evoked by the exon 4 skipping *arl15b*-MO by RT-qPCR using specific primers that discriminate for the correctly spliced (functional) *arl15b* mRNA. Data were calculated using the Livak method ($2^{-\Delta\Delta Ct}$) and they represent the mean fold difference (mean ± SEM, n = 10) from the control group (fish injected with the control-MO). $^{*}P < 0.05$ was considered statistically significant when compared with the control group. (**e**) Distribution of morphological phenotypes in the zebrafish larvae (5 dpf) used for the quantification of the *arl15b* knockdown by RT-qPCR. Numbers on top of the bars indicate the number of animals in each experimental condition. (**f**) Illustrative picture showing the characteristic phenotype (normal) evoked by knockdown of *arl15b* (2 ng/embryo of exon 4 skipping *arl15b*-MO).

SUPPLEMENTARY TABLES

Supplementary Table 1. Summary statistics for the genome-wide meta-analysis of serum Mg^{2+} levels.

	Effect allele	Other allele	Mean effect allele frequency	Effect size discovery (SE)	*P* value discovery	Effect size replica (SE)	*P* value replica	Effect size combined analysis (SE)	*P* value combined analysis	Direction of effects of individual cohorts	I^2
rs4460629	T	C	0.56	-0.144 (0.02)	4.89×10^{-13}	-0.100 (0.04)	1.15 x10-2	-0.136 (0.018)	4.45×10^{-14}	--?-	14.6

The effect size sign for each individual cohort on the last but one column is represented by the sign – or +. The cohort displaying a "?" is for the Carlantino cohort, not having data for rs4460629. The last column shows the I^2 value, representing the heterogeneity across cohorts.

Supplementary Table 2. Imputation status and quality for rs35929 and rs3824347.

SNP	COLAUS	CARLANTINO	KORCULA	LBC1936	SPLIT	VAL BORBERA	VIS
rs35929	I(0.95)	I (0.81)	I (1)	I(1)	I(1)	I(1)	I(1)
rs3824347	I(0.97)	I(0.76)	I(0.95)	I(0.97)	I(0.98)	I(0.97)	I(0.98)

Imputation status (G= genotyped, I=imputed) for both SNPs of interest in each cohort. Between brackets is the r^2 value representing imputation quality.

Supplementary Table 3. Association of *ARL15* variants with metabolic phenotypes.

Source	Trait	SNP	p-value of association in published GWAS	Chr	Position	Gene Region	Context	PubMed	reference allele	p-value for uMg/uCreat in Meta-analysis	Beta for uMg/uCreat in Meta-analysis	Standard error of Beta for uMg/uCreat in Meta-analysis
dbGaP	Body Weight	rs2042313	2.45x10-7	5	53212417	ARL15	Intron	17903300	NA	NA	NA	NA
dbGaP	Body Weight	rs2042313	5.15x10-7	5	53212417	ARL15	Intron	17903300	NA	NA	NA	NA
NHGRI GWAS Catalog	Adiponectin	rs6450176	6.00x10-8	5	53298025	ARL15	Intron	22479202	a	0.59	0.0091	0.0169
NHGRI GWAS Catalog	Cholesterol, HDL	rs6450176	5.00x10-8	5	53298025	ARL15	Intron	20686565	a	0.59	0.0091	0.0169
NHGRI GWAS Catalog	Adiponectin	rs4311394	3.00x10-8	5	53300662	ARL15	Intron	20011104	a	0.63	-0.0079	0.0165
dbGaP	Uric Acid	rs10513040	3.55x10-6	5	53502295	ARL15	Intron	17903292	a	0.052	-0.0663	0.0341

Summary of previously associated SNPs in *ARL15* in published GWAS. The SNP associated with body weight is not present in our study. The 3 other SNPs are not significantly associated in the present uMg-to-creatinine meta-analysis, as shown in the last 3 columns.
Data were exported from dbGAP browser: http://www.ncbi.nlm.nih.gov/gap.

Supplementary Table 4. Study characteristics.

Study	CoLaus	INGI-Val Borbera	INGI-Carlantino	CROATIA-Vis	CROATIA-Korcula	CROATIA-Split	LBC1936
Sample size	5265	1541	281	195	889	489	660
Female % (N)	53%	56%	56.80%	58%	63.80%	56.50%	47.90%
Age, years mean (SD)	53.4 (10.7)	55 (18)	48 (19.7)	56.36 (15.5)	56.3 (13.9)	49.25 (14.7)	72.74 (0.75)
Serum Mg (mg/dl) mean (SD)	2.06 (0.166)	2.2 (0.3)	2.1 (0.2)	NA	2.04 (0.21)	NA	NA
Serum creatinine (mg/dl) mean (SD)	1.05 (0.24)	0.87 (0.25)	0.8 (0.2)	0.99 (0.32)	0.92 (0.18)	0.93 (0.15)	NA
Urine Mg (mg/dl) mean (SD)	6.9 (4.0)	8.4 (4.8)	8.1 (5)	5.93 (4.52)	7.6 (4)	8.76 (4.9)	8.70 (5.61)
Urine creatinine (mg/dl) mean (SD)	161.9 (81.4)	105.4 (59.1)	80.5 (42.1)	103.18 (65.8)	133.8 (63.8)	154.72 (72.98)	115.75 (62.20)
Urine Mg/creat ratio (mg/gr) mean (SD)	46.51 (25.98)	88.6 (36.5)	104.6 (44.8)	62.55 (33.37)	63.7 (32.5)	60.6 (26.8)	82.03 (42.23)
FEMg mean (SD)	3.27 (1.65)	5.2 (2.5)	6.0 (2.6)	NA	2.55 (1.33)	NA	NA
eGFR (mean, SD)	89.39 (20.03)	89.23 (23.28)	NA	89.41 (21.18)	87.72 (21.16)	94.92 (23.34)	NA

Supplementary Table 5. Study genotyping characteristics.

Study	CoLaus	INGI-Val Borbera	INGI-Carlantino	CROATIA-Vis	CROATIA-Korcula	CROATIA-Split	LBC1936
Array type	Affymetrix 500K	Illumina 370k	Illumina 370k	Illumina HumanHap300v1	Illumina HumanHap370CNV	Illumina HumanHap370CNV	Illumina 610
Genotype calling	BRLMM	BeadStudio analysis software	BeadStudio analysis software	Genome Studio	Genome Studio	Genome Studio	Genome studio
QC filters for genotyped SNPs used for imputation	pHWE<1e-7; individual call rate <90%; SNP call rate<70%; MAF<0.01	call rate >= 90%; MAF >= 1%; pHWE p > 0.0001	call rate >= 90%; MAF >= 1%; pHWE p > 0.0001	SNP Call rate<=0.98, MAF<0..01, pHWE<1e-6, Individual Call rate<0.95	SNP Call rate<=0.98, MAF<0..01, pHWE<1e-6, Individual Call rate<0.95	SNP Call rate<=0.98, MAF<0..01, pHWE<1e-6, Individual Call rate<0.95	pHWE<p < 1x10-3 individual call rate <95%; SNP call rate<98%; MAF<0.01
No of SNPs used for imputation	390'631	332'887	309’430	289'827	307'625	321'456	~500,000
Imputation	IMPUTE v0.2	MACH	MACH	MACH 1.0.16	MACH 1.0.16	MACH 1.0.16	MACH
Imputation Backbone for phased CEU haplotypes (NCBI build)	HapMap release 21 (build 35)	HapMap release 22 (build 36)	HapMap release 22 (build 36)	HapMap release 22 (build 36)	HapMap release 22 (build 36)	HapMap release 22 (build 36)	HapMap II (build 36)
Filtering of imputed genotypes	None	Rsq>0.3	Rsq>0.3	None	None	None	none
Data management and statistical	QUICKTEST	R, GenABEL, ProbABEL (mmscore function was used to	R, GenABEL, ProbABEL (mmscore	R, GenABEL, ProbABEL (mmscore	R, GenABEL, ProbABEL (mmscore function	R, GenABEL, ProbABEL (mmscore function	mach2qtl

analysis		account for relatedness)	function was used to account for relatedness)	function was used to account for relatedness)	was used to account for relatedness)	was used to account for relatedness)	
Population stratification or Principal Components	We included the first 3 principal components as covariates	We included the first 3 principal components as covariates	We included the first 3 principal components as covariates	We included the first 3 principal components as covariates	We included the first 3 principal components as covariates	We included the first 3 principal components as covariates	We included the first 4 principal components as covariates

Supplementary Table 6. Urine (U) parameters in mice fed different Mg^{2+}-containing diets.

Baseline	**Control diet (n=10)**	**Mg^{2+} deficient diet (n= 11)**	**Mg^{2+} excess diet (n=10)**
Body weight (g)	23.7 ± 0.4	23.9 ± 0.8	25.6 ± 0.4*
Diuresis (µl/16h)	1307 ± 162	1467 ± 244	1985 ± 285
Diuresis (µl/min.gBW)	0.058 ± 0.007	0.066 ± 0.012	0.080 ± 0.012
U Na^+ (nmol/min)	164 ± 16	170 ± 19	177 ± 15
U K^+ (nmol/min)	413 ± 40	479 ± 42	501 ± 46
U Cl^- (nmol/min)	229 ± 21	263 ± 29	265 ± 26
U Mg^{2+} (nmol/min)	586 ± 59	621 ± 54	656 ± 78

Day 5	**Control diet (n=10)**	**Mg^{2+} deficient diet (n= 11)**	**Mg^{2+} excess diet (n=10)**
Body weight (g)	24.3 ± 0.5	24.3 ± 0.8	25.8 ± 0.5*
Diuresis (µl/16h)	1064 ± 49	1390 ± 168	1126 ± 132$^{\neq}$
Diuresis (µl/min.gBW)	0.046 ± 0.002	0.060 ± 0.01	0.045 ± 0.005$^{\neq}$
U Na^+ (nmol/min)	156 ± 14	171 ± 20	123 ± 20
U K^+ (nmol/min)	382 ± 36	393 ± 45	327 ± 52$^{\neq}$
U Cl^- (nmol/min)	210 ± 20	239 ± 28	168 ± 30$^{\neq}$
U Mg^{2+} (nmol/min)	478 ± 42	13 ± 3*$^{,\neq}$	1269 ± 184*$^{,\neq}$

Day 10	**Control diet (n=10)**	**Mg^{2+} deficient diet (n= 11)**	**Mg^{2+} excess diet (n=10)**
Body weight (g)	24.1 ± 0.4	24.3 ± 0.9	25.9 ± 0.5*
Diuresis (µl/16h)	1516 ± 136§	1447 ± 149	1334 ± 124$^{\neq}$
Diuresis (µl/min.gBW)	0.066 ± 0.006§	0.062 ± 0.005	0.053 ± 0.005$^{\neq}$
U Na^+ (nmol/min)	189 ± 16§	176 ± 23	140 ± 18
U K^+ (nmol/min)	532 ± 46§	465 ± 43	409 ± 51
U Cl^- (nmol/min)	287 ± 26$^{\neq,\S}$	263 ± 33	195 ± 28*$^{,\neq}$
U Mg^{2+} (nmol/min)	723 ± 49§	8.1 ± 1.7*$^{,\neq,\S}$	1399 ± 149*$^{,\neq}$

*P < 0.05 versus control diet; $^{\neq}$ P < 0.05 versus baseline; § P < 0.05 versus day 5

Supplementary Table 7. Plasma (P) parameters in mice fed different Mg^{2+}-containing diets.

Day 10	Control diet (n=10)	Mg^{2+} deficient diet (n= 11)	Mg^{2+} excess diet (n=10)
Body weight (g)	23.4 ± 0.5	23.3 ± 0.8	24.5 ± 0.6
P urea (mg/dl)	51.4 ± 1	64.7 ± 3.9*	52.0 ± 2.6$^{\neq}$
P creatinine (mg/dl)	0.07 ± 0.01	0.07 ± 0.01	0.08 ± 0.01
P Na^+ (mmol/l)	154 ± 1	157 ± 1*	152 ± 1*,$^{\neq}$
P K^+ (mmol/l)	4.0 ± 0.2	4.4 ± 0.1*	4.7 ± 0.2*
P Cl^- (mmol/l)	110 ± 1	111 ± 1	108 ± 1
P Ca^{2+} (mmol/l)	2.26 ± 0.03	2.06 ± 0.03*	2.29 ± 0.03$^{\neq}$
P Mg^{2+} (mg/dl)	2.95 ± 0.10	1.08 ± 0.11*	3.13 ± 0.13$^{\neq}$

*P < 0.05 versus control diet; $^{\neq}P < 0.05$ versus Mg^{2+} deficient diet

Supplementary Table 8. Primer oligonucleotide sequences used in the present study during RT-qPCR measurements.

Primer sequence 5' → 3'		Species	Amplicon size (bp)	Efficiency (%)
Actb		Mouse	102	102
Forward	TGCCCATCTATGAGGGCTAC			
Reverse	CCCGTTCAGTCAGGATCTTC			
Arl15		Mouse	133	98
Forward	TCATCAAGACAAGCCAGCAG			
Reverse	GCTGTCCTTCAGTGTGTCCA			
Gapdh		Mouse	176	104
Forward	TGCACCACCAACTGCTTAGC			
Reverse	GGATGCAGGGATGGGGGAGA			
Podocin		Mouse	162	103
Forward	GTCTAGCCCATGTGTCCAAA			
Reverse	CCACTTTGATGCCCCAAATA			
Pvalb		Mouse	136	97
Forward	GACGCCATTCTTCTGGAAAT			
Reverse	ATACCCCCACTGCCCTAAAA			
Arbp		Mouse	150	99
Forward	CTTCATTGTGGGAGCAGACA			
Reverse	TTCTCCAGAGCTGGGTTGTT			
Ncc		Mouse	148	101
Forward	CATGGTCTCCTTTGCCAACT			

Reverse	TGCCAAAGAAGCTACCATCA			
Nkcc2		Mouse	154	99
Forward	CCGTGGCCTACATAGGTGTT			
Reverse	GGCTCGTGTTGACATCTTGA			
Aqp2		Mouse	147	103
Forward	TCACTGGGTCTTCTGGATCG			
Reverse	CGTTCCTCCCAGTCAGTGT			
Ppia		Mouse	139	102
Forward	CGTCTCCTTCGAGCTGTTTG			
Reverse	CCACCCTGGCACATGAATC			
Hprt1		Mouse	162	99
Forward	ACATTGTGGCCCTCTGTGTG			
Reverse	TTATGTCCCCCGTTGACTGA			
Sglt2		Mouse	164	101
Forward	TTGGGCATCACCATGATTTA			
Reverse	GCTCCCAGGTATTTGTCGAA			
Trpm6		Mouse	156	100
Forward	CACAAGCCAGTGACCACCTA			
Reverse	GAGGCTCTTGAGGGCTTTTT			
Snat3		Mouse	109	99
Forward	GTTATCTTCGCCCCCAACAT			
Reverse	TGGGCATGATTCGGAAGTAG			
Alpha Enac		Mouse	151	96
Forward	CCTGGGCAGCTTCATCTTTA			

Reverse	GACTCCAGGCATGGAAGACA			
Casr		Mouse	150	97
Foward	CTCTGCTGCTTCTCCAGCT			
Reverse	GGCCTCAAATACCAGGAGGA			
Cabd28		Mouse	154	101
Forward	CTGACAGAGATGGCCAGGTT			
Reverse	AGCAAAGCATCCAGCTCATT			
arl15b		Zebrafish	133	104
Forward	AAGGAACTCGGAGGAGCAGACTCA			
Reverse	AGTGGAGCTCTGTACGCGCC			
elf1α		Zebrafish	89	100
Forward	GAGGCCAGCTCAAACATGGGC			
Reverse	AGGGCATCAAGAAGAGTAGTACCGC			

SUPPLEMENTARY REFERENCES

1. Firmann M, Mayor V, Vidal PM, Bochud M, Pécoud A, Hayoz D, Paccaud F, Preisig M, Song KS, Yuan X, Danoff TM, Stirnadel HA, Waterworth D, Mooser V, Waeber G, Vollenweider P: The CoLaus study: a population-based study to investigate the epidemiology and genetic determinants of cardiovascular risk factors and metabolic syndrome. *BMC Cardiovasc Disord* 8**:** 6, 2008.
2. Vitart V, Rudan I, Hayward C, Gray NK, Floyd J, Palmer CN, Knott SA, Kolcic I, Polasek O, Graessler J, Wilson JF, Marinaki A, Riches PL, Shu X, Janicijevic B, Smolej-Narancic N, Gorgoni B, Morgan J, Campbell S, Biloglav Z, Barac-Lauc L, Pericic M, Klaric IM, Zgaga L, Skaric-Juric T, Wild SH, Richardson WA, Hohenstein P, Kimber CH, Tenesa A, Donnelly LA, Fairbanks LD, Aringer M, McKeigue PM, Ralston SH, Morris AD, Rudan P, Hastie ND, Campbell H, Wright AF: SLC2A9 is a newly identified urate transporter influencing serum urate concentration, urate excretion and gout. *Nat Genet* 40**:** 437-442, 2008.
3. Polasek O, Marusić A, Rotim K, Hayward C, Vitart V, Huffman J, Campbell S, Janković S, Boban M, Biloglav Z, Kolčić I, Krzelj V, Terzić J, Matec L, Tometić G, Nonković D, Nincević J, Pehlić M, Zedelj J, Velagić V, Jurić D, Kirac I, Belak Kovacević S, Wright AF, Campbell H, Rudan I: Genome-wide association study of anthropometric traits in Korčula Island, Croatia. *Croat Med J* 50**:** 7-16, 2009.
4. Rudan I, Marusić A, Janković S, Rotim K, Boban M, Lauc G, Grković I, Dogas Z, Zemunik T, Vatavuk Z, Bencić G, Rudan D, Mulić R, Krzelj V, Terzić J, Stojanović D, Puntarić D, Bilić E, Ropac D, Vorko-Jović A, Znaor A, Stevanović R, Biloglav Z, Polasek O: "10001 Dalmatians:" Croatia launches its national biobank. *Croat Med J* 50**:** 4-6, 2009.
5. Deary IJ, Gow AJ, Taylor MD, Corley J, Brett C, Wilson V, Campbell H, Whalley LJ, Visscher PM, Porteous DJ, Starr JM: The Lothian Birth Cohort 1936: a study to examine influences on cognitive ageing from age 11 to age 70 and beyond. *BMC Geriatr* 7**:** 28, 2007.
6. Deary IJ, Gow AJ, Pattie A, Starr JM: Cohort profile: the Lothian Birth Cohorts of 1921 and 1936. *Int J Epidemiol* 41**:** 1576-1584, 2012.
7. Traglia M, Sala C, Masciullo C, Cverhova V, Lori F, Pistis G, Bione S, Gasparini P, Ulivi S, Ciullo M, Nutile T, Bosi E, Sirtori M, Mignogna G, Rubinacci A, Buetti I, Camaschella C, Petretto E, Toniolo D: Heritability and demographic analyses in the

large isolated population of Val Borbera suggest advantages in mapping complex traits genes. *PLoS One* 4**:** e7554, 2009.

8. Glaudemans B, Terryn S, Gölz N, Brunati M, Cattaneo A, Bachi A, Al-Qusairi L, Ziegler U, Staub O, Rampoldi L, Devuyst O: A primary culture system of mouse thick ascending limb cells with preserved function and uromodulin processing. *Pflügers Arch* 466**:** 343-356, 2014.
9. Hoenderop, JGJ, Dardenne, O, van Abel, M, van der Kemp, AW, van Os, CH, St -Arnaud, R, Bindels, RJM: Modulation of renal Ca^{2+} transport protein genes by dietary Ca^{2+} and 1,25-dihydroxyvitamin D_3 in 25-hydroxyvitamin D_3-1a-hydroxylase knockout mice. *FASEB J* 16**:** 1398-1406, 2002.
10. Ferrè, S, de Baaij, JHF, Ferreira, P, Germann, R, de Klerk, JB, Lavrijsen, M, van Zeeland, F, Venselaar, H, Kluijtmans, LA, Hoenderop, JGJ, Bindels, RJM: Mutations in PCBD1 cause hypomagnesemia and renal magnesium wasting. *J Am Soc Nephrol* 25**:** 574-586, 2014.
11. Nijenhuis, T, Hoenderop, JGJ, Loffing, J, van der Kemp, AWCM, van Os, CH, Bindels, RJM: Thiazide-induced hypocalciuria is accompanied by a decreased expression of Ca^{2+} transport proteins in kidney. *Kidney Int* 64**:** 555-564, 2003.
12. Voets T, Nilius B, Hoefs S, van der Kemp AW, Droogmans G, Bindels RJM, Hoenderop JGJ: TRPM6 forms the Mg^{2+} influx channel involved in intestinal and renal Mg^{2+} absorption. *J Biol Chem* 279**:** 19-25, 2004.
13. Groenestege WM, Hoenderop JGJ, van den Heuvel L, Knoers N, Bindels RJM: The epithelial Mg^{2+} channel transient receptor potential melastatin 6 is regulated by dietary Mg^{2+} content and estrogens. *J Am Soc Nephrol* 17**:** 1035-1043, 2006.
14. Wingert RA, Selleck R, Yu J, Song HD, Chen Z, Song A, Zhou Y, Thisse B, Thisse C, McMahon AP, Davidson AJ: The cdx genes and retinoic acid control the positioning and segmentation of the zebrafish pronephros. *PLoS Genet* 3**:** e189, 2007.
15. Wang Y-F, Tseng Y-C, Yan J-J, Hiroi J, Hwang P-P: Role of SLC12A10.2, a Na-Cl cotransporter-like protein, in a Cl uptake mechanism in zebrafish (*Danio rerio*). *Am J Physiol Regul Integr Comp Phys* 296**:** R1650-R1660, 2009.
16. Arjona FJ, Chen Y-X, Flik G, Bindels RJM, Hoenderop JGJ: Tissue-specific expression and in vivo regulation of zebrafish orthologues of mammalian genes related to symptomatic hypomagnesemia. *Pflügers Arch* 465**:** 1409-1421, 2013.

17. Hyatt TM, Ekker SC: Vectors and techniques for ectopic gene expression in zebrafish. In: *Methods in Cell biology,* edited by Detrich HW, Westerfield M, Zon LI, 1998, pp 117-126.

18. Mahmood F, Mozere M, Zdebik AA, Stanescu HC, Tobin J, Beales PL, Kleta R, Bockenhauer D, Russell C: Generation and validation of a zebrafish model of EAST (epilepsy, ataxia, sensorineural deafness and tubulopathy) syndrome. *Dis Model Mech* 6**:** 652-660, 2013.

19. Arjona FJ, de Baaij JHF, Schlingmann KP, Lameris ALL, van Wijk E, Flik G, Regele S, Korenke GC, Neophytou B, Rust S, Reintjes N, Konrad M, Bindels RJM, Hoenderop JGJ: CNNM2 mutations cause impaired brain development and seizures in patients with hypomagnesemia. *PLoS Genet* 10**:** e1004267, 2014.

20. Bustin SA, Benes V, Garson JA, Hellemans J, Huggett J, Kubista M, Mueller R, Nolan T, Pfaffl MW, Shipley GL, Vandesompele J, Wittwer CT: The MIQE guidelines. *Clin Chem* 55**:** 611-622, 2009.

21. Jouret F, Auzanneau C, Debaix H, Wada GH, Pretto C, Marbaix E, Karet FE, Courtoy PJ, Devuyst O: Ubiquitous and kidney-specific subunits of vacuolar H+-ATPase are differentially expressed during nephrogenesis. *J Am Soc Nephrol* 16**:** 3235-3246, 2005.

22. Parreira KS, Debaix H, Cnops Y, Geffers L, Devuyst O: Expression patterns of the aquaporin gene family during renal development: influence of genetic variability. *Pflügers Arch* 458**:** 745-759, 2009.

23. McCurley AT, Callard GV: Characterization of housekeeping genes in zebrafish: male-female differences and effects of tissue type, developmental stage and chemical treatment. *BMC Mol Biol* 9**:** 102, 2008.

Genome-wide Meta-analysis Unravels Novel Interactions Between Magnesium Homeostasis and Metabolic Phenotypes

METHODS

Meta-GWAS of urinary Mg^{2+} in European cohorts (n = 9,099)

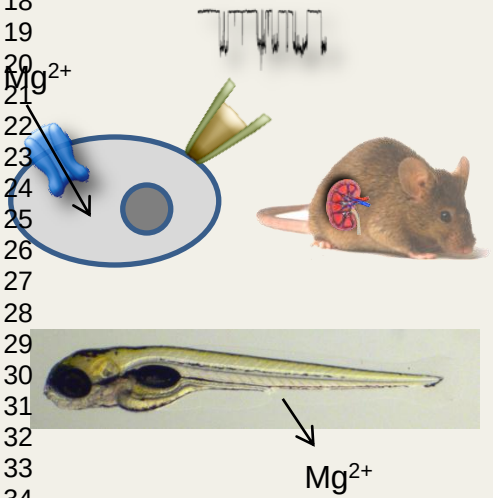

In vitro and *in vivo* studies of renal Mg^{2+} handling

RESULTS

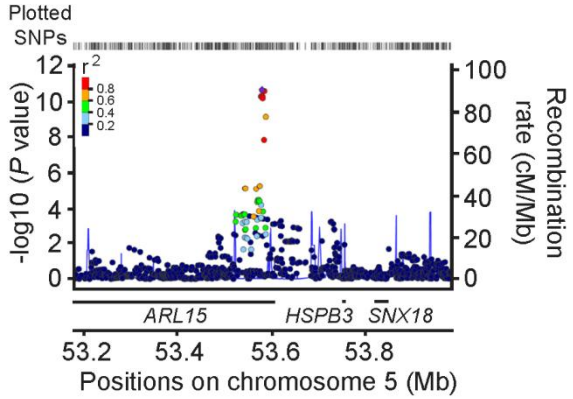

ARL15 is associated with urinary Mg^{2+} in the population

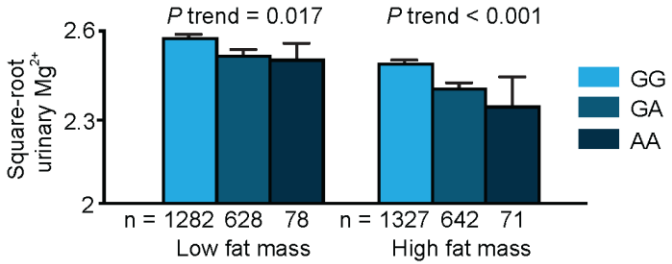

SNP-by-environment interaction

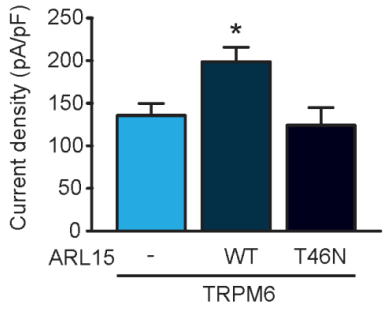

Renal cells

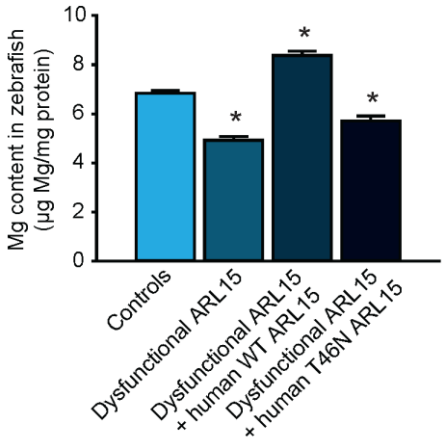

Zebrafish

CONCLUSION ARL15 is a new player for renal Mg^{2+} handling that provides the first genetic link between Mg^{2+} balance and metabolism

Ganguy Corre*, Francisco J. Arjona*, Caroline Hayward*, Sonia Youhanna, Jeroen H.F. de Baaij, Hendrica Belge, Nadine Nägele, Huguette Debaix, Maxime G. Blanchard, Michela Traglia, Sarah E. Harris, Sheila Ulivi, Rico Rueedi, David Lamparter, Aurélien Macé, Cinza Sala, Stefania Lenarduzzi, Belen Ponte, Menno Pruijm, Daniel Ackermann, Georg Ehret, Daniela Baptista, Ozren Polasek, Igor Rudan, Toby Hurd, Nicholas D. Hastie, Veronique Vitart, Gerard Waeber, Zoltán Kutalik, Sven Bergmann, Rosa Vargas-Poussou, Martin Konrad, Paolo Gasparini, Ian J. Deary, John M. Starr, Daniela Toniolo, Peter Vollenweider, Joost G.J. Hoenderop, René J.M. Bindels#, Murielle Bochud#, and Olivier Devuyst#: **Genome-wide Meta-analysis Unravels Novel Interactions Between Magnesium Homeostasis and Metabolic Phenotypes**. J Am Soc Nephrol: doi: 10.1681/ASN. *equally contributed to the study; #co-directed the study

JASN
JOURNAL OF THE AMERICAN SOCIETY OF NEPHROLOGY